



PHS6317 - Nanoingénierie des couches minces - Nanoengineering of thin films

Thermal spray processes and coatings

Christian Moreau

Concordia University

Canada Research Chair in Thermal Spray and Surface Engineering

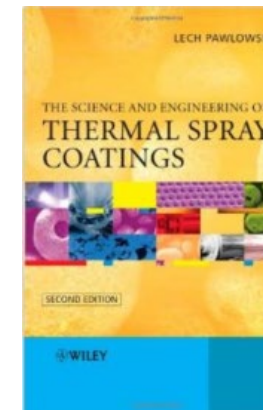
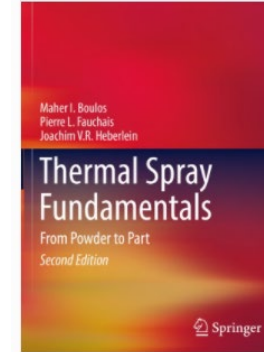
Polytechnique Montréal, February 9, 2024

Outline

- Introduction to thermal spray processing
- Plasma spray
 - Air plasma spray
 - Suspension plasma spray
- Combustion processes:
 - Flame
 - HVOF / HVAF
- Arc Spray
- Cold spray / Kinetic spray
- Applications

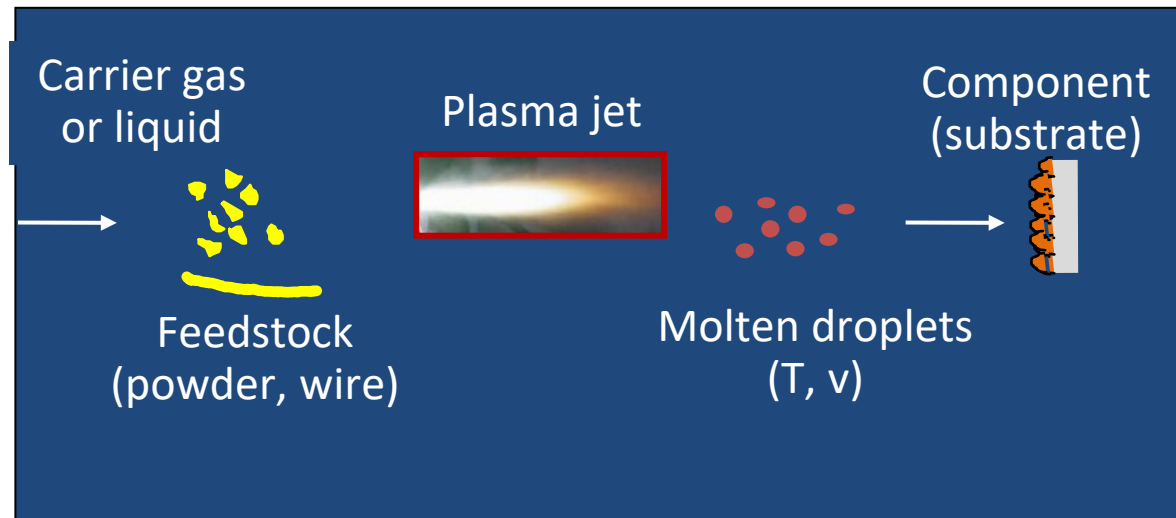
References

- Maher I. Boulos, Pierre L. Fauchais, Joachim V.R. Heberlein,, “**Thermal Spray Fundamentals: From Powder to Part** “, 2nd Edition, Springer, 2021, 1136 p
- **ASM Handbook, Volume 5A: Thermal Spray Technology**, Robert C. Tucker, Jr. , Ed., 2013, 412 p.
- L. Pawlowski, “**The Science and Engineering of Thermal Spray Coatings**”, Wiley, 2008, 656 p



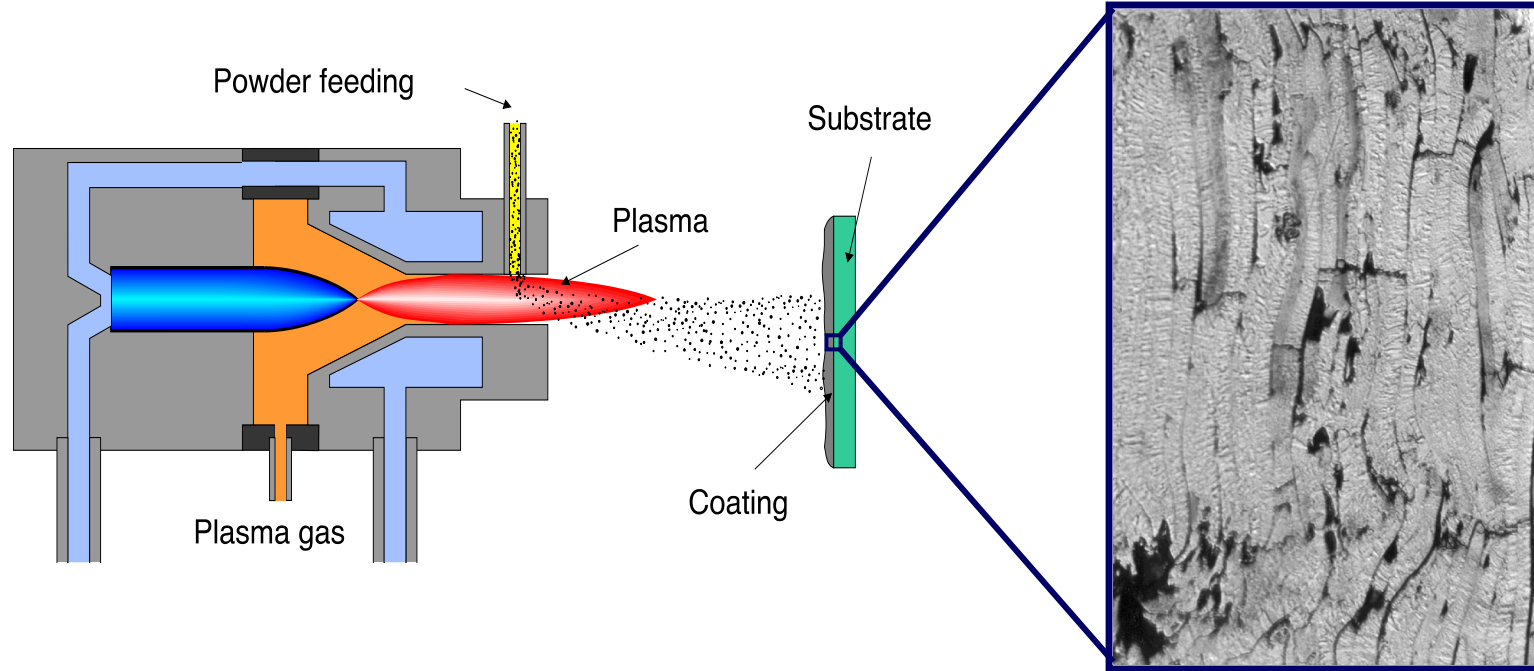
What Is Thermal Spraying?

- A family of processes in which a finely divided surfacing material is sprayed in a molten or semi-molten state on a prepared substrate to form a coating.



What Is Plasma Spraying?

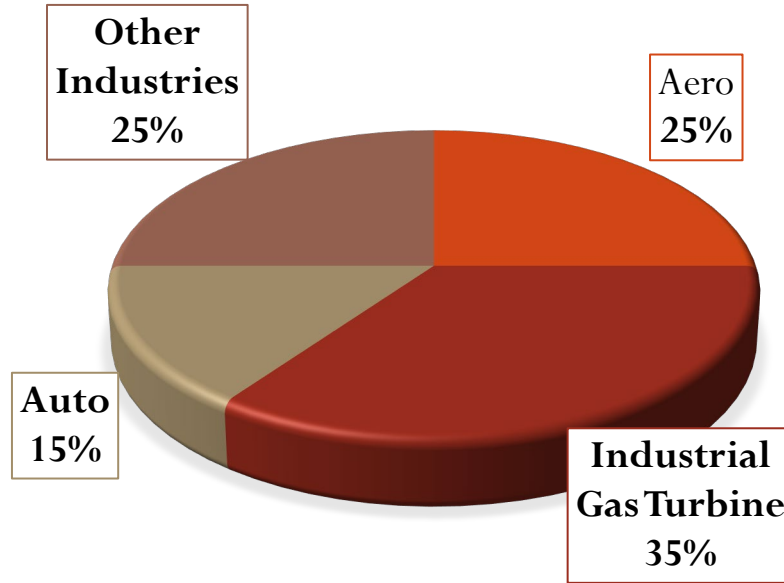
- The flame is a thermal plasma jet heated by a high intensity dc current arc between the anode and cathode (300-800 A, 30-80V)



Coating cross-section showing the lamellar structure

Thermal Spray Markets

□ Global market estimated at \$7.5 billion US(Dorfman, MS&T 2011)



Other Industries

- Printing, pulp and paper
- Biomedical
- Mining, metal processing
- Petrochemical
- Electronics
- Etc.



*Images courtesy of NRC Canada

Plasma Spraying

- The plasma torch is scanned in front of the substrate as many times as necessary to get the required coating thickness (10 microns – millimetres)

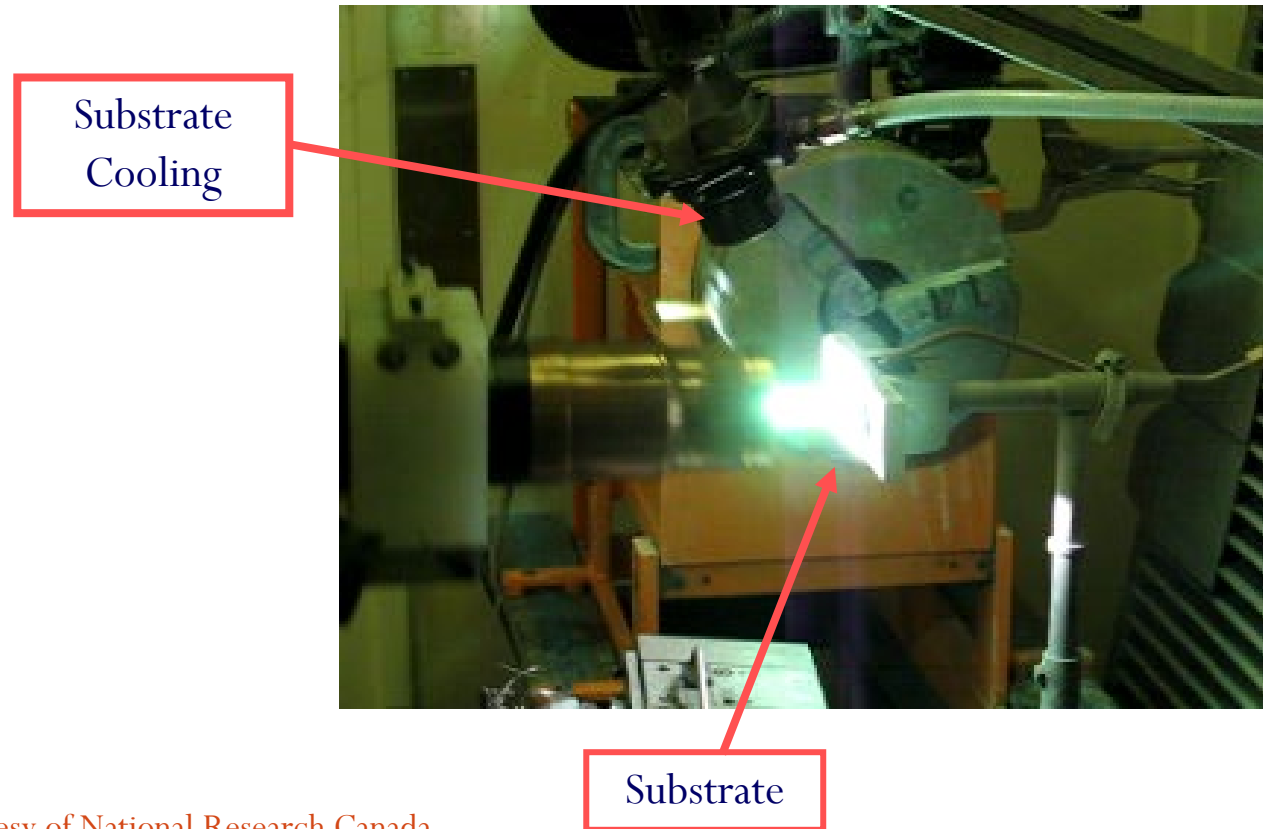
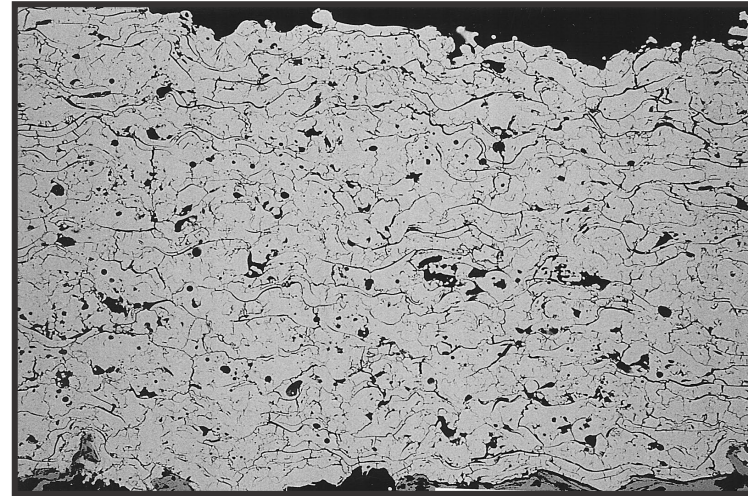
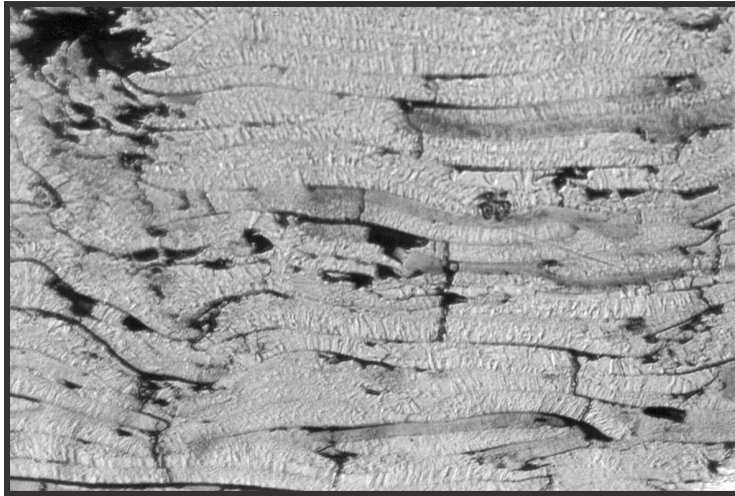


*Image courtesy of National Research Canada

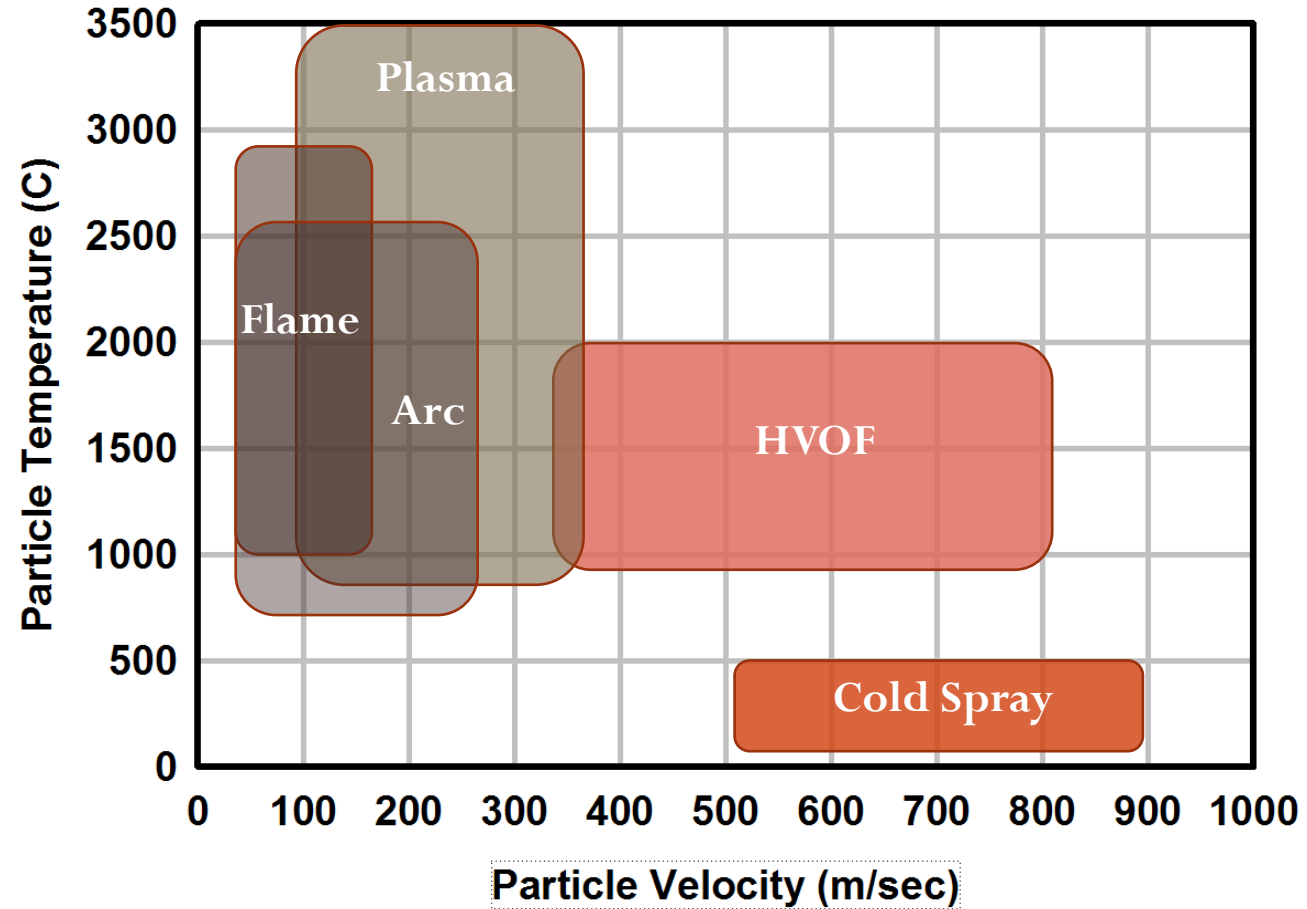
Coating Structure

- Coatings are built by the accumulation of molten or partially molten particles impacting on the substrate surface

- Lamellar structure
- Pores and cracks



Thermal Spray Processes: Particle Characteristics



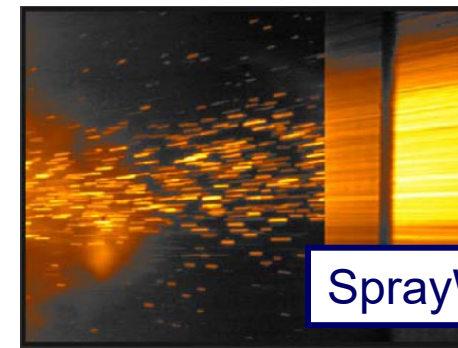
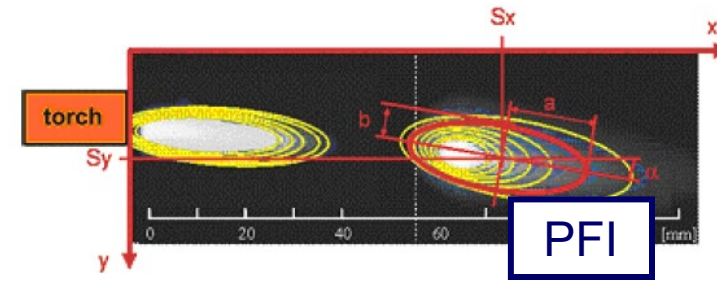
In-flight Particle Diagnostics: Commercial Sensors

- Detection of thermal radiation emitted by the hot particles
- Camera for monitoring the orientation, width and intensity of the particle jet
- Commercial systems for monitoring particle jet characteristics:



Accuraspray/PlumeSpector

DPV 2000

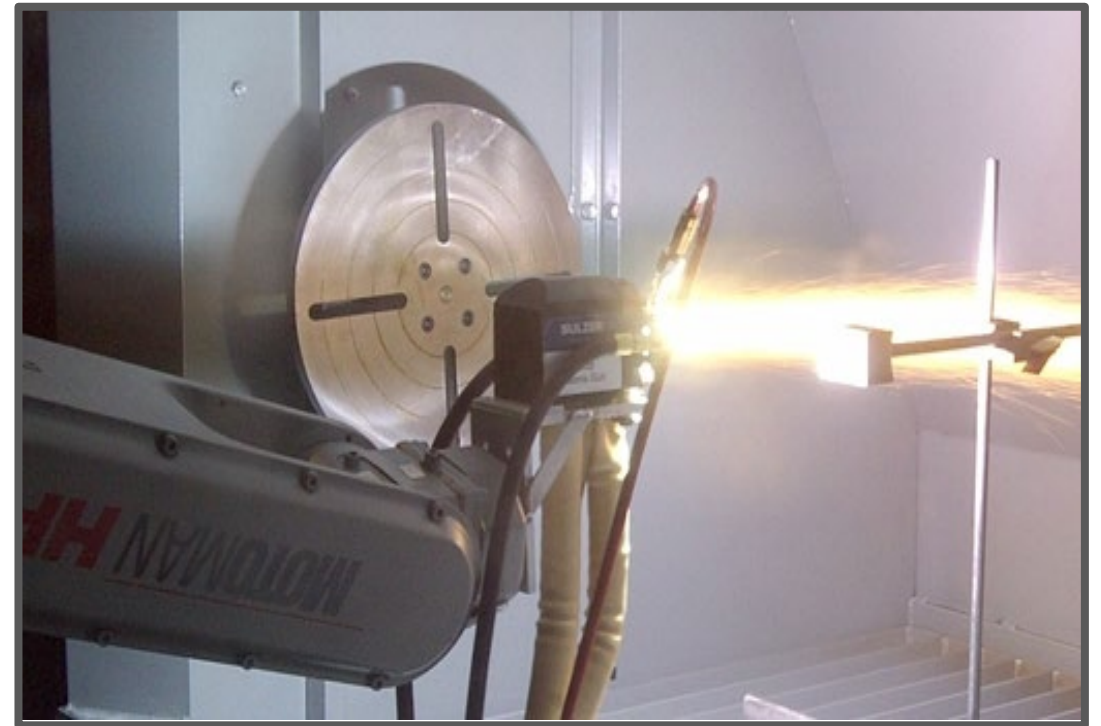


SprayWatch

Plasma Spray

Plasma Spray

Air Plasma Spray
Concordia



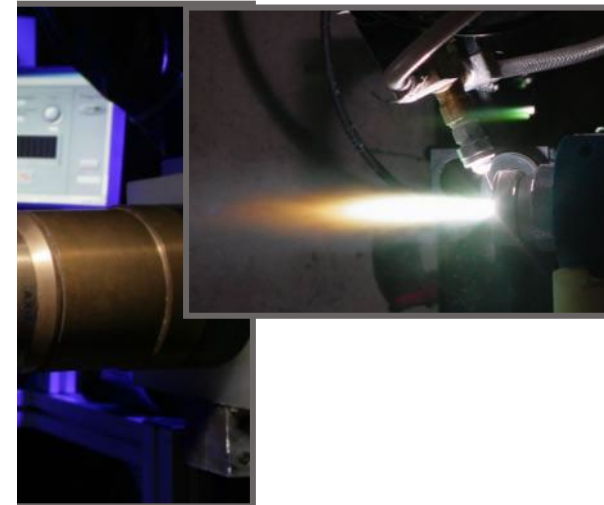
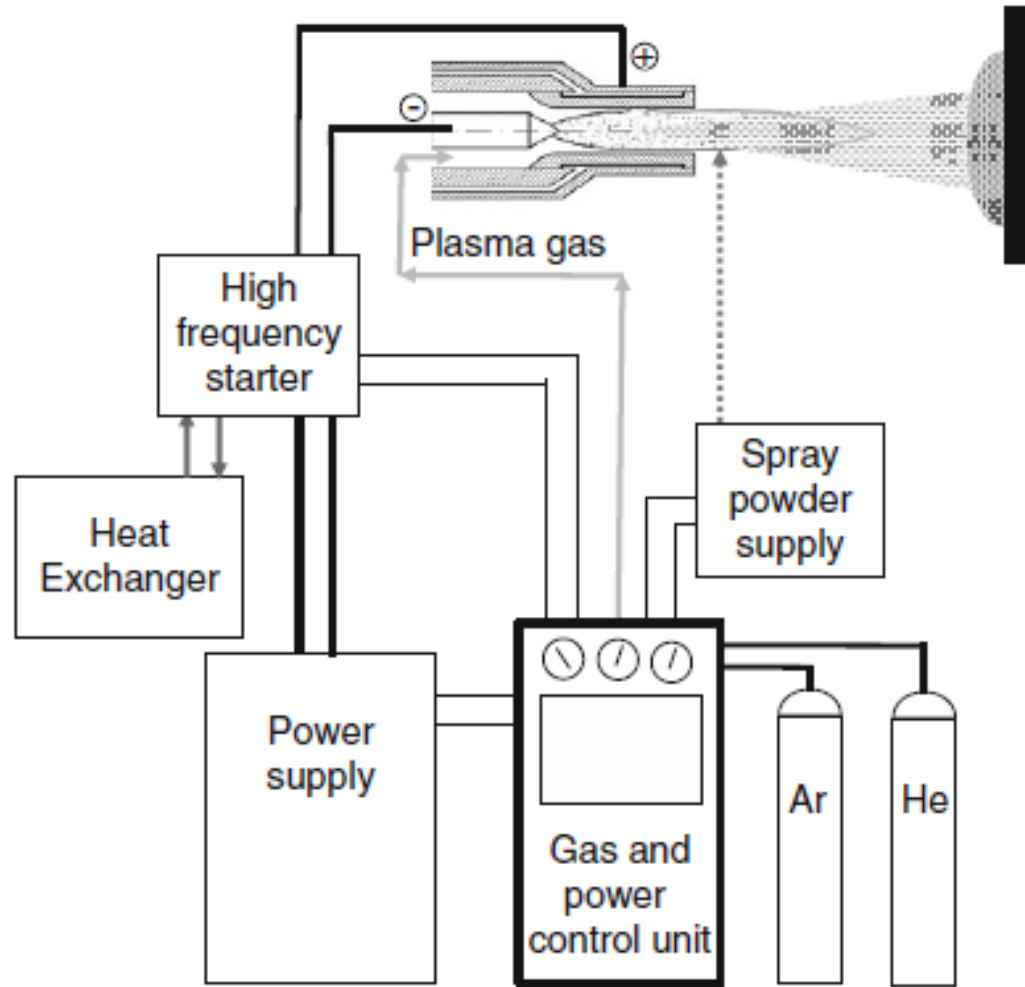
Plasma Spraying

- Particle characteristics
 - temperature $\sim 800\text{-}3500^\circ\text{C}$
 - speed $\sim 100\text{-}350\text{ m/s}$
- Materials - ceramics, metals and cermets
 - deposition efficiency $\sim 30\text{ to }70\%$
 - spray rate $\sim 1\text{ to }3\text{ kg/hour}$
- Coating characteristics
 - density $\sim 5\text{ to }20\%$ porosity
- The plasma temperature reaches $10,000\text{K}$ and more. Thus any material that can melt without decomposition or sublimation can be sprayed
 - Well adapted for ceramics and refractory metals

Spray Parameters

Parameters	Torch	Plasma Jet	Spray Particles	Substrate
Input	<ul style="list-style-type: none"> • Current • Primary and secondary gas flow rate • Cooling water flow 		<ul style="list-style-type: none"> • Feed rate • Carrier gas flow rate 	<ul style="list-style-type: none"> • Surface preparation • Heating/cooling • Motion relative to the torch • Spray distance
Operating	<ul style="list-style-type: none"> • Voltage • Voltage fluctuations • Thermal efficiencies 	<ul style="list-style-type: none"> • Plasma jet T and v • Plasma jet stability 	<ul style="list-style-type: none"> • Particle injection speed • Particle trajectories • Particle T, v and flux 	<ul style="list-style-type: none"> • Substrate temperature • Deposition efficiency
Other	<ul style="list-style-type: none"> • Torch assembly • Electrode wear 		<ul style="list-style-type: none"> • Particle characteristics (size, shape, etc.) 	<ul style="list-style-type: none"> • Substrate material

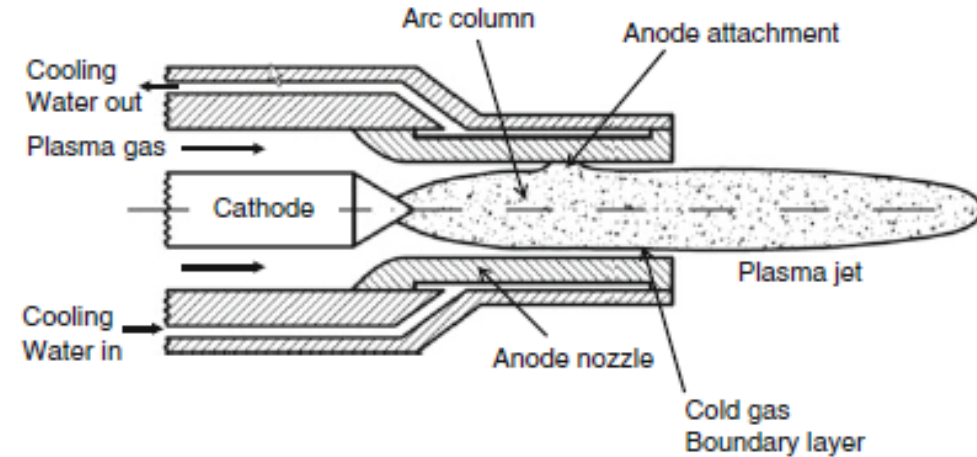
Equipment and Process Parameters



Thermal Spray Fundamentals, Fauchais et al., 2014

Images courtesy of NRC Canada

Plasma Torch



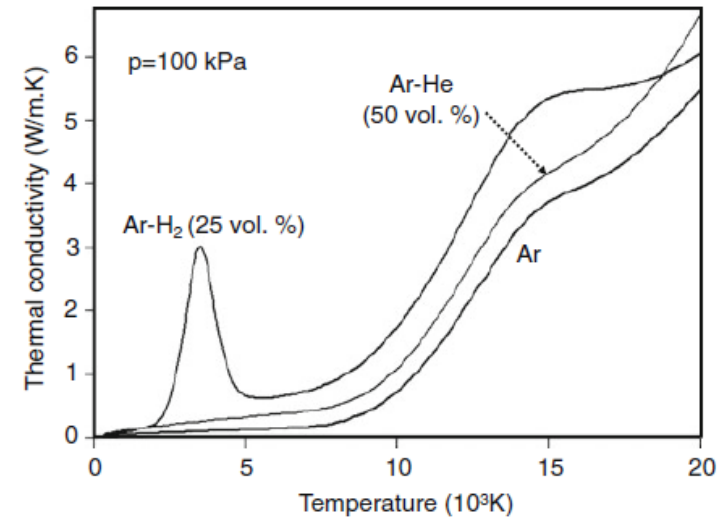
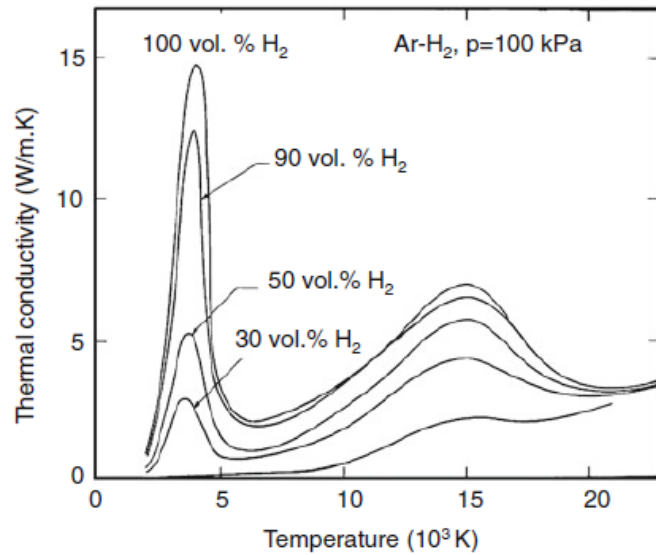
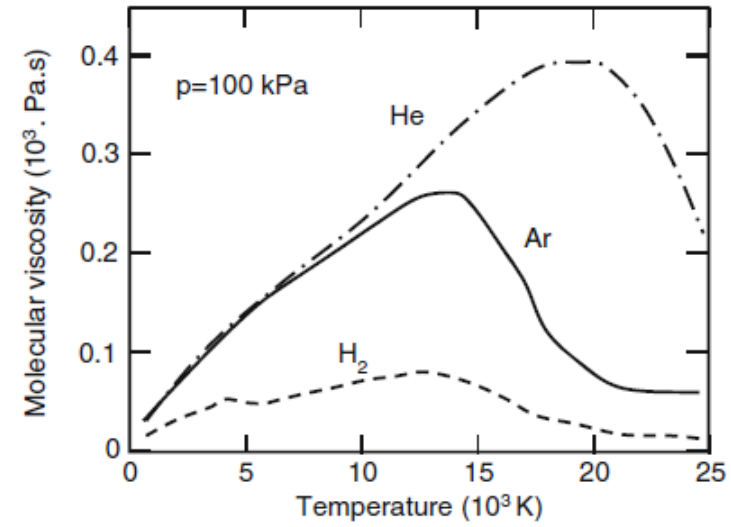
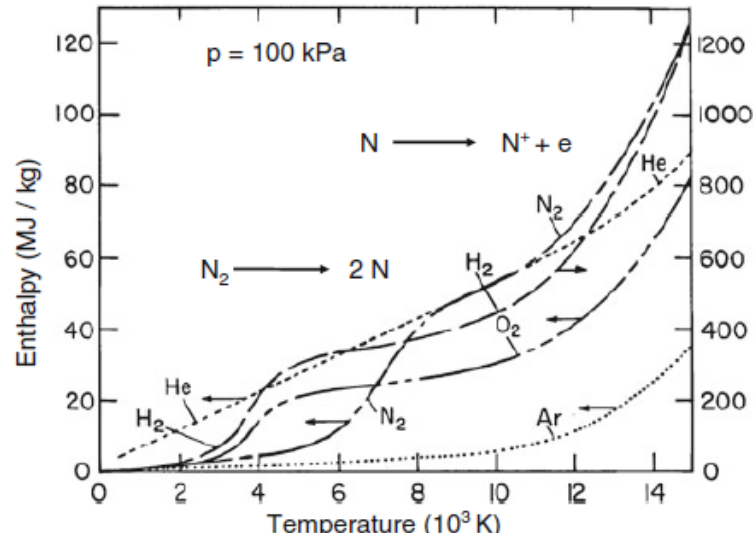
- Integral energy balance (integrated over the radial coordinate):

$$\dot{m} \frac{\Delta \bar{h}}{\Delta z} + Q_{\text{cond}} + Q_{\text{Rad}} = I \times E$$

- Energy balance for the torch:

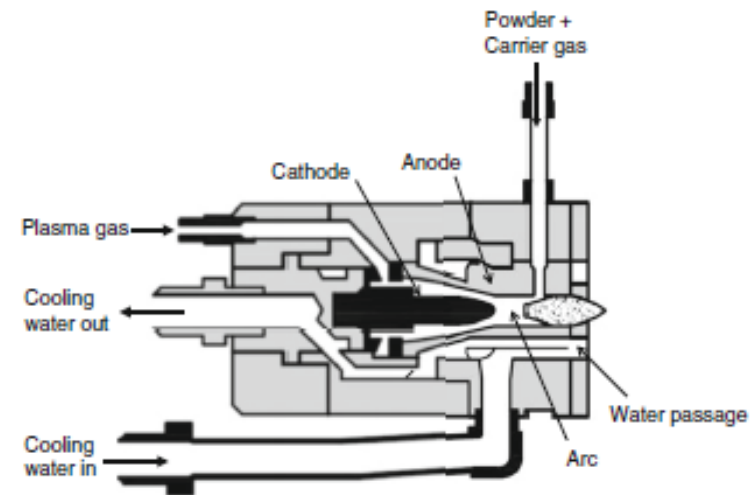
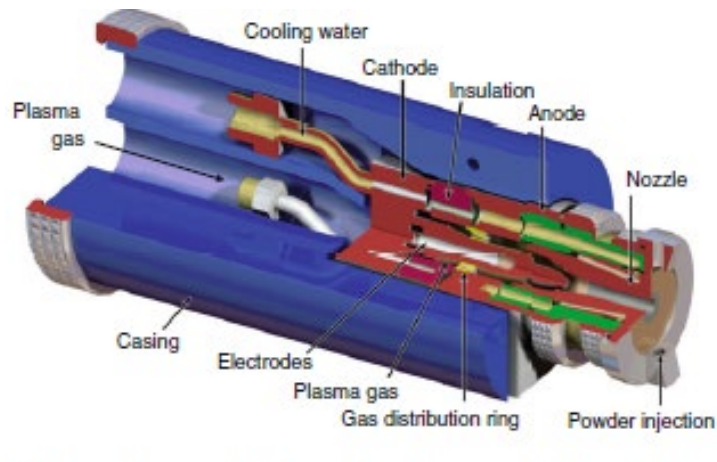
$$\dot{m} h_{\text{ave}} = \eta P_{\text{el}} = P_{\text{el}} - Q_{\text{Loss}}$$

Key Properties of Plasma Gases



Plasma Torches

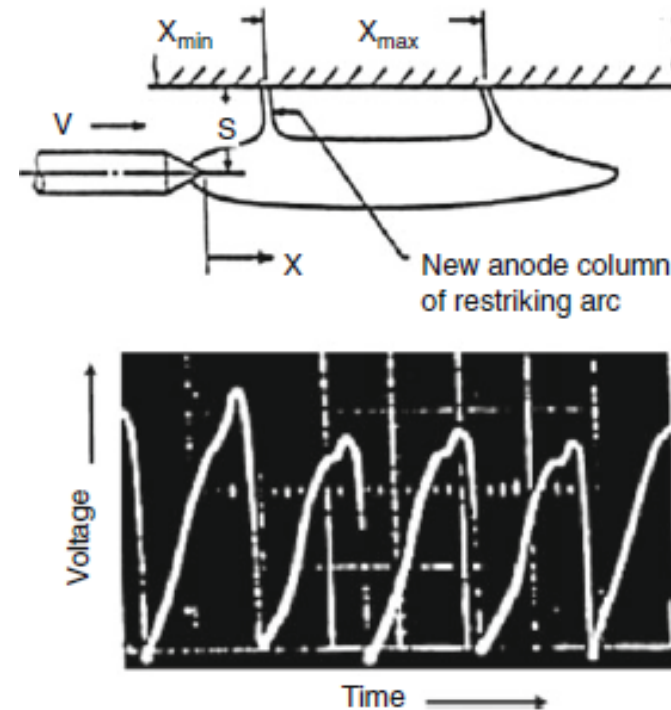
- Numerous different torches are available on the marketplace with different characteristics (power 15-200 kW, spray rate, size, radial or axial injection, etc.)
- Oerlikon Metco F4
- Praxair SG100



Thermal Spray Fundamentals, Fauchais et al., 2014

Plasma Jet Stability

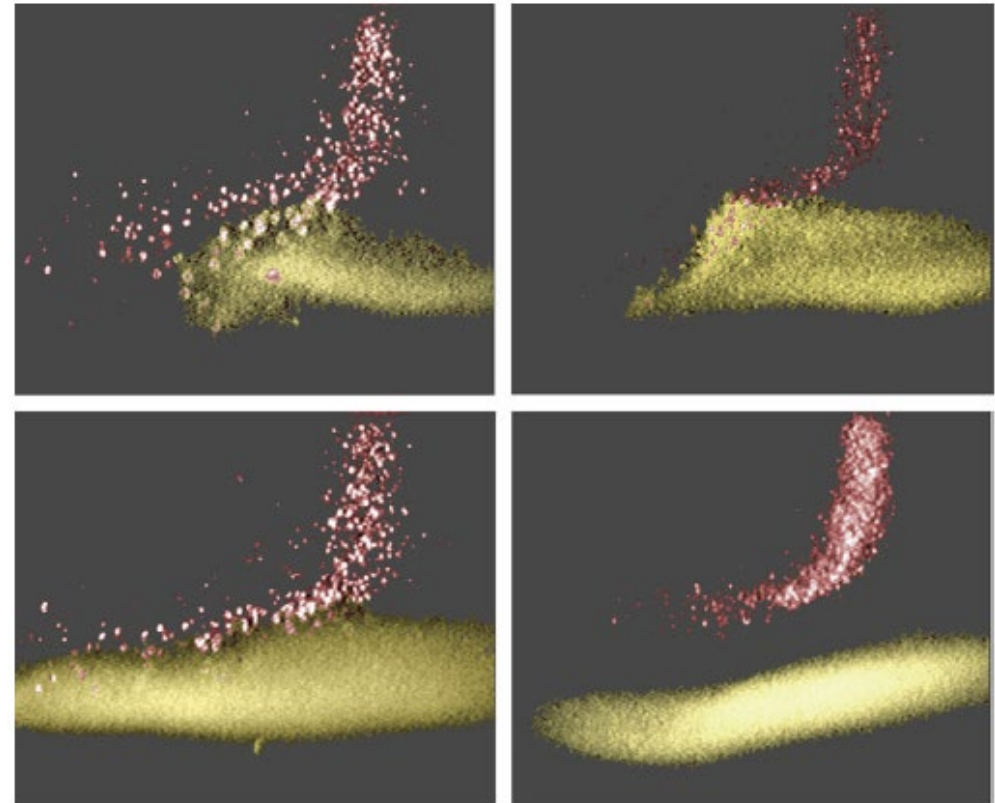
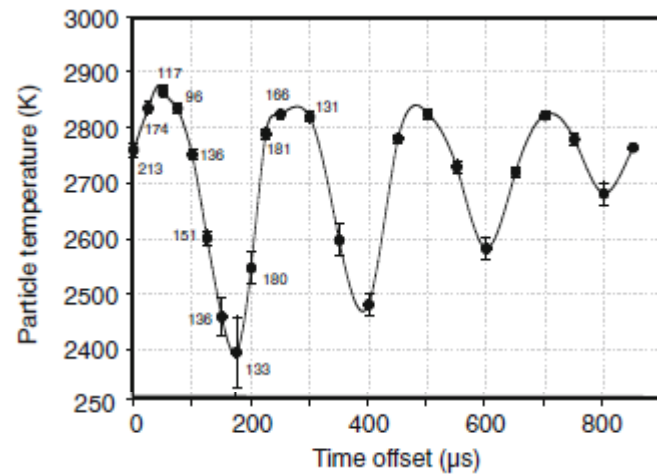
- The arc root moves along the anode surface under the influence of:
 - drag force exerted by the cold flow in the boundary layer
 - Lorentz forces due the magnetic field induced by the curvature of the current flow.
- The voltage (and power) changes with the length of the arc
- Arc fluctuation frequency typically observed between 2-5 kHz



Thermal Spray Fundamentals, Fauchais et al., 2014

Plasma-particle Interaction

- The plasma fluctuations induced variations in the temperature and velocity of the spray particles



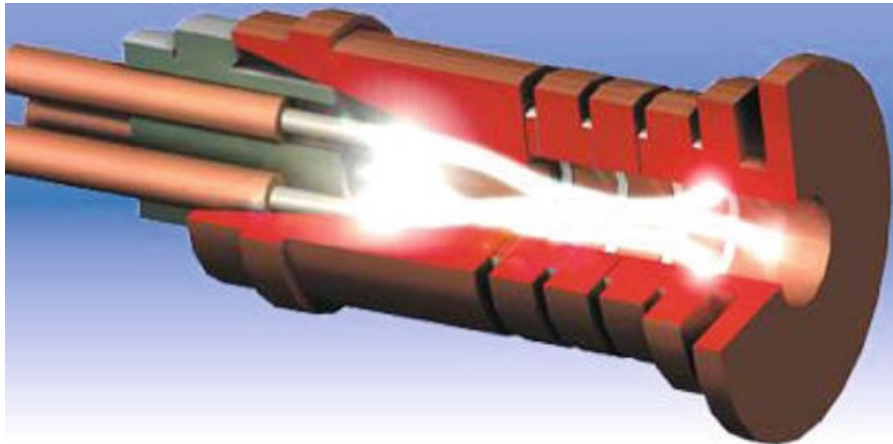
JF Bisson et al., *J Therm. Spray Technol.*, 12 (2003)38–43

P. Fauchais, *Understanding plasma spraying. J Phys D Appl Phys* 37 (2004) 86–108

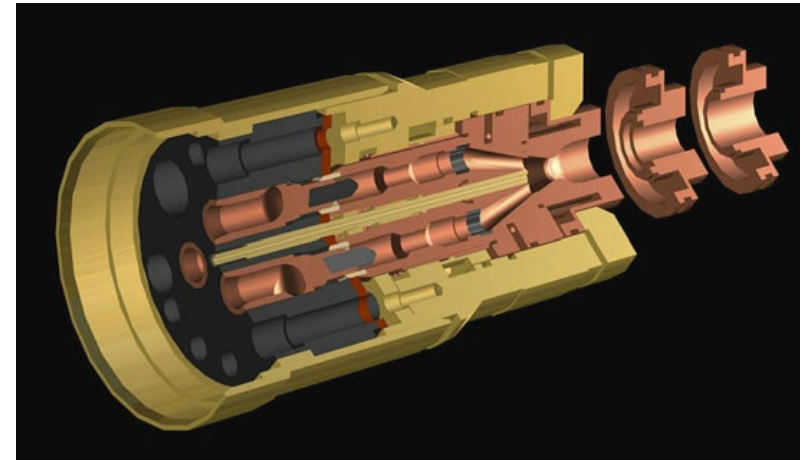
Recent Developments

- More stable plasma torches typically operating at lower current and higher voltage:
 - Cascaded torch
 - Current is carried through 3 separate arcs

Triplex, Oerlikon Metco



Axial III, Mettech Corp.



Thermal Spray Fundamentals, Fauchais et al., 2014

Average Plasma Characteristics Downstream the Torch Exit

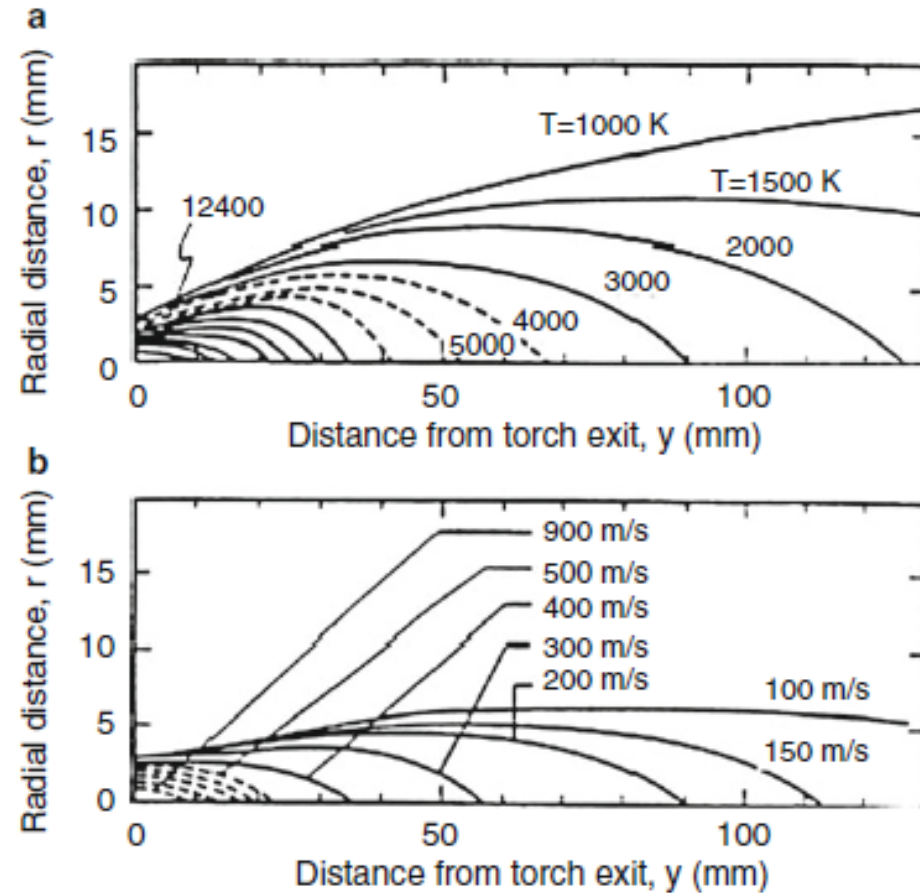


Fig. 7.21 Temperature and velocity contours in d.c. plasma spray jet operated with nitrogen-hydrogen mixture [76] (with kind permission from Springer Science+Business Media B.V.)

Turbulent Plasma Flow

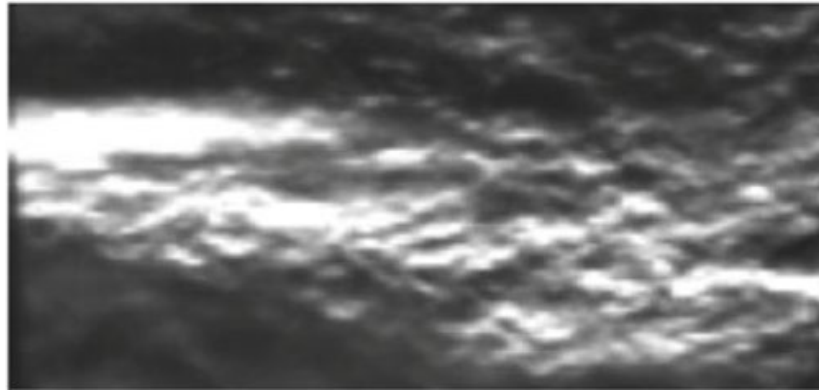
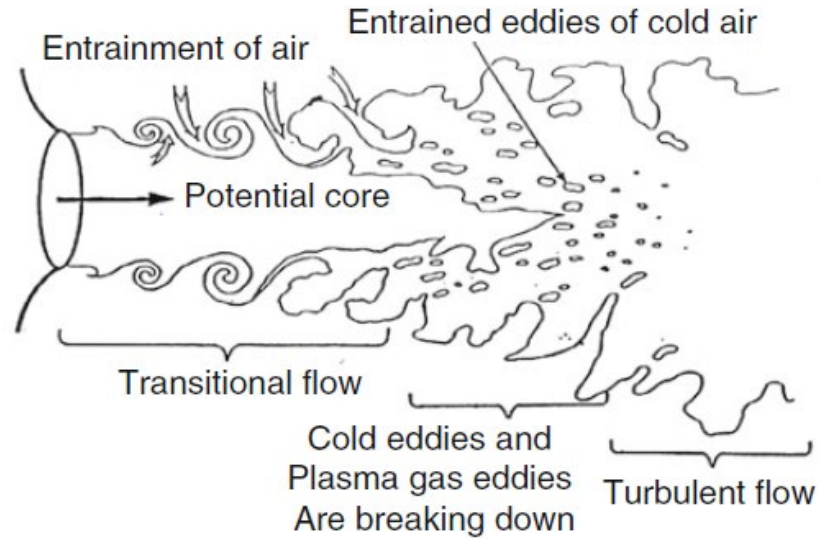
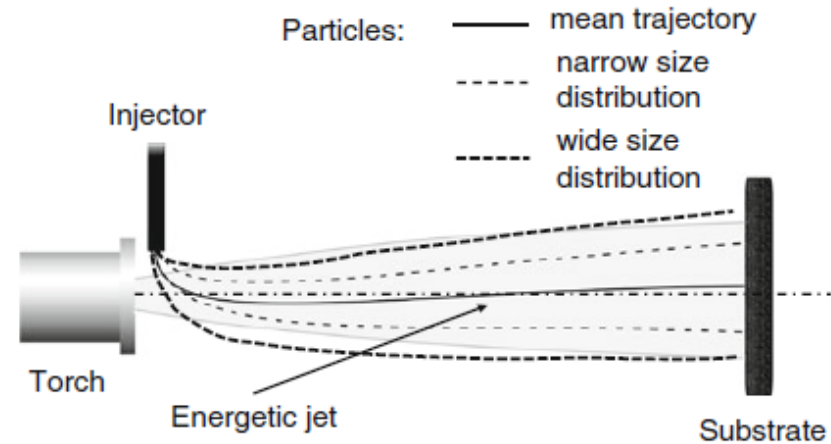


Fig. 7.37 Schematic of the large-scale turbulence and cold gas entrainment in a plasma jet issuing into a cold gas environment and Schlieren images of a turbulent plasma jet [92]. Reprinted with permission of ASM International. All rights reserved

Powder Injection and Trajectories

Fig. 2.18 Envelope of trajectories of particles injected radially for two powder size distributions (with one larger than the other) with the same mean size and same optimum trajectory



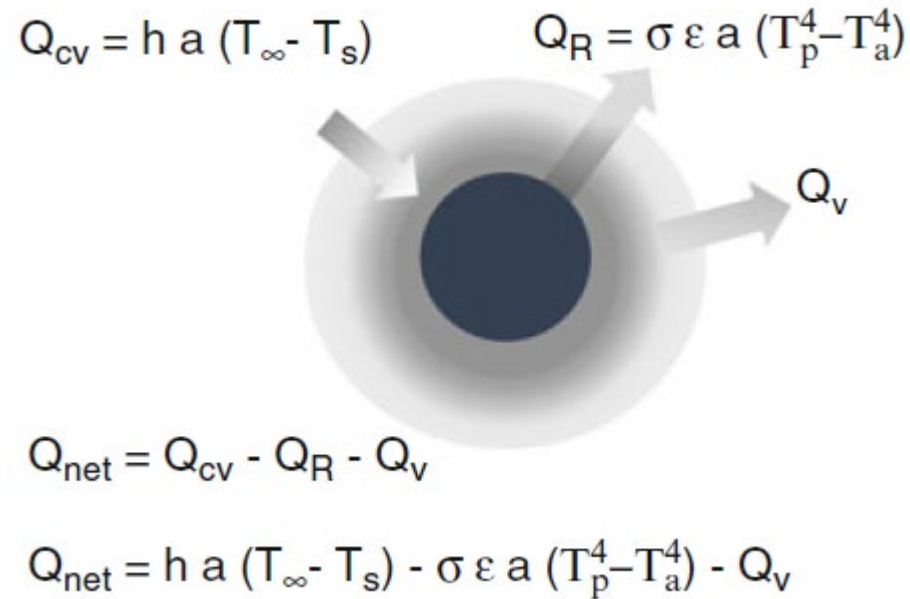
- Forces: inertia, drag (gravity negligible)

$$F_i = \frac{\pi d_p^3}{6} \cdot \rho_p \cdot \frac{du_p}{dt}$$
$$F_D = \frac{\pi d_p^2}{4} \cdot C_D \cdot \frac{1}{2} \rho \cdot u_R^2$$

Heat Transfer

$$Q = h(\pi d_p^2)(T_\infty - T_s) - (\pi d_p^2)\epsilon\sigma_s(T_s^4 - T_a^4)$$

Fig. 4.20 Schematic of the net heat transfer to a particle, q_{net} , where, q_R radiative loss from the surface of a solid particle and q_v , heat loss from radiating vapor



In-flight Particle Characteristics

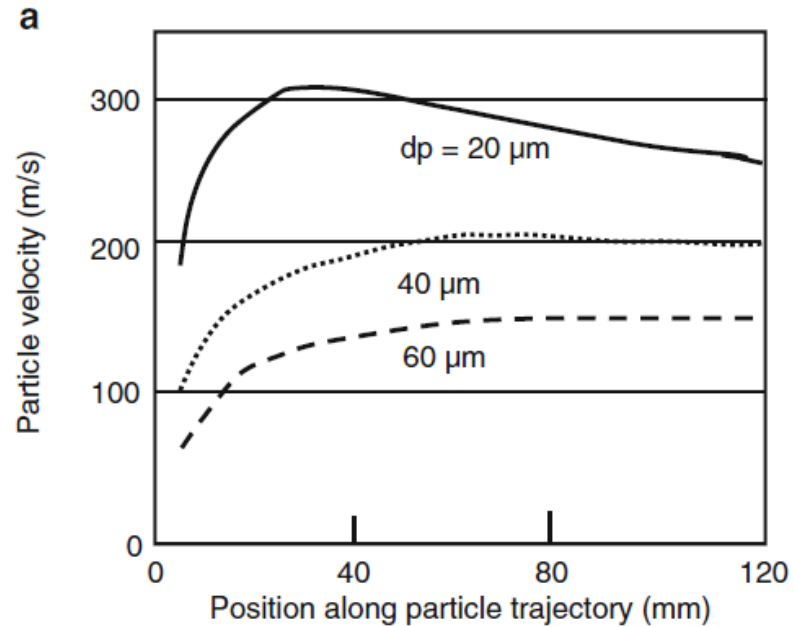
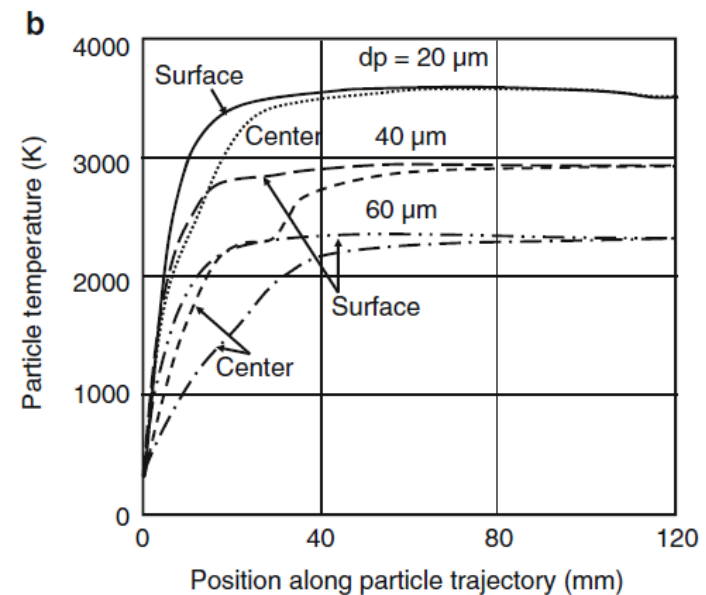


Fig. 4.38 Computed particle velocity (a) and temperature history (b) for dense Zirconia particles injected into an Ar-H₂ DC plasma jet: nozzle i.d. 6 mm, 35 slm Ar, 12 slm H₂, $I = 600 \text{ A}$, $P = 35 \text{ kW}$, $\eta_{\text{th}} = 55 \%$ [87]



Feedstock - Powders

- Powder characteristics must be controlled tightly as they influence the particle injection and trajectories in the plasma and the resulting coating characteristics:
 - Particle size distribution
 - Particle shape
 - No segregation
 - Low humidity
 - Etc.

Powder Characteristics

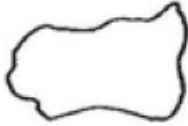
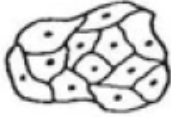
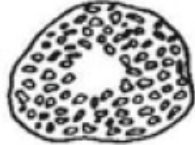
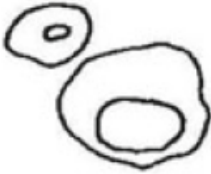

Powder type Manufacturer	Fused and milled	Sintered and milled	Agglomerated and sintered	Spheroidized	Atomized
					
Particle shape	Blocky - angular	Blocky - angular	Spherical	Spherical	Spherical -irregular
Porosity	Dense	Dense - porous	Porous	Dense - hollow	Porous - hollow
Crystalline size	Course- fine	Course - fine	Medium - fine	Medium - fine	Fine
Homogeneity	Alloyed	Alloyed	Alloyed - heterogeneous	Alloyed - heterogeneous	Alloyed

Fig. 11.39 Specific $ZrO_2-8 \text{ wt}\% Y_2O_3$ powder characteristics depending on their manufacturing route. Reprinted with kind permission from Elsevier [47]

Surface Preparation

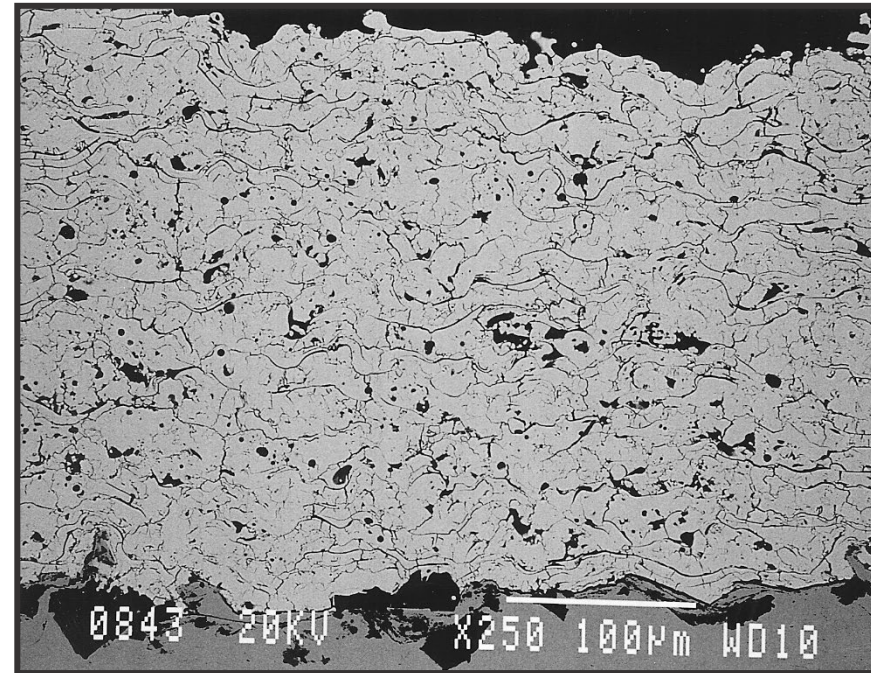
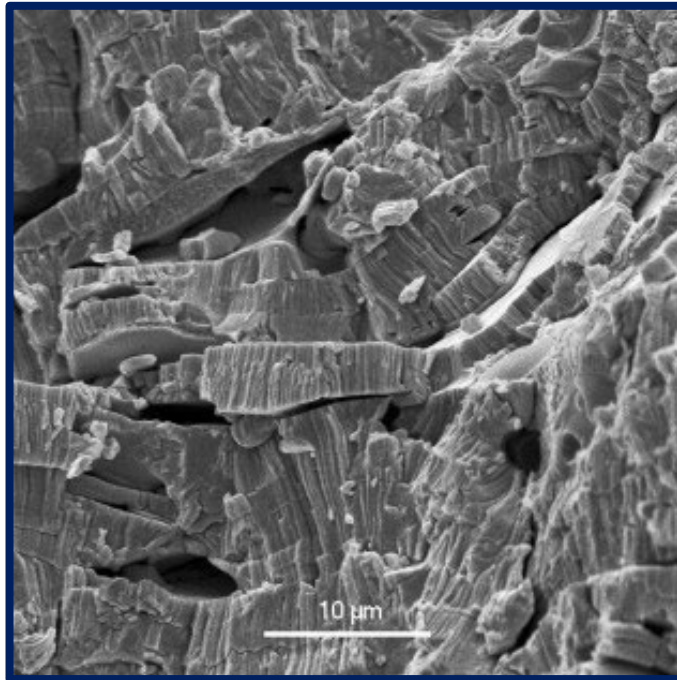
- Adhesion mostly mechanical
- Majority of coating failures due to poor surface preparation
- Grit blasting
 - 36 to 60 grit Al₂O₃
 - Sand blasting is NOT acceptable
- Water Jet
- Laser cleaning



Progressive Technologies

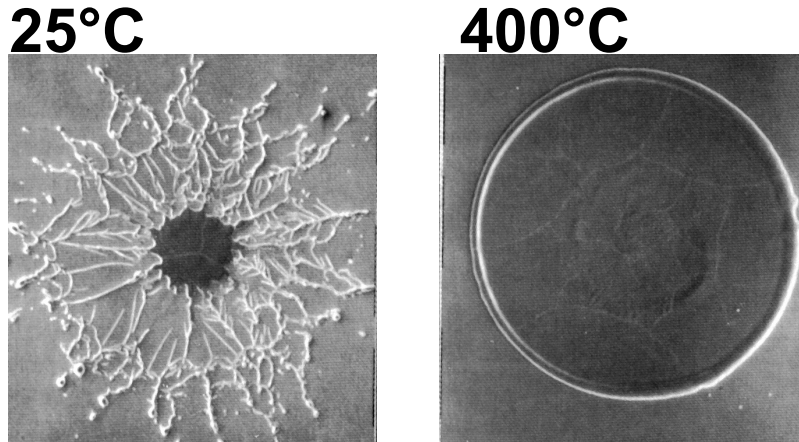
Plasma-sprayed Ceramic Coatings

Thermal Barrier Coating: Yttria partially stabilized zirconia

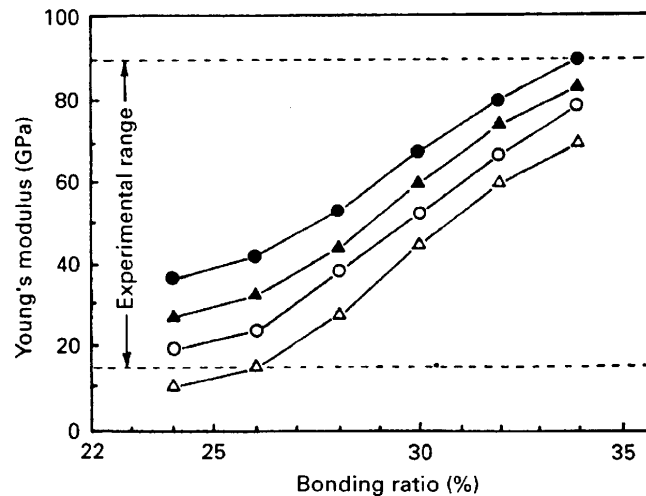


Clyne et al., Acta Metal., 2008

Effect of Substrate Temperature

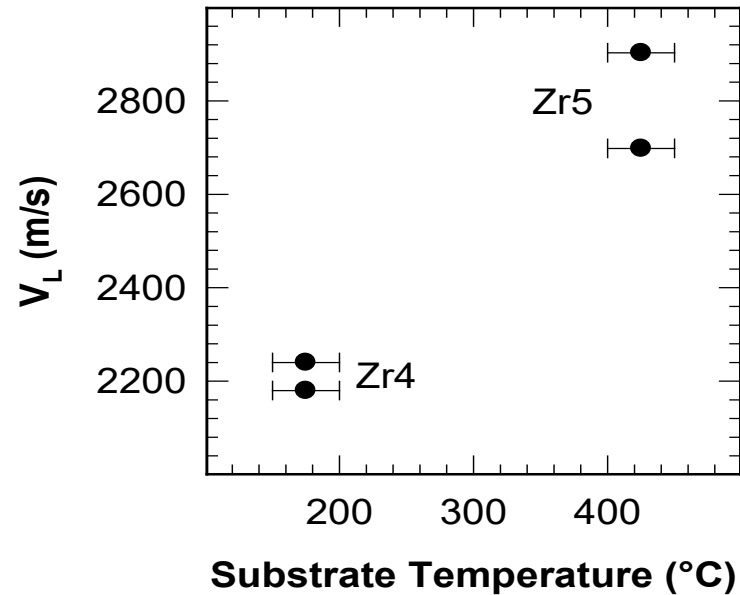


after Fukomoto *et al.*, Proc. Int. Thermal Spray Conf., Kobe, 1995, p.353-8

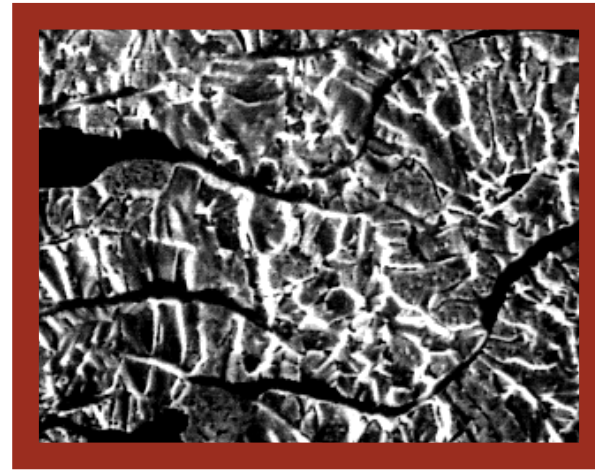
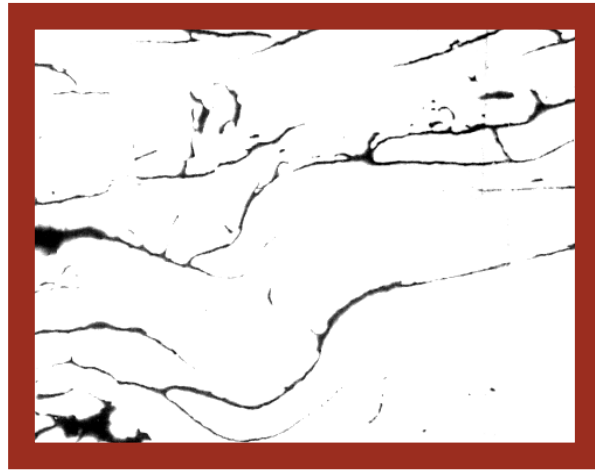


after C.J. Li *et al.*, J. Mat. Science 32 (1997) 997

$$Velocity = \sqrt{\frac{Elastic\ modulus}{Density}}$$



W Coating Structure – Cu infiltrated



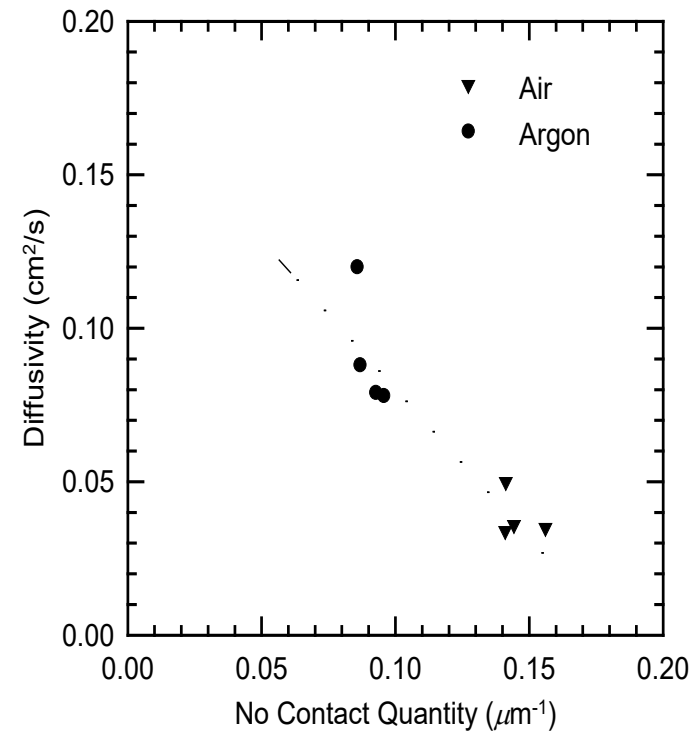
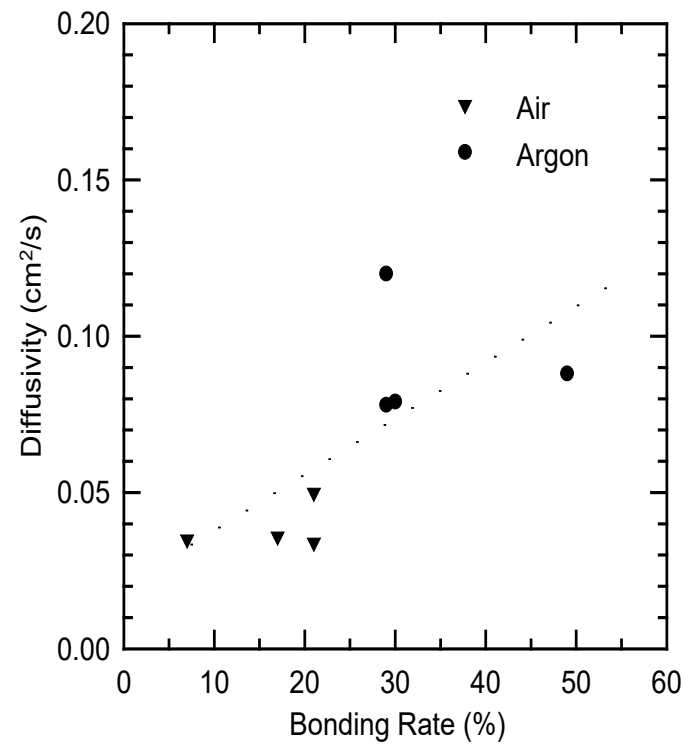
—
20 μm

Polished

Etched

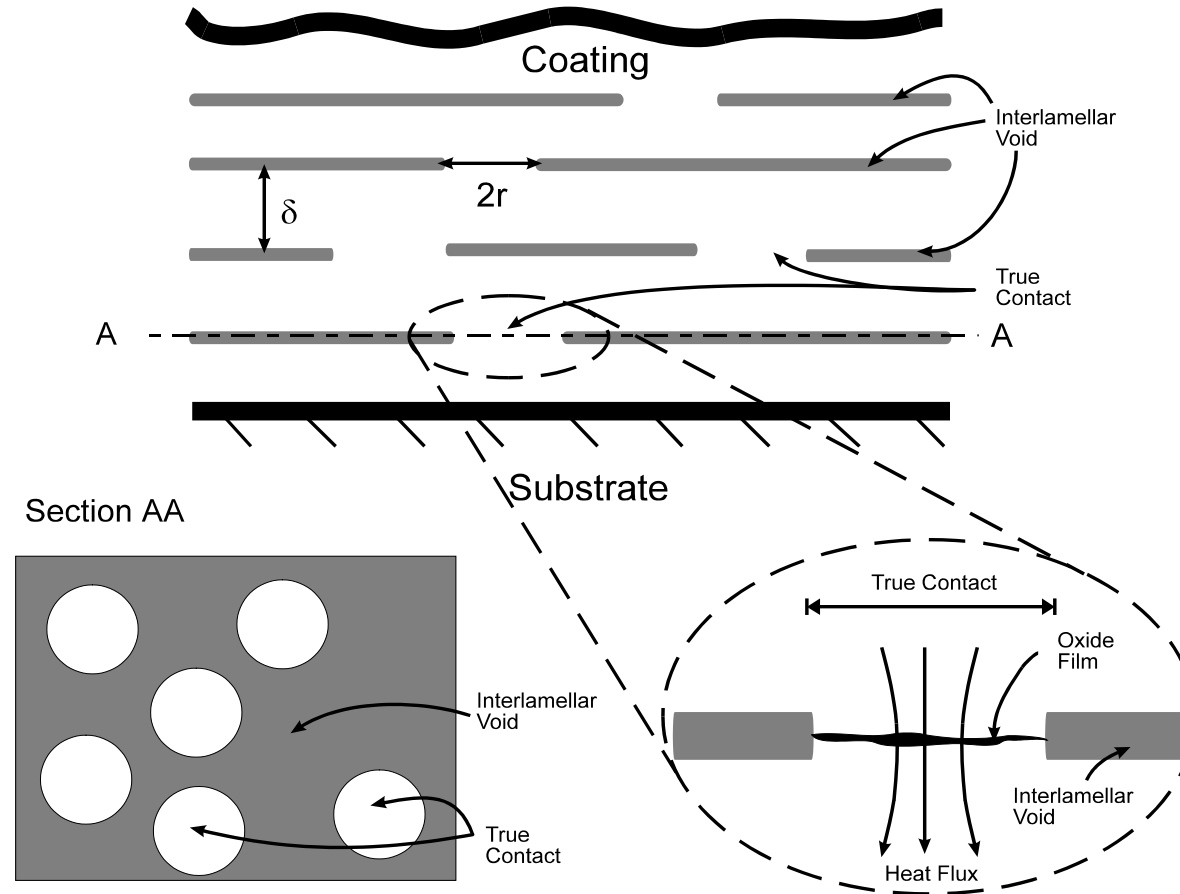
S. Boire-Lavigne et al., *J Therm. Spray Technol.*,
4 (1995) 261-267

Thermal Conductivity of W Coatings



S. Boire-Lavigne et al., *J Therm. Spray Technol.*,
4 (1995) 261-267

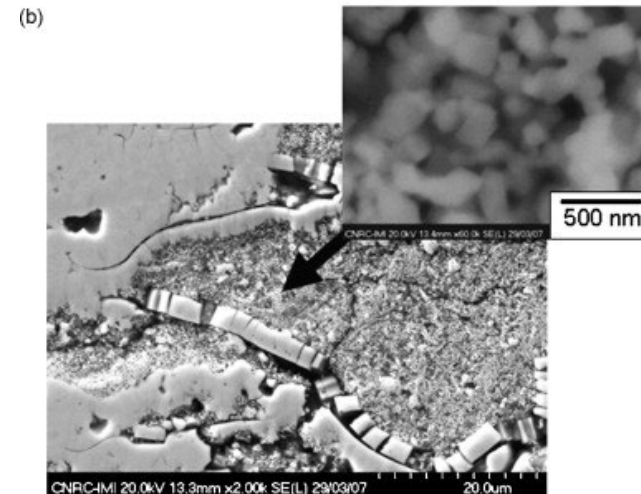
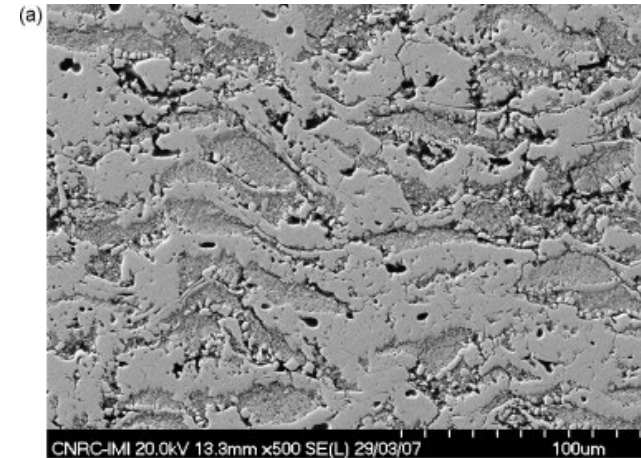
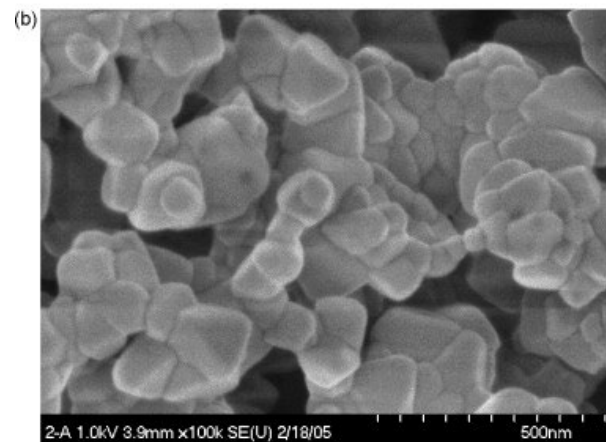
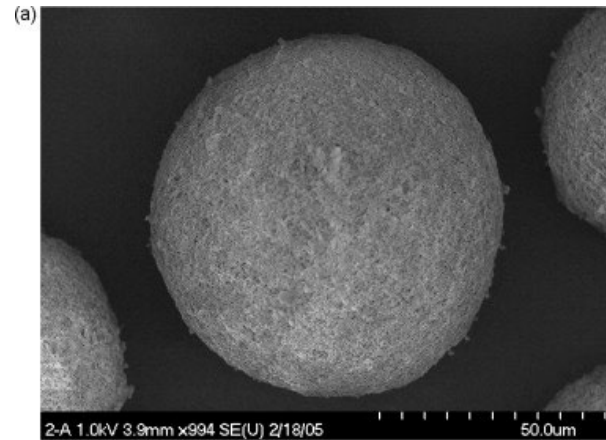
Lamellar Structure



S. Boire-Lavigne et al., J Therm. Spray Technol.,
4 (1995) 261-267

Nanostructured YSZ TBCs

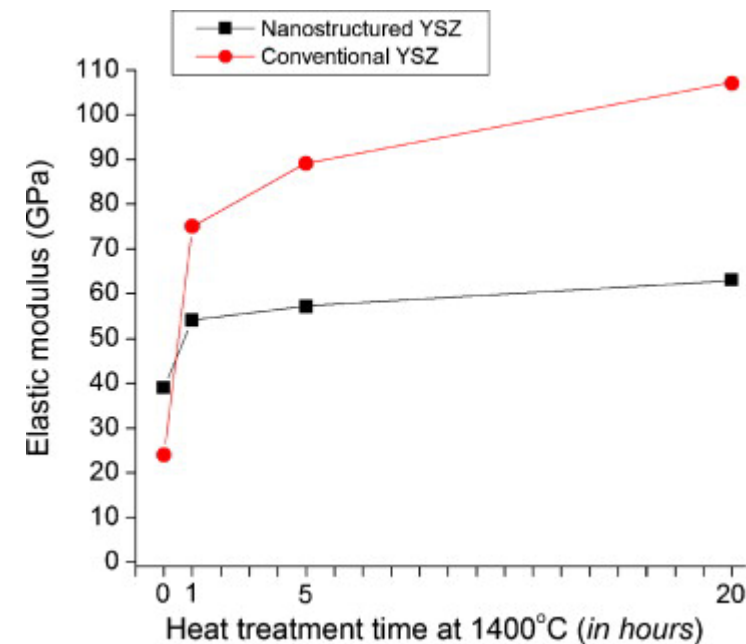
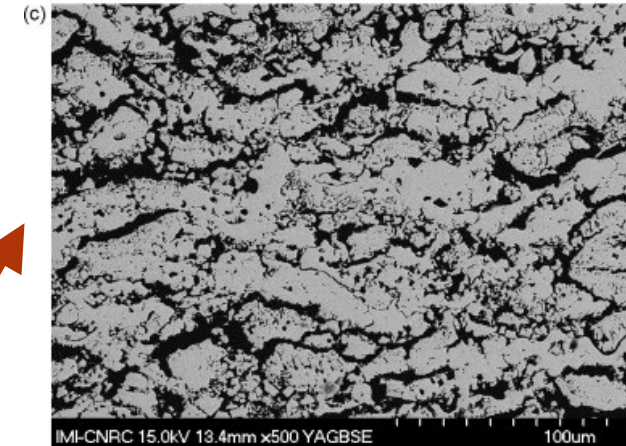
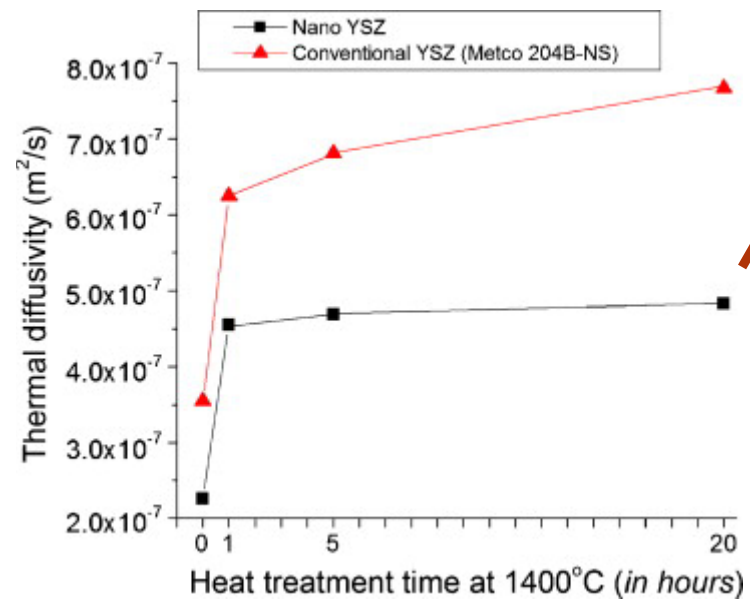
- Nanostructured porous powders and coatings



R. Lima and B. Marple, *Mat. Sci. & Eng. A*, 485 (2008) p. 182-193

Nanostructured YSZ TBCs

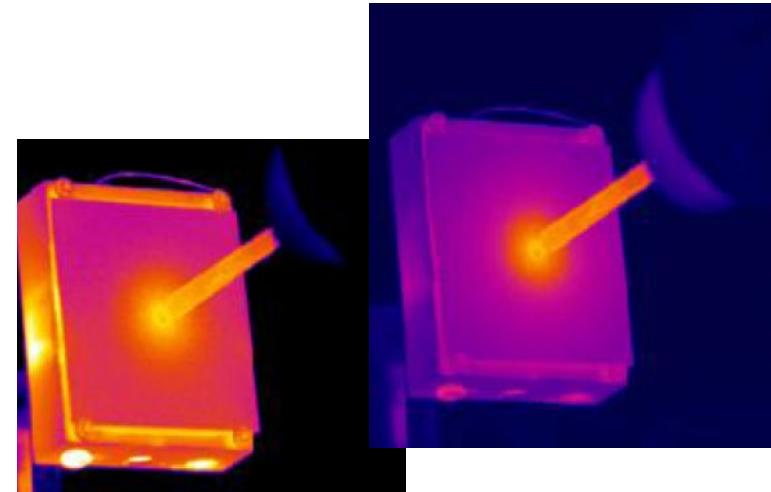
- Lower thermal diffusivity
- Lower elastic modulus



R. Lima and B. Marple, *Mat. Sci. & Eng. A*, 485 (2008) p. 182-193

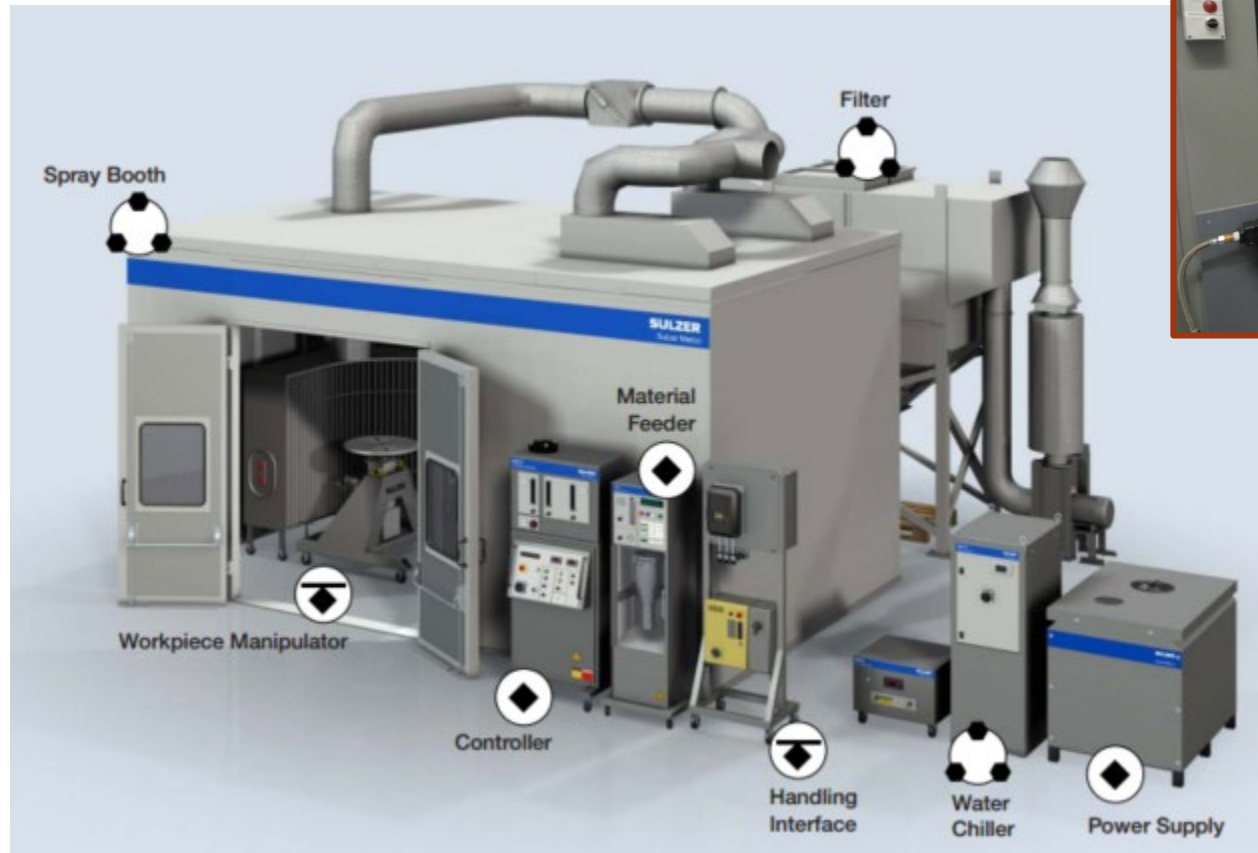
Substrate and Coating Temperature

- Influence on:
 - interface quality between lamellae
 - residual stresses
 - crack formation
 - thermal conductivity
 - elastic modulus, etc.
- Measuring techniques:
 - one- or two-color pyrometer
 - infrared camera



Images courtesy of NRC Canada

Spray Booth



Oerlikon Metco : <http://www.oerlikon.com/metco/en/products-services/coating-equipment/thermal-spray/systems/plasma/>

Safety Consideration

- Safety issues:
 - Noise
 - UV light
 - Dust and fumes
 - Heat
 - Robot
 - Electrical shocks

Measures:

- Adequate thermal spray booth design
- Personal protection
- Adequate gas and fuel handling infrastructure
- Adequate operation practices

More at: <http://tss.asminternational.org/portal/site/tss/SafetyGuidelines/>

Suspension Thermal Spraying

- Fine droplets formed by injection of submicron powders (STS) in the flame
- Cooling rates exceeding 10 million °C/sec → formation of nanograins

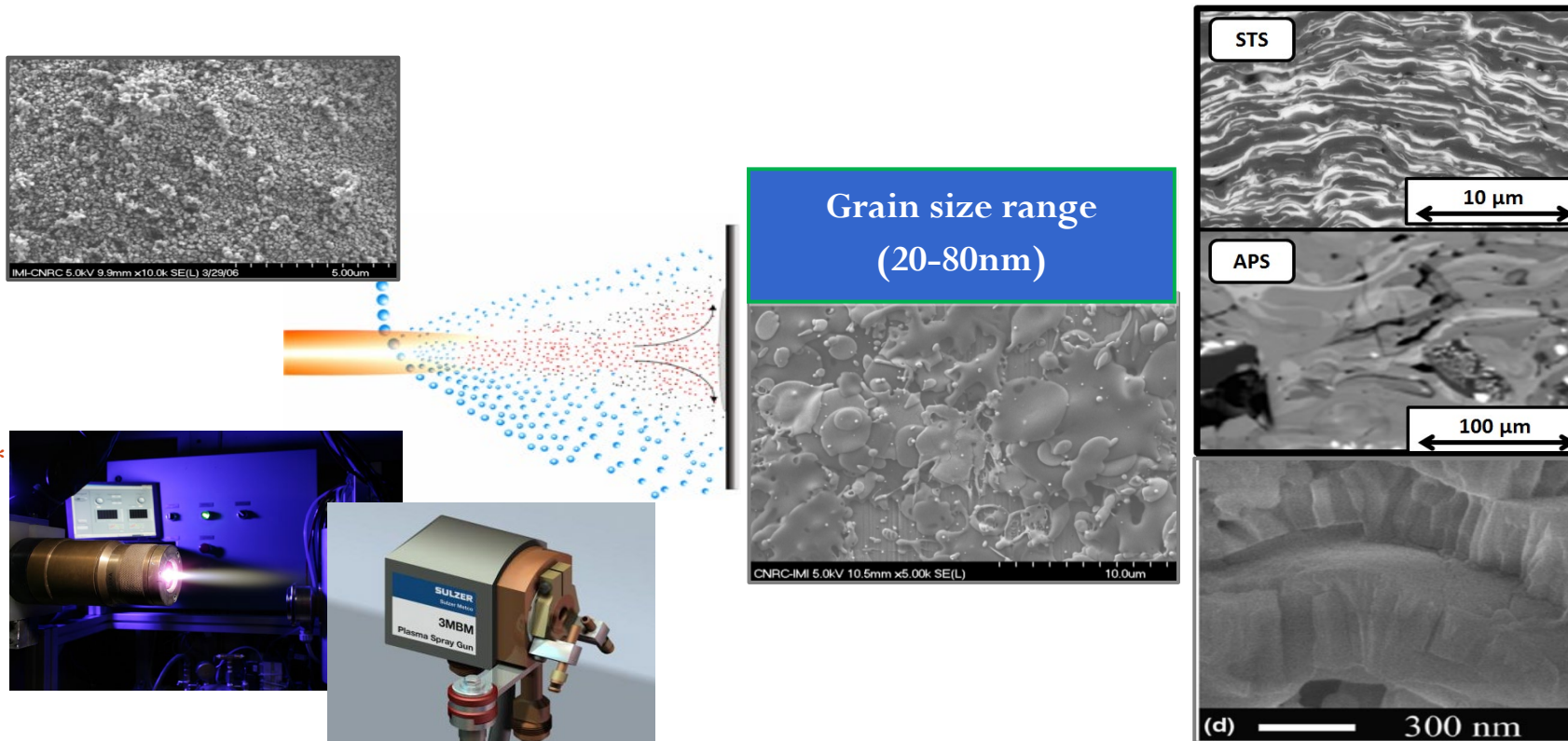
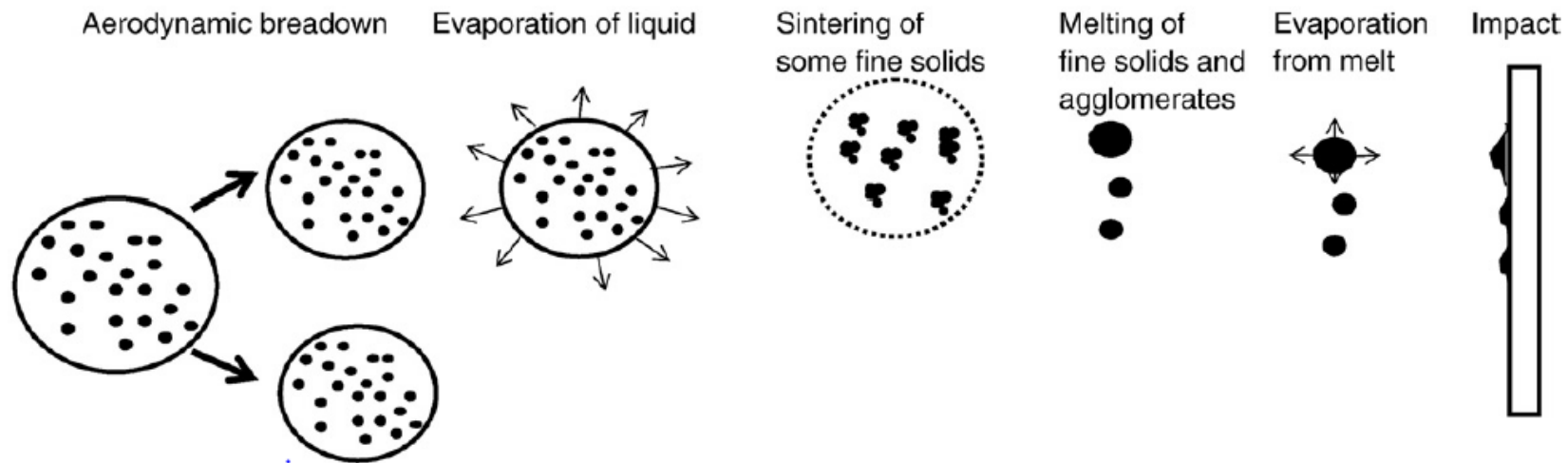


*Image courtesy of NRC Canada

VanEvery et al., JTST, Vol. 20 (2011) p. 817

Suspension/Jet Interaction

- Complex phenomena occur sequentially:
- Primary and secondary atomization
- Liquid evaporation
- Sintering and melting of the spray material

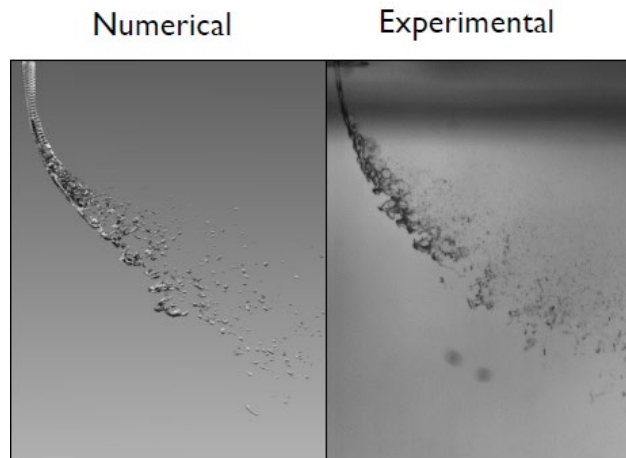


L. Pawlowski, *Surface and Coating Technol.* 203 (2009) 2807-2829

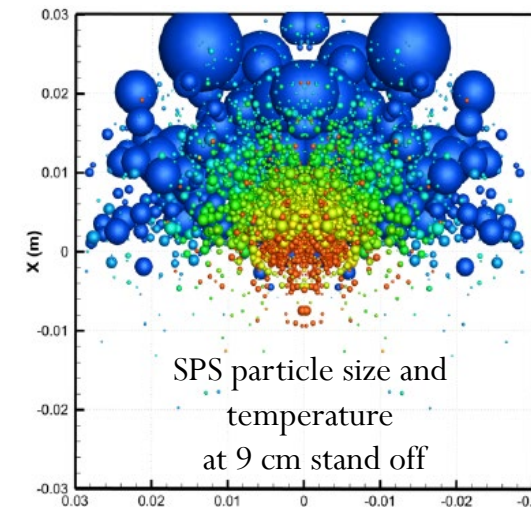
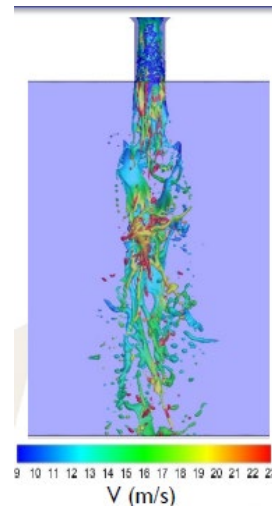
Modelling and Simulation

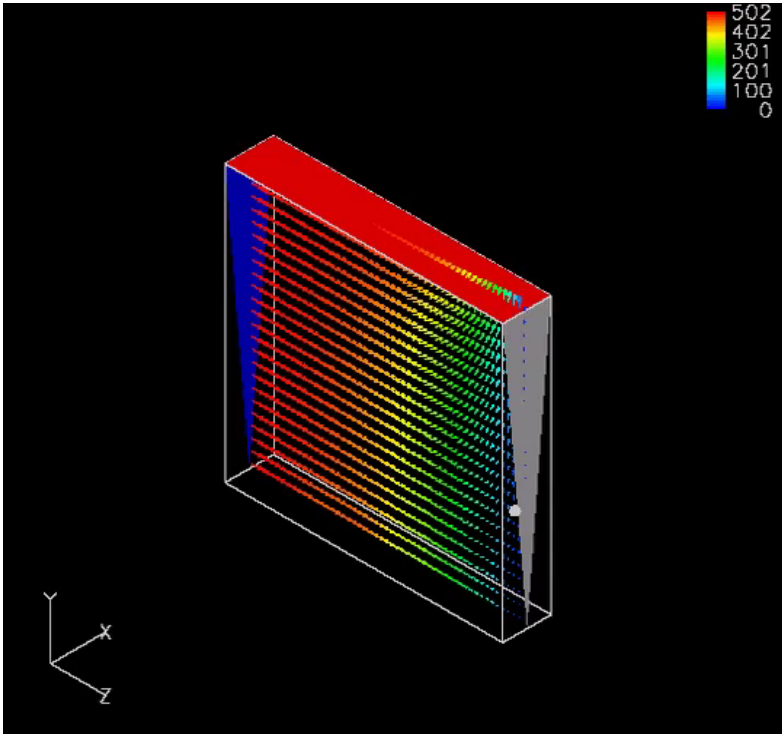
- Atomization behaviour of multiphase fluids containing nanoparticles. Nanoparticle/ fluid thermal interaction
- Determination of in-flight particle characteristics by numerical modelling
- Multiscale modeling of nanomaterials properties

Liquid jet in cross flow



Modeling of an effervescent atomizer

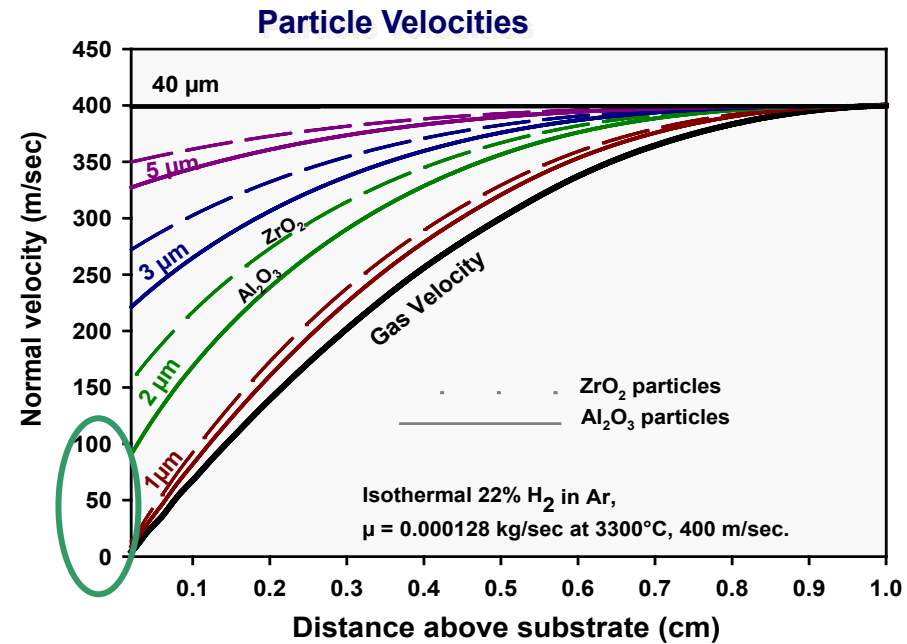




Gas Flow Simulation with CFD 2000
Adaptive Research®

Reduced Particle Impact Velocity

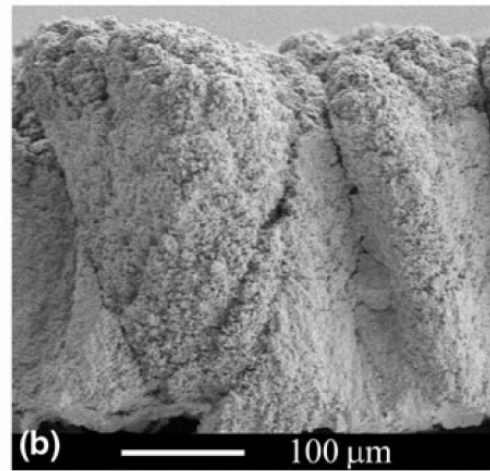
- Critical to control the microstructure



- Highly sensitive to particle size and material density
- Higher free stream velocities can dramatically increase the impact velocity of small particles

Coating Build-up

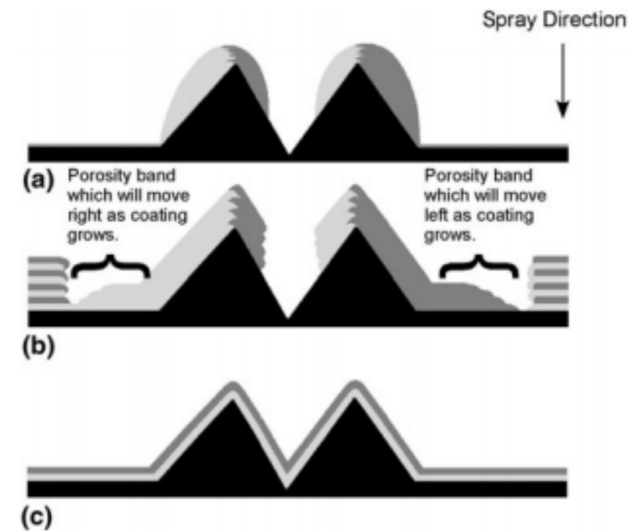
- STS typical microstructure formation depends strongly on the particle velocity at impact:
 - Normal direction
 - Parallel direction



Deflection of the particle trajectory depends on the Stokes number St :

$$St = \frac{\rho_p d_p^2 v_p}{\mu_g l_{BL}}$$

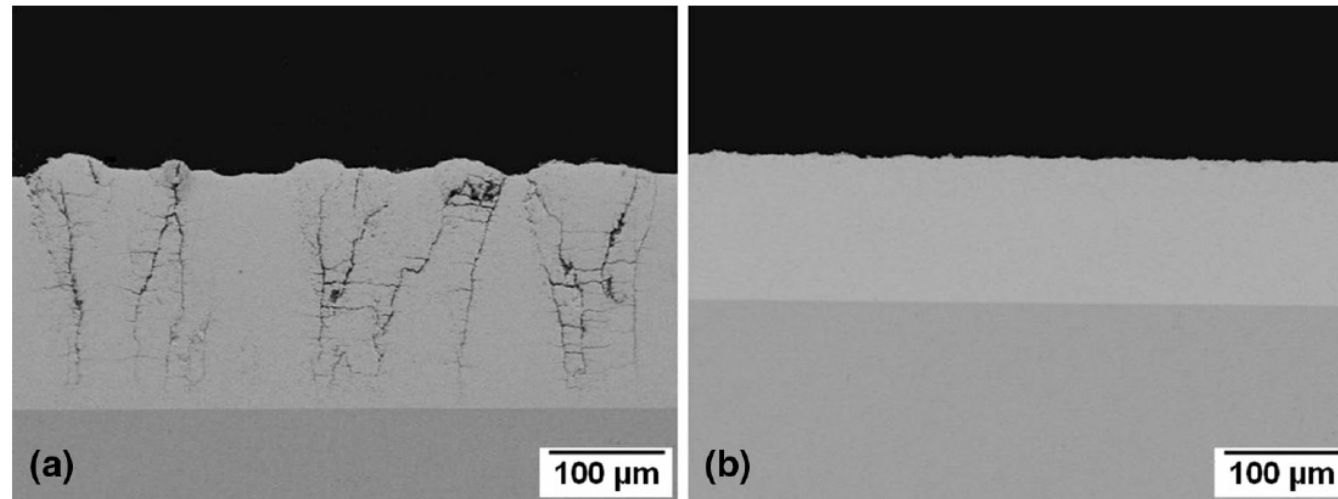
P. Fauchais, et al., JTST, 17 (2008) 31-59



K. VanEvery, et al., JTST, 20 (2011) 817-828

Controlling SPS Coating Structure

- A designed cooling system allows:
- driving out the low-velocity particles before their impact onto the substrate
- maintaining the nominal temperature of the substrate by playing on the cooling gas flow rate

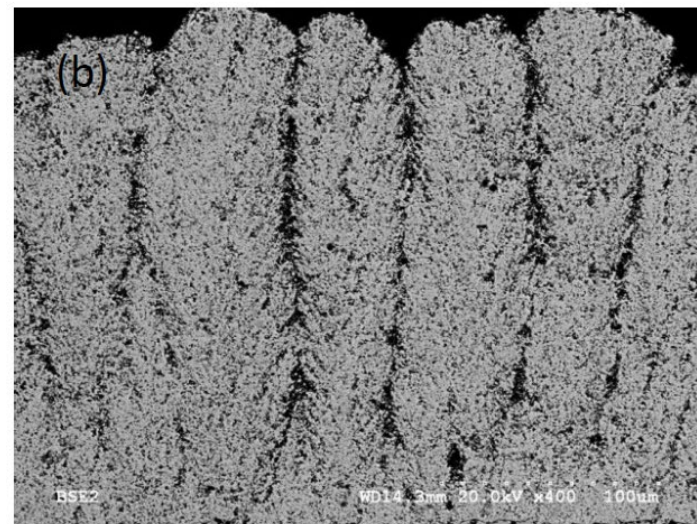
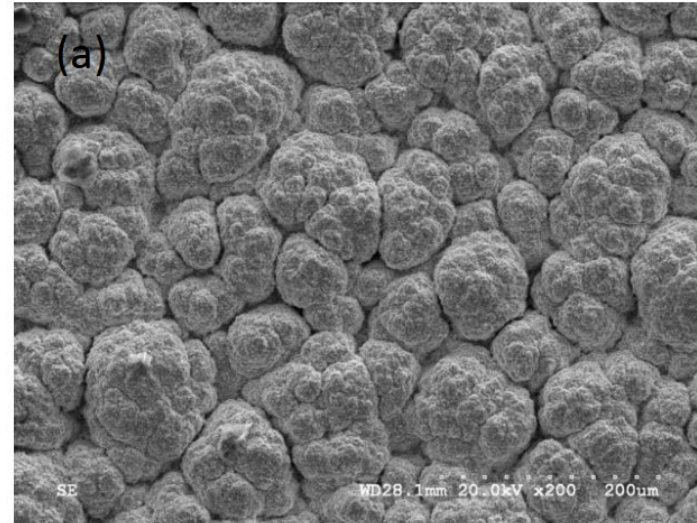


A. Joulia, et al., Published online 8 Nov. 2014

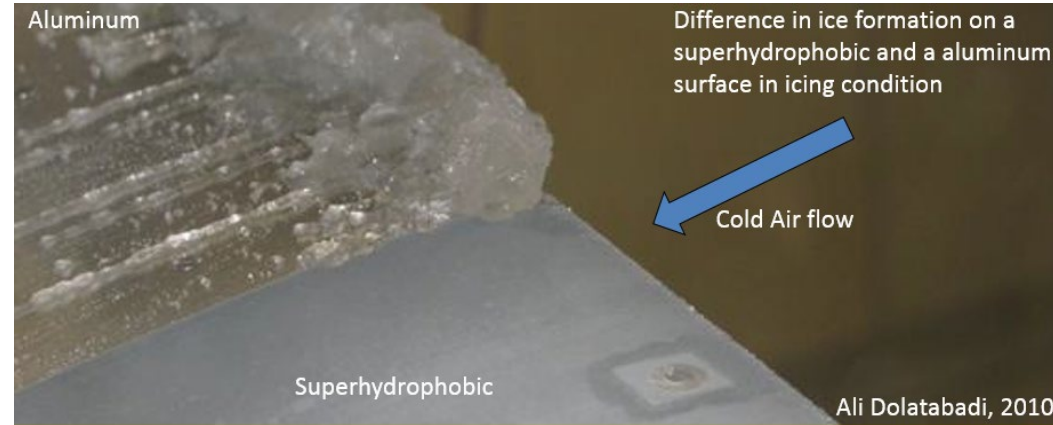
Suspension Plasma Spraying for Thermal Barrier Coatings (TBCs)

- Promising coating process:
 - SPS coating structures comparable with EB-PVD coatings
 - Important potential cost savings

- After Z. Tang, H. Kim, I. Yaroslavski, G. Masindo, Z. Celler and D. Ellsworth, « **Novel Thermal Barrier Coatings Produced by Axial Suspension Plasma Spray** », ITSC 2011, Hamburg, Germany

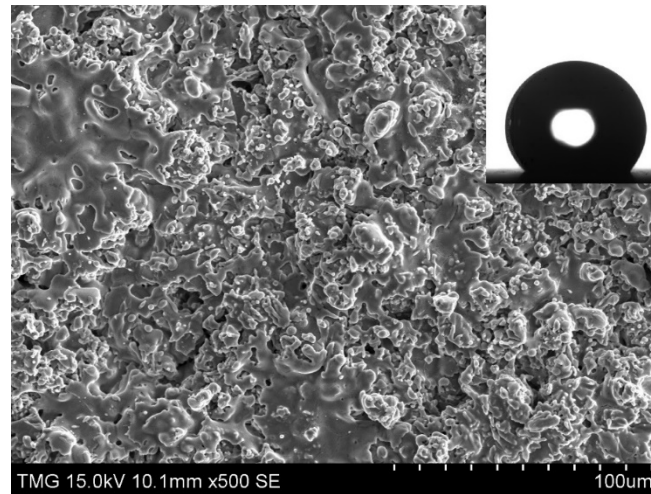


Superhydrophobic Coatings for Reduction of Ice Accumulation

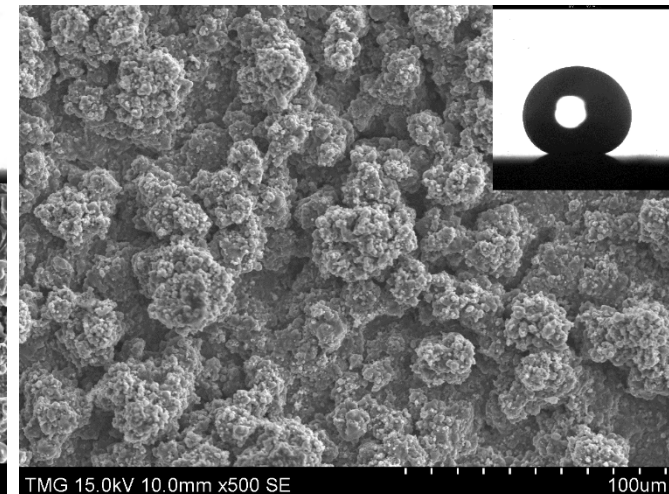


- APS and SPS TiO₂ coatings treated with stearic acid solution

APS Contact angle $\approx 145^\circ$



SPS Contact angle $\approx 167^\circ$



Combustion Processes

Combustion Temperature

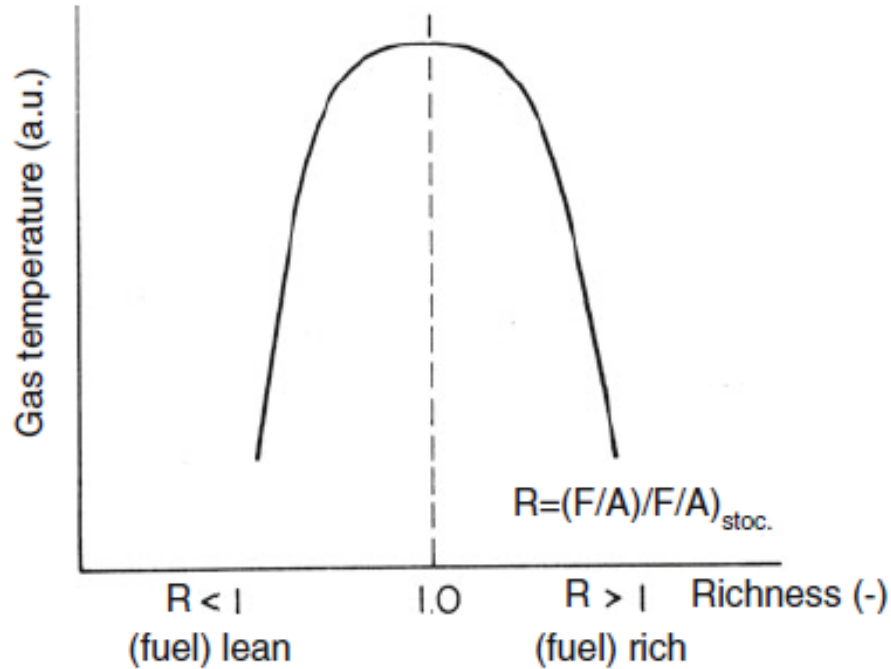


Fig. 3.1 Variation of combustion temperature with richness ratio [1], reprinted with the kind permission of Elsevier

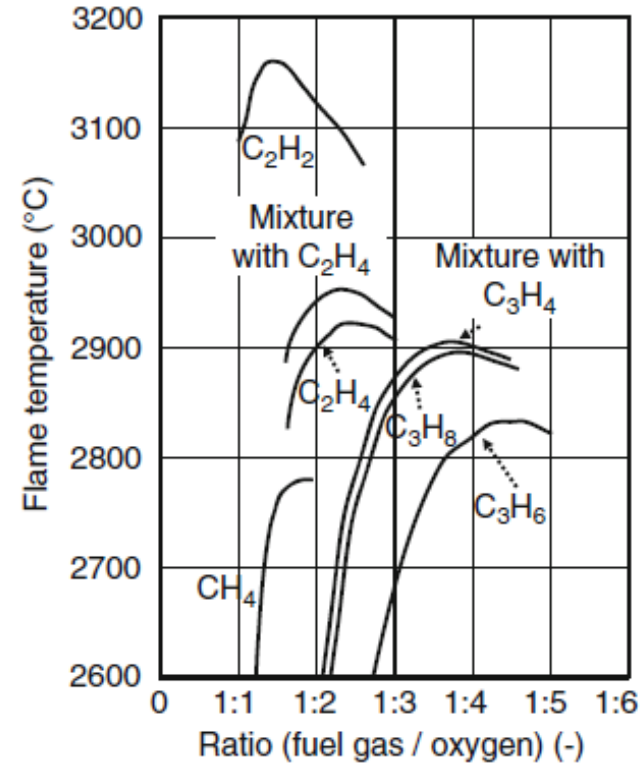


Fig. 3.2 Flame temperatures as function of the fuel/oxygen ratio for different mixtures fuel/oxygen by volumes (m³/m³) and for different hydrocarbon fuel gases [2], reprinted with the kind permission of Linde Co

Combustion with Air and Oxygen

Table 3.1 Approximate flame temperatures of various stoichiometric mixtures (initial temperature 298 K, atmospheric pressure) [1], reprinted with the kind permission of Elsevier

Fuel	Flame temperature (K)	
	Air as oxidizer	Oxygen as oxidizer
Acetylene	2,600 ^a	3,410 ^b
Carbon monoxide	2,400	3,220
Heptane	2,290	3,100
Hydrogen	2,400	3,080
Methane	2,210	3,030

^aThis maximum exists at $R' = 1.3$

^bThis maximum exists at $R' = 1.7$

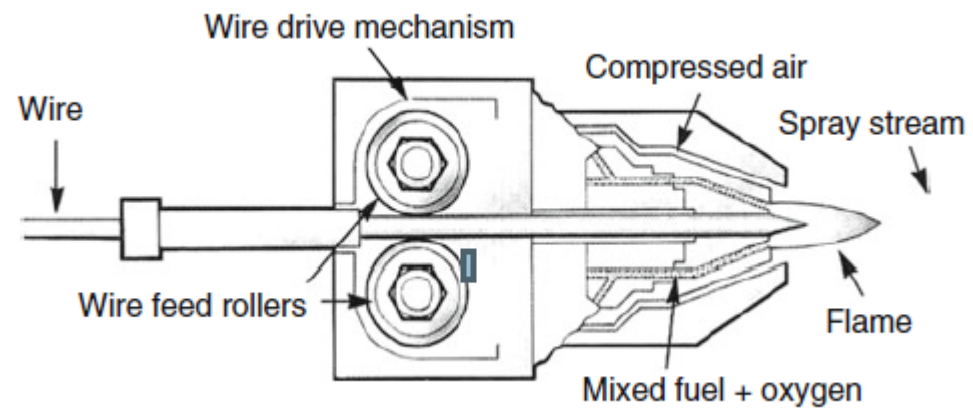
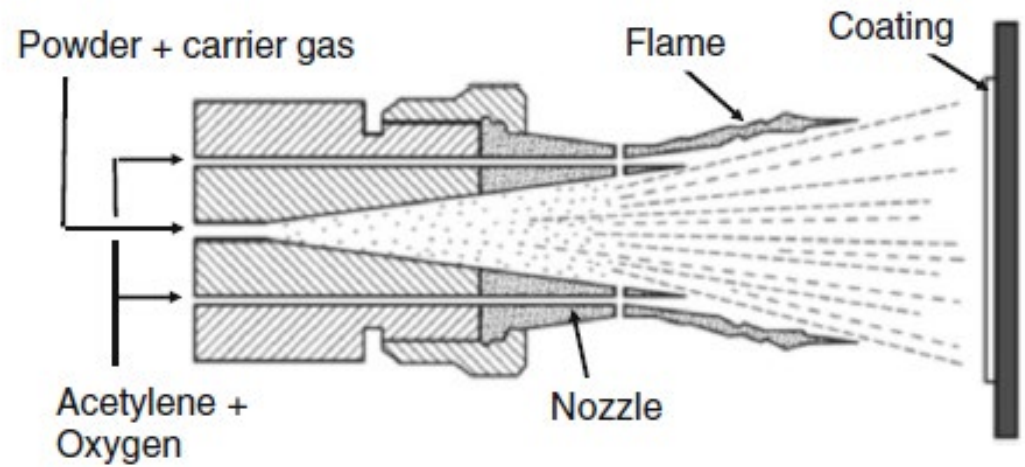
Combustion: Spray Processes History

Table 5.1 Major dates related to the development of the major thermal spray processes

Year	Process	Energy generation	Inventor(s)	References
1909	Flame spraying (FS)	Combustion (diffusive)	Schoop (Switzerland)	[1]
1955	Detonation gun spraying (D-Gun)	Combustion (detonation)	Gfeller and Baiker ^a (USA)	[2]
1983	Supersonic flame spraying (HVOF)	Combustion (deflagration)	Browning (USA)	[3]

^aUnion Carbide, today Praxair Surface Technology (USA)

Flame Spray: Powder and Wire

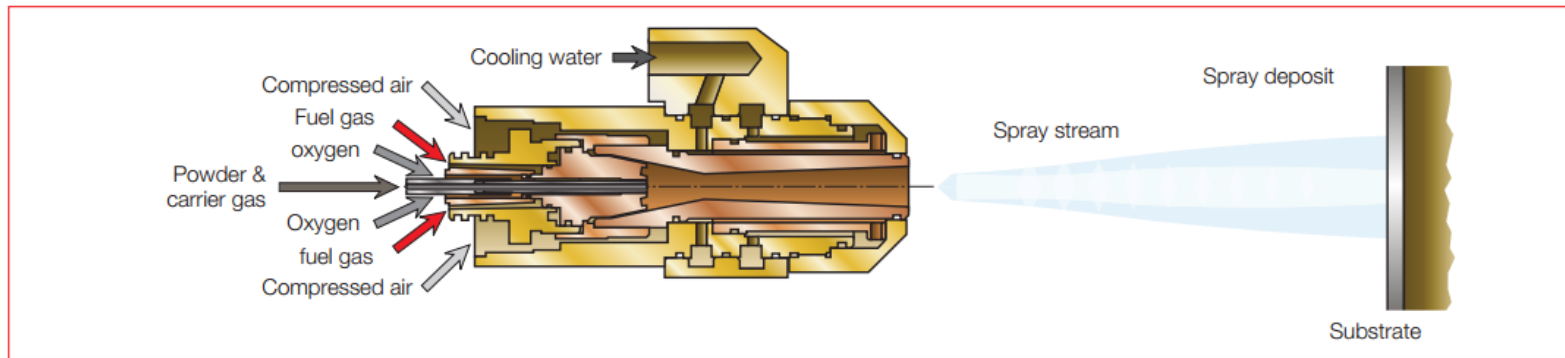


Flame Spaying

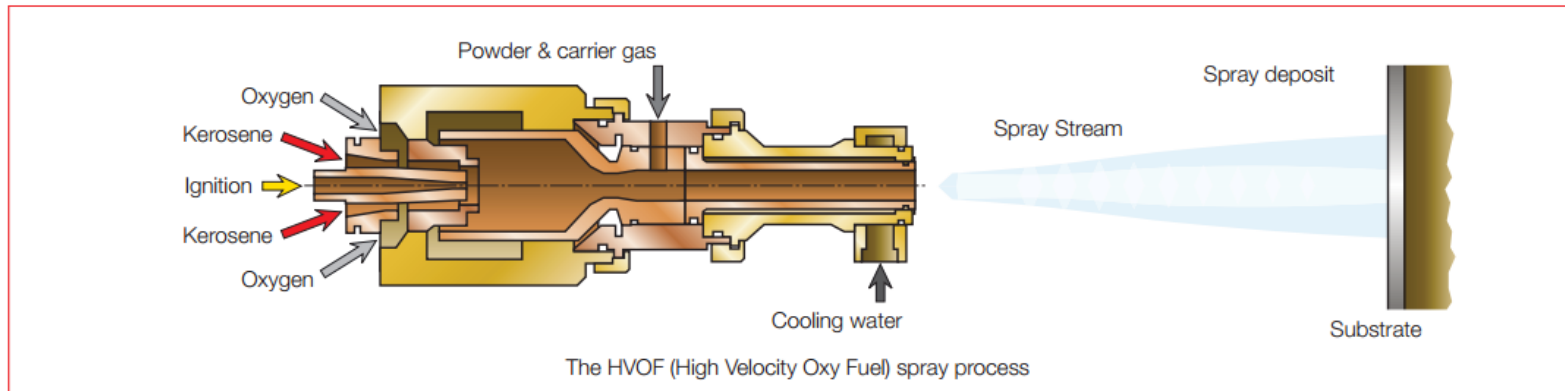
- Particle characteristics
 - temperature $\sim 300\text{-}3000^\circ\text{C}$
 - speed $\sim 30\text{-}50\text{ m/s}$
- Materials - polymers, metals and ceramics
 - spray rate $\sim 2\text{ to }3\text{ kg/hour}$
- Coating characteristics
 - density $\sim 5\text{ to }15\%$ porosity

HVOF: Gas and Liquid Fueled

Gas-fuel HVOF gun



Liquid fuel HVOF gun



High Velocity Oxy-Fuel (HVOF) Solutions, Oerlikon Metco:

http://www.oerlikon.com/ecomaXL/files/metco/oerlikon_HVOFSolutions_EN6.pdf&download=1

HVOF: Gas and Liquid Fueled

Comparison	Gas fuel HVOF	Liquid fuel HVOF
Gun	Water-cooled Diamond Jet Gun	WokaJet™-410-Si Gun
General characteristics		
Fuel options	H ₂ , CH ₄ , C ₂ H ₄ , C ₃ H ₆ , C ₃ H ₈	Jet-A or Kerosene
Combustion pressure	~ 0.55 MPa (80 PSI)	0.55 – 0.83 MPa (80 – 120 PSI)
Gas velocity	1800 – 2100 m/s (5900 – 6900 ft/s)	2000 – 2200 m/s (6500 – 7200 ft/s)
Particle velocity	450 – 600 m/s (1475 – 1975 ft/s)	475 – 700 m/s (1550 – 2300 ft/s)
Powder injection	Axial feed (hotter zone)	Radial feed (cooler zone)
Powder injection pressure	Higher	Lower
Spray rate	up to 120 g/min (16 lb/h)	up to 200 g/min (26.5 lb/h)
Consumption comparison (typical utility consumption per hour of operation)		
Fuel	43800 liters (1670 ft ³) H ₂ , or 5280 liters (200 ft ³) C ₃ H ₆ , or 5280 liters (200 ft ³) C ₃ H ₈	28 liters (7.3 gal) kerosene
Oxygen	18420 liters (700 ft ³)	61400 liters (2335 ft ³)
Water	600 liters (160 gal)	2375 liters (625 gal)

High Velocity Oxy-Fuel (HVOF) Solutions, Oerlikon Metco:

http://www.oerlikon.com/ecomaXL/files/metco/oerlikon_HVOFSolutions_EN6.pdf&download=1

HVOF Guns

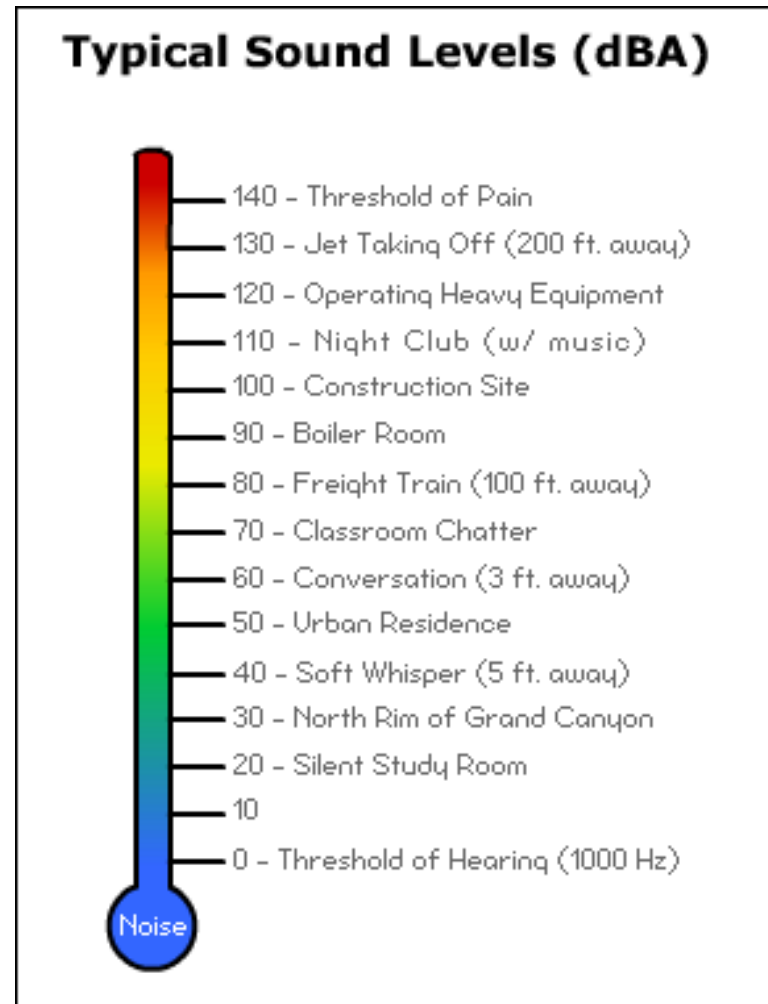


Images courtesy of NRC Canada

Progressive Surface: <https://www.youtube.com/watch?v=BS10TaQK0ss&t=4s>

HVOF: Noise (dB)

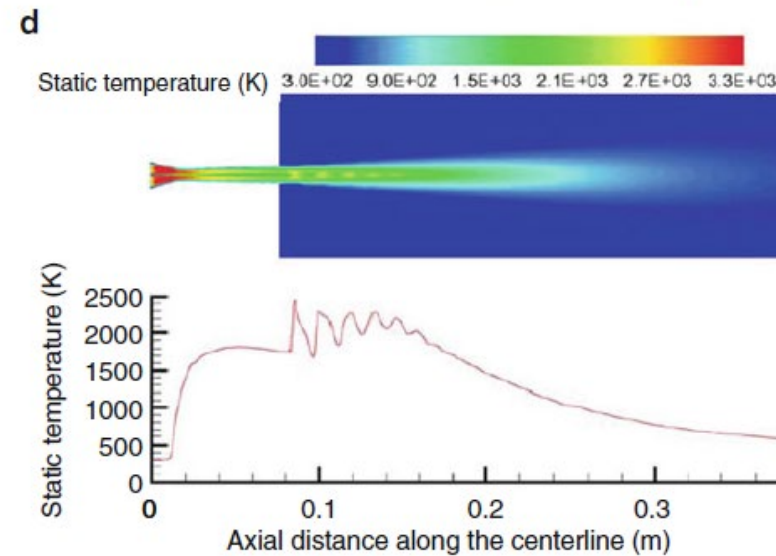
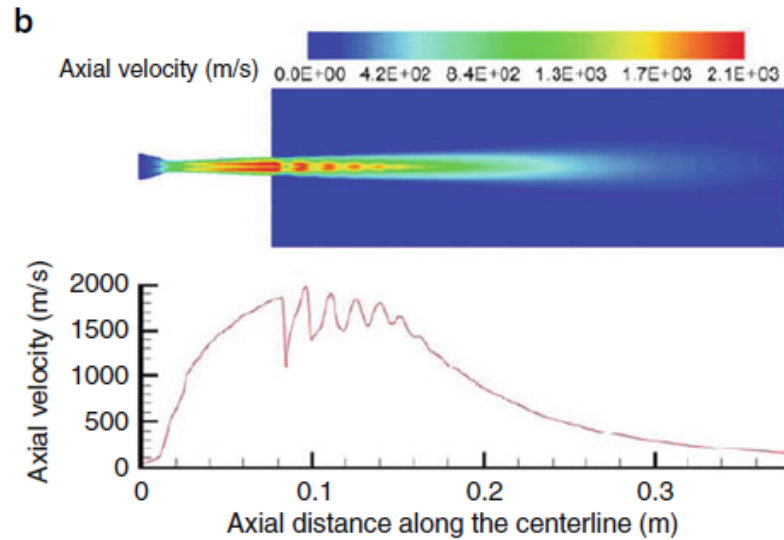
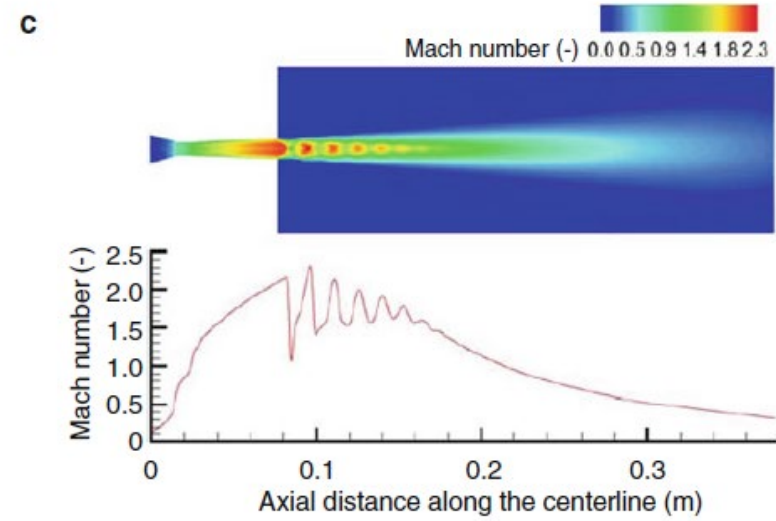
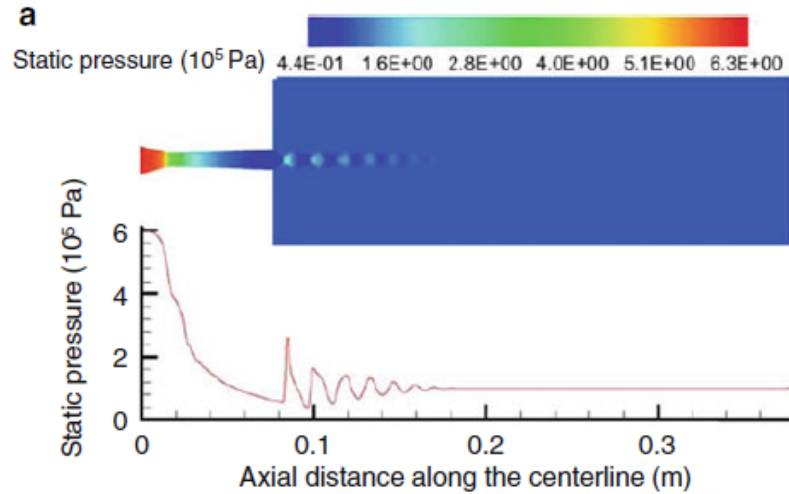
- Can reach 125 dB



Occupational Safety & Health Administration

https://www.osha.gov/dts/osta/otm/new_noise/#decibles

Modeled Gas Characteristics



High Velocity Oxy-Fuel (HVOF)

- Particle characteristics
 - temperature $\sim 1500-3000^{\circ}\text{C}$
 - speed $\sim 300-900\text{ m/s}$
- Materials - metals and cermets
 - deposition efficiency $\sim 45-80\%$
 - spray rate $\sim 1\text{ to }5\text{ kg/hour}$
- Coating characteristics
 - high density ($< 2\%$ porosity)
 - tensile or compressive stress (thick coatings possible)

Residual Stress

- In thermal spray coatings, residual stress results from:
 - Rapid quenching and concomitant shrinkage of the solidified splat during cooling to the deposition temperature (quenching stress; always in tension)
 - Differential thermal contraction stress: when coating and substrate cool together from the deposition temperature to room temperature
 - Volume change due to phase transformation
 - Peening effect

Quenching Stress

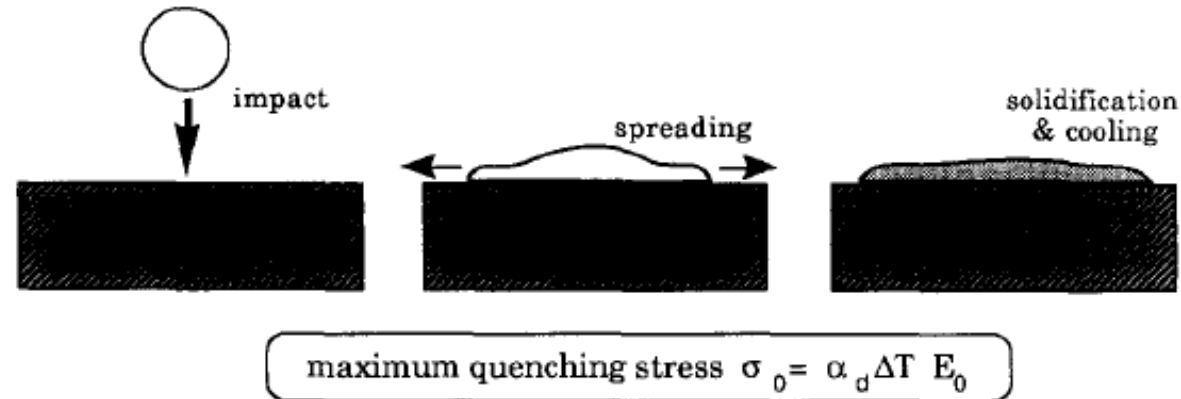


Fig. 1. Schematic depiction of impact, spreading and cooling of a single splat.

TABLE I

COMPARISON OF STRAIN AND STRESS FROM THERMAL CONTRACTION FOR A RANGE OF MATERIALS

<i>Material</i>	α_0 (10^{-6} K^{-1})	E_0 (GPa)	$\alpha_0 \Delta T$ (mstrain for $\Delta T = 100 \text{ K}$)	$\alpha_0 \Delta T E_0$ (MPa)
Molybdenum	4.9	325	0.49	160
Nickel	12.8	200	1.28	255
Aluminium	23	71	2.3	162
Al_2O_3	8	370	0.8	300

After Kuroda and Clyne, Thin Solid Film, 200 (1991) 49-66

Quenching Stress: Relaxation

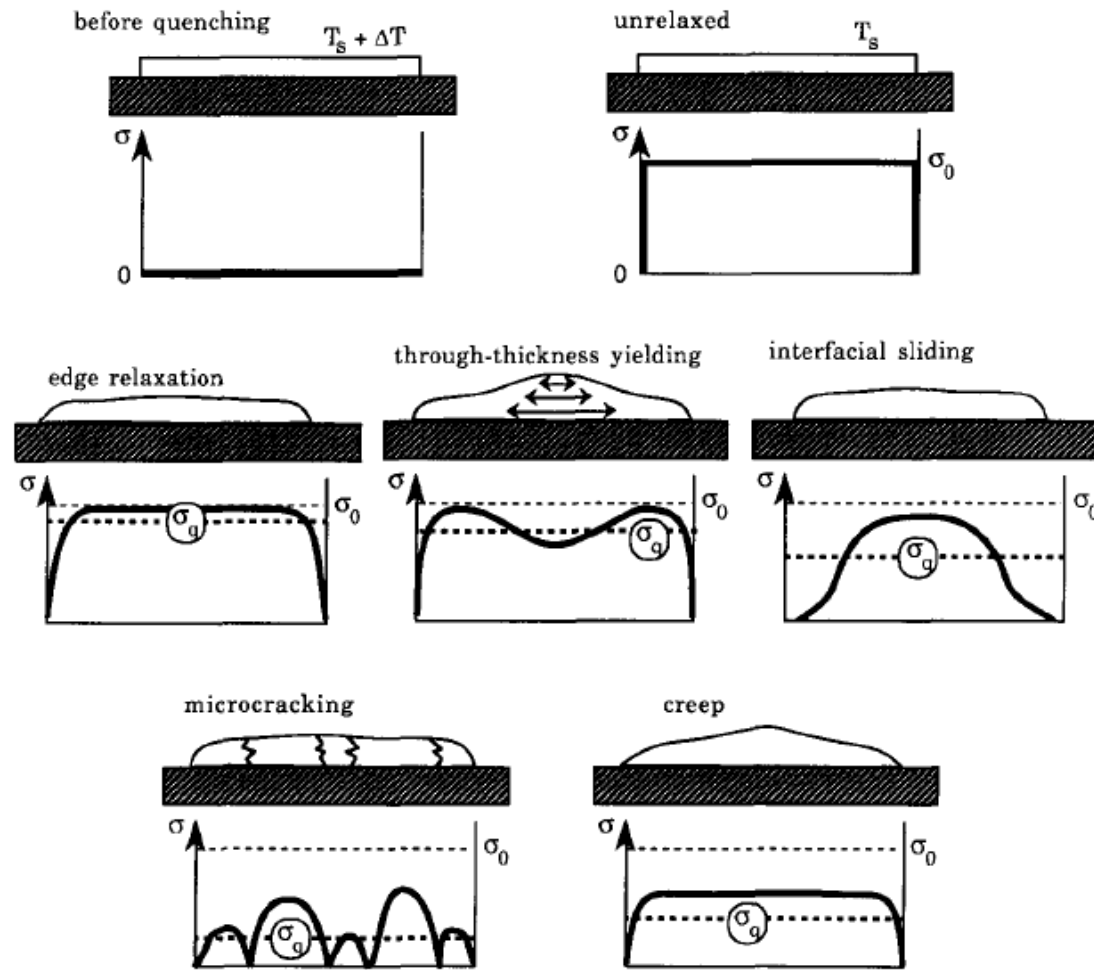


Fig. 2. Schematic illustration of the stress distributions within a single splat before and after various stress relaxation phenomena have taken place.

Residual Stress

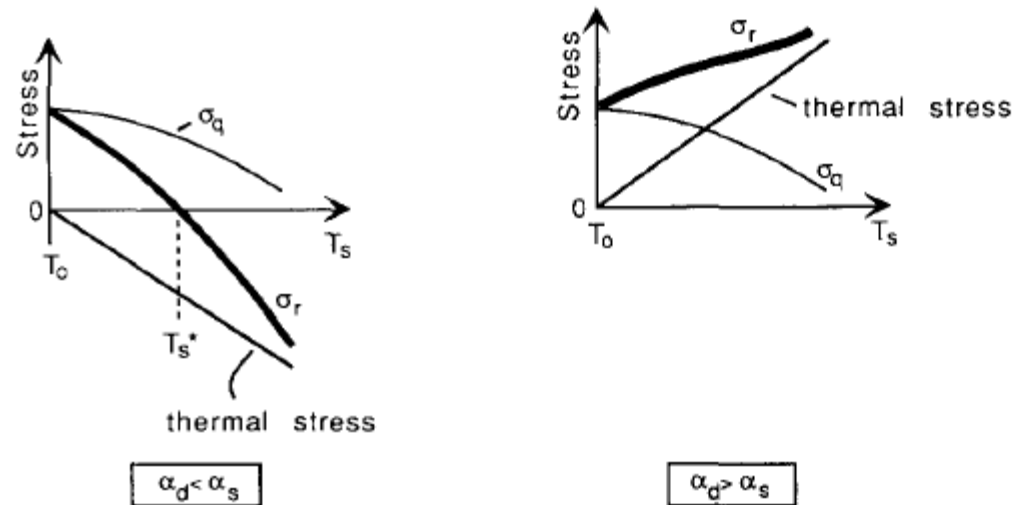


Fig. 3. Schematic diagram of the variation of the final residual stress with substrate temperature T_s during spraying. $\sigma_r(T_0)$ is the final residual stress after the sprayed deposit and the substrate cool down to T_0 .

$$\sigma_r(T_0) = \{ \sigma_q(T_s) / E_d(T_s) + (\alpha_d - \alpha_s)(T_s - T_0) \} E_d(T_0)$$

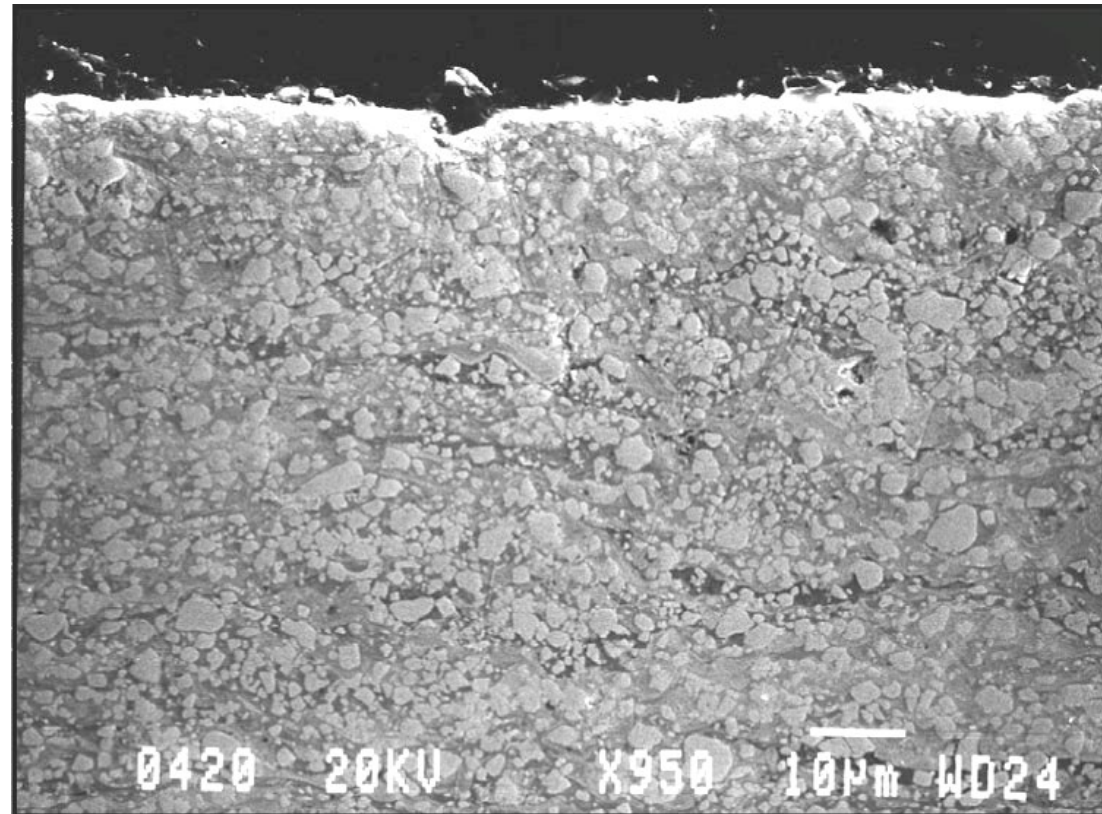
After Kuroda and Clyne, Thin Solid Film, 200 (1991) 49-66

Residual Stress

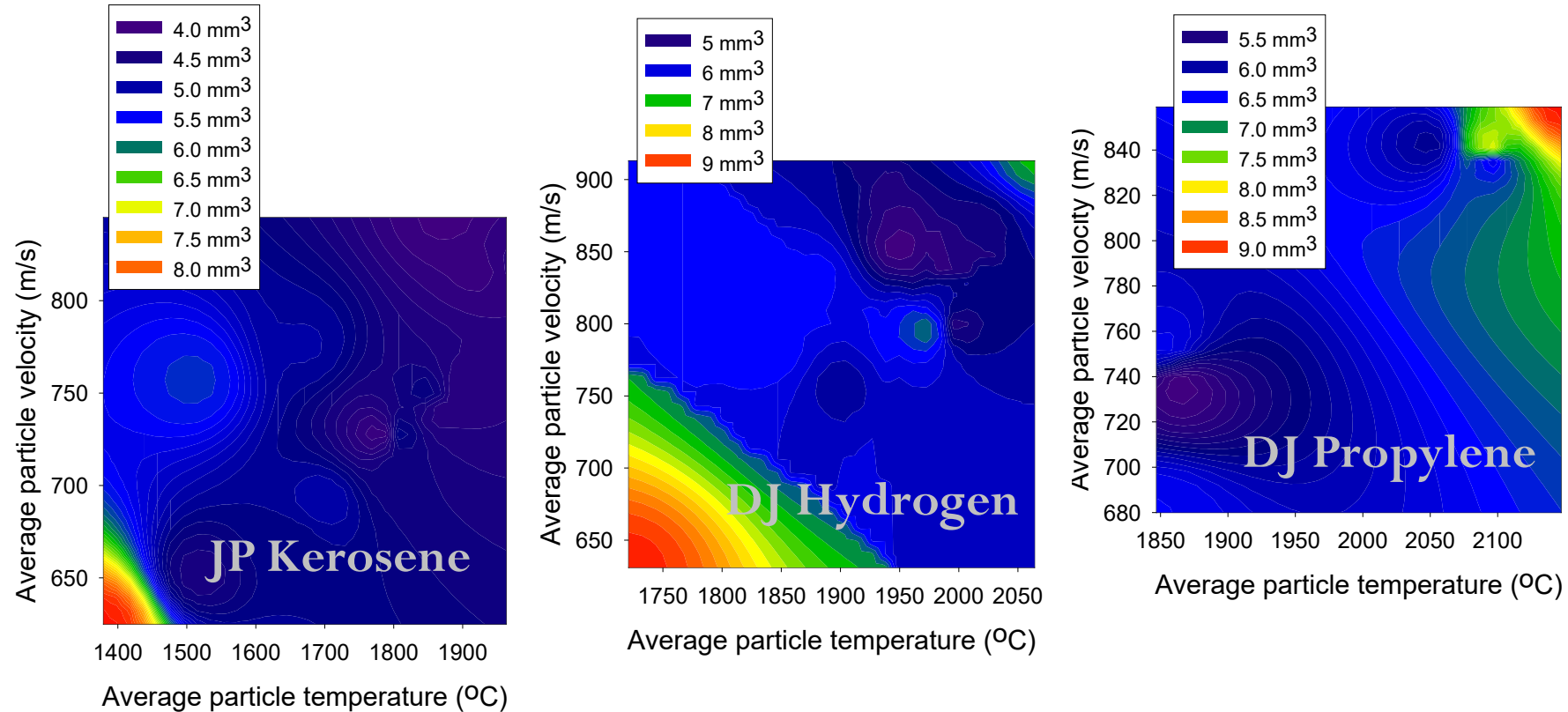
- In HVOF, the peening effect is large due to the high impact velocities of the spray particles
- Resulting residual stresses can be in:
 - Compression (liquid fuel)
 - Neutral (gas fuel)
 - Tension (gas fuel)

HVOF Coating

- Wear-resistant WC-Co coating



Abrasion Maps for WC-CO Coatings

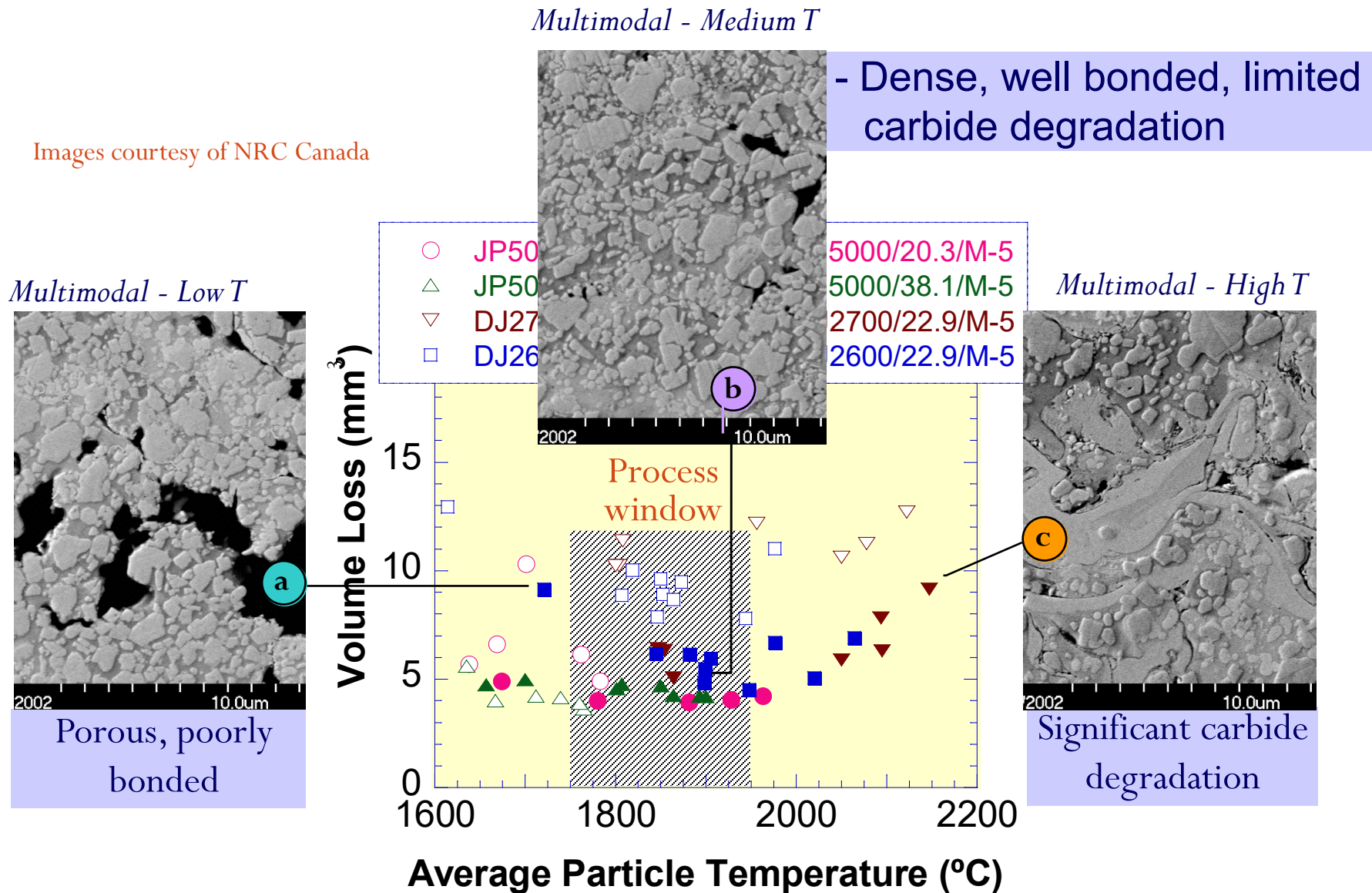


- **Optimum region for coating production:**
 - high abrasion resistance
 - robust parameters (small change in performance for large changes in particle conditions)

Images courtesy of NRC Canada

Process / Wear Map WC-Co

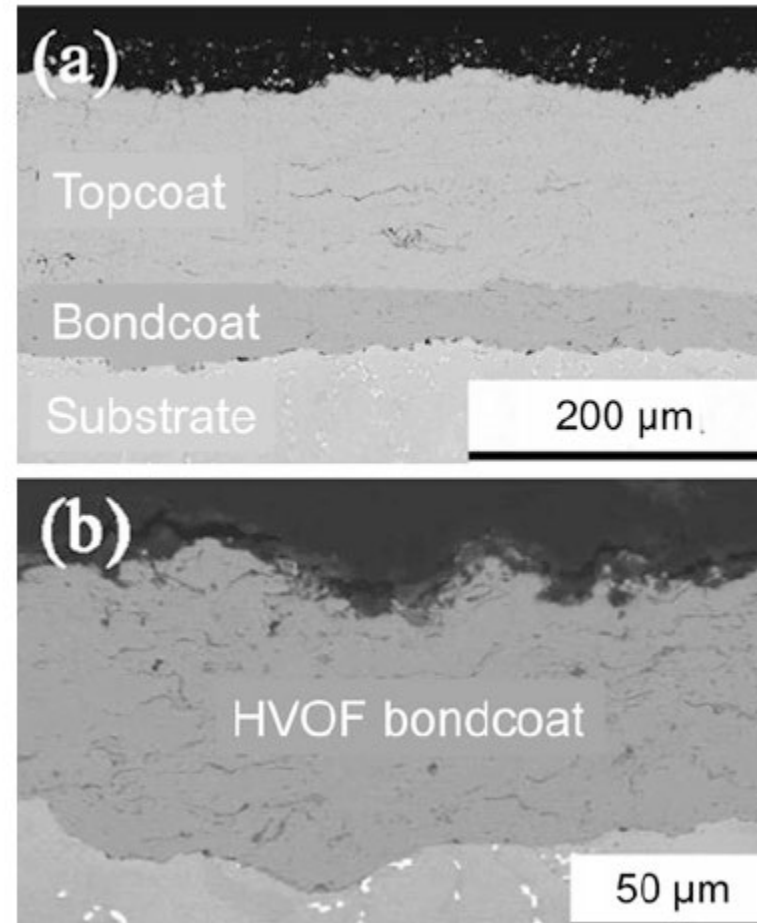
Images courtesy of NRC Canada



HVOF Coatings

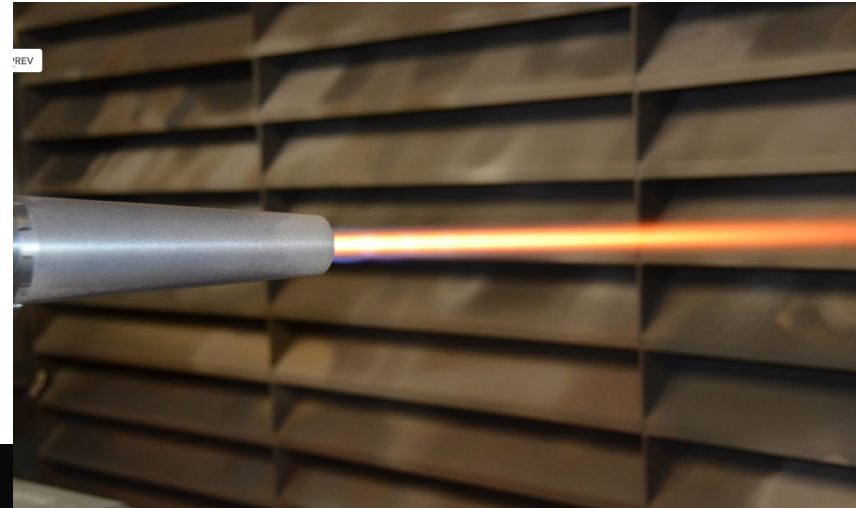
- Metals

Fig. 5.38 (a) Cross section of detonation-sprayed TBC using hollow sphere YSZ powder D-gun sprayed with the HVOF bond coat. (b) Microstructure of the HVOF NiCrAlY coating in the as-sprayed state. Reprinted with kind permission from Elsevier [113]



High Velocity Air-Fuel (HVAF)

- Air is used instead of oxygen
- Many versions developed by Browning

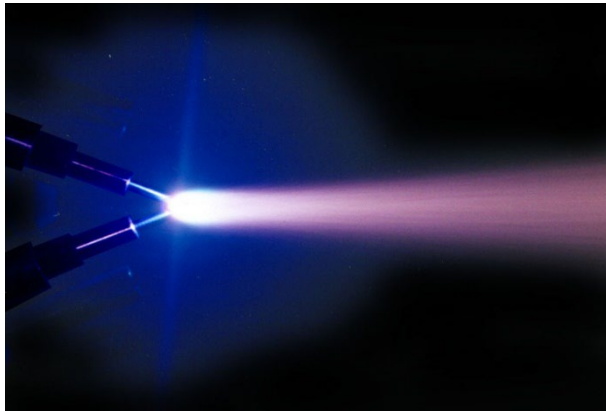
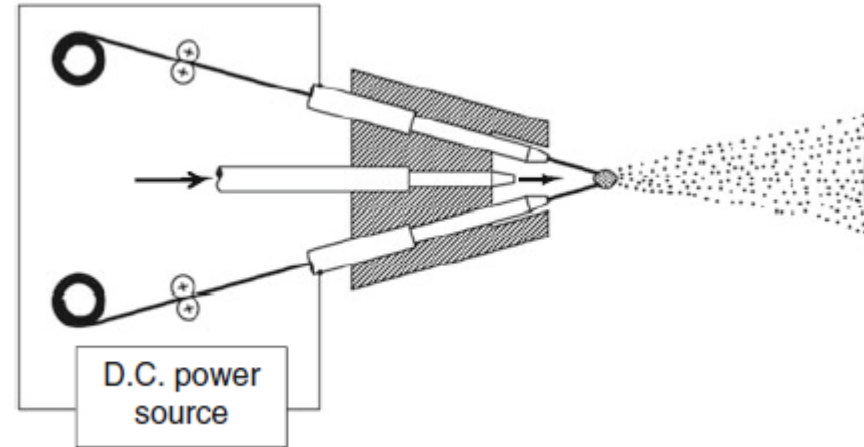


<http://uniquecoat.com/>



Arc Spray

Arc Spray



Courtesy of Praxair - Tafa

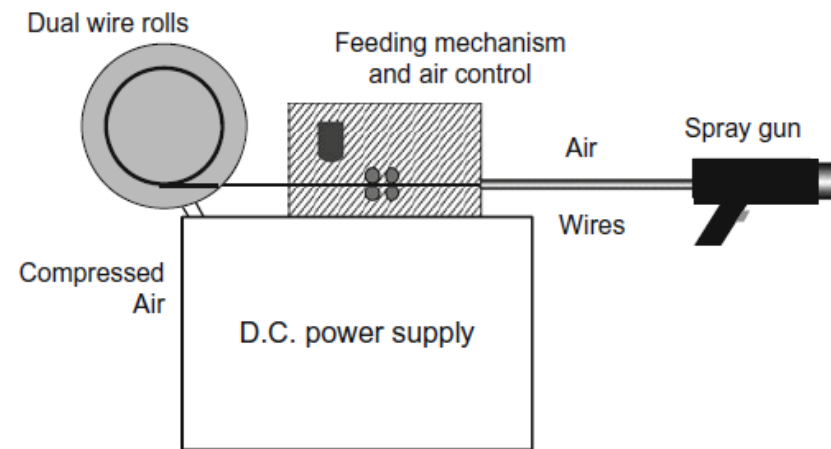


Fig. 9.3 Schematic of wire arc spray system with power supply, control unit, wire supply rolls, compressed gas line, and torch

Atomization Process

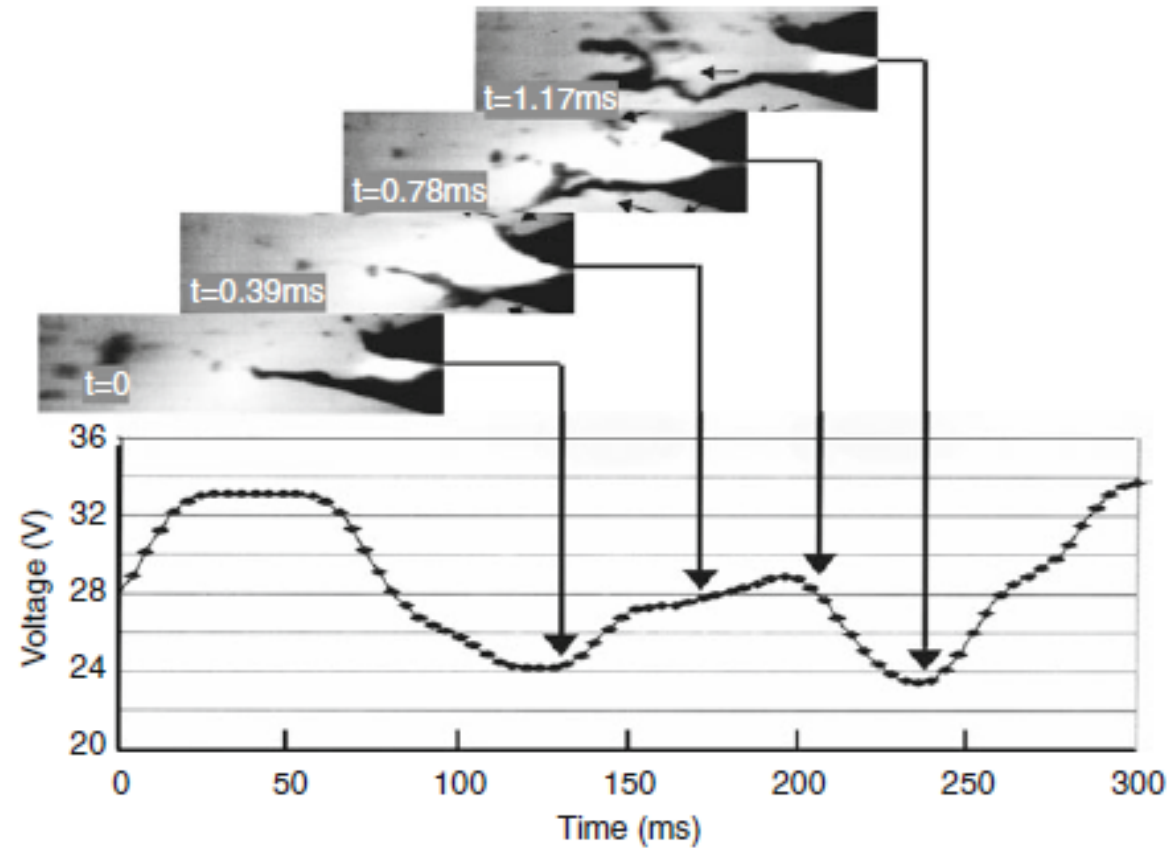
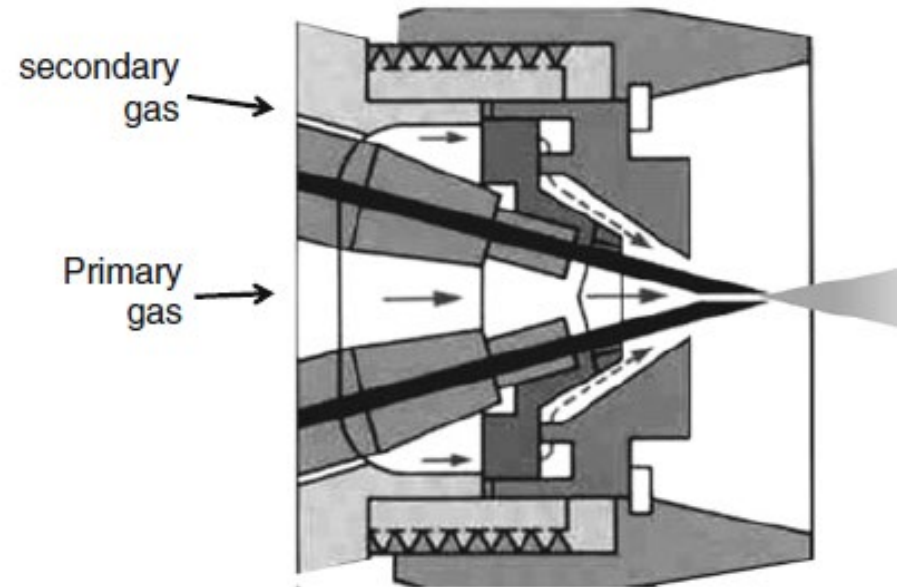


Fig. 9.8 High-speed images of metal droplet formation synchronized with arc voltage trace, showing the forward movement of the anode arc attachment with the associated increase in voltage. Operating parameters: $V = 33$ V, $I = 300$ A, $p = 69$ kPa [40] (Copyright © ASM International. Reprinted with permission)

Primary and Secondary Gas Flows

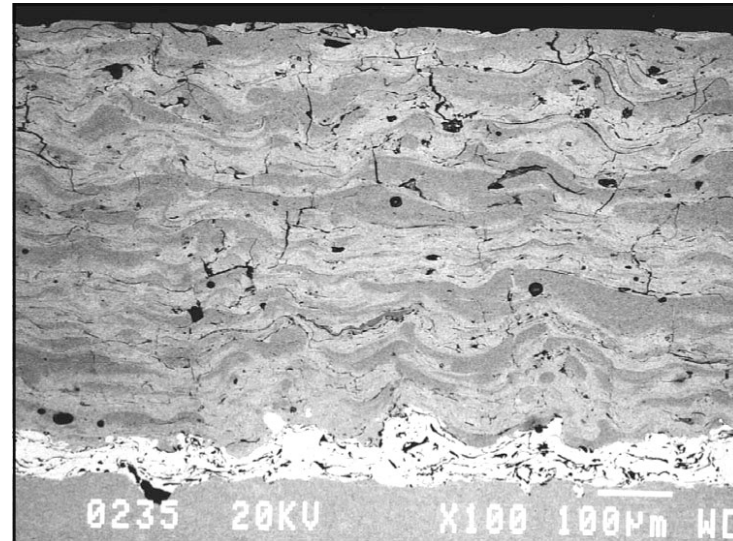
Fig. 9.6 Schematic of wire arc spray head with primary and secondary gas flow (Reproduced with kind permission of Praxair TAFE)



Typical Spray Conditions

- Arc voltage: 20–40 V
- Arc current: 100–400 A
- Wire feed speed: 7–10 m/min
- Standoff distance: 10–20 cm
- Gases: Air, nitrogen, CO₂
- Gas flow rates: 800–2,400 slm
- Gas supply pressure: 0.27–0.6 MPa

Arc Spray



Arc Spraying

- Particle characteristics
 - temperature $\sim 1500\text{-}3000^\circ\text{C}$
 - speed $\sim 50\text{-}200\text{ m/s}$
- Materials - metals and cermets
 - spray rate $\sim 5\text{ to }50\text{ kg/hour}$
- Coating characteristics
 - density $\sim 5\text{ to }20\%$ porosity
 - Relatively high oxide content
 - Low cost

Wire for Arc Spray

- Metals, alloys and cored wires
- Examples from Praxair:

<https://www.praxairsurfacetechologies.com/en/materials-and-equipment/materials/wires>

Pure metal and metal alloy wires

- » Nickel-based wires
- » Iron-based wires
- » Aluminum-based wires
- » Copper-based wires
- » Zinc-based wires
- » Specialty wires, such as titanium, molybdenum, and indium

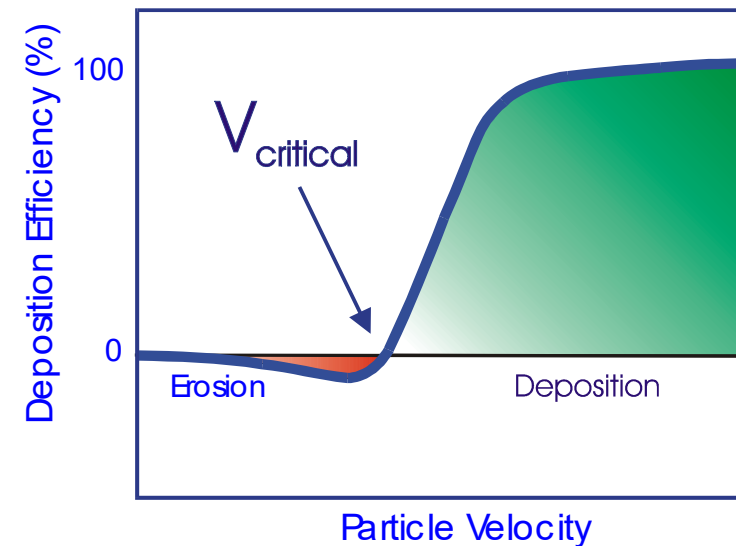
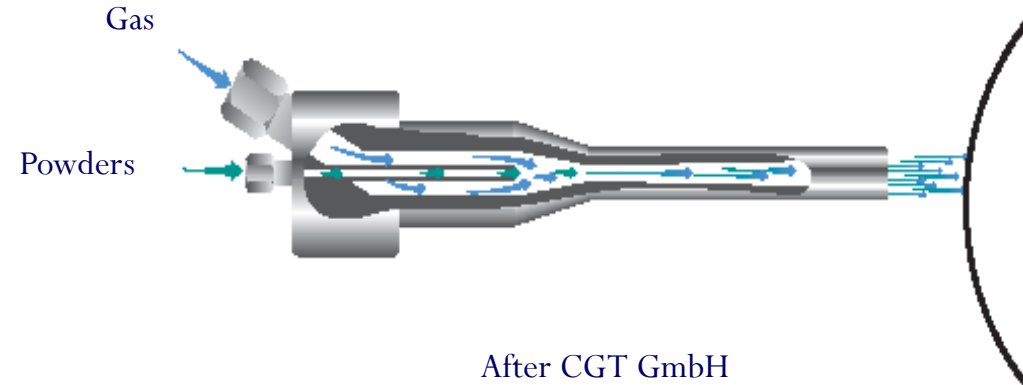
Cored wires

- » Nickel-based cored wires
- » Iron-based cored wires
- » Cobalt-based cored wires
- » Tungsten-cored wires
- » Nano-composite cored wires

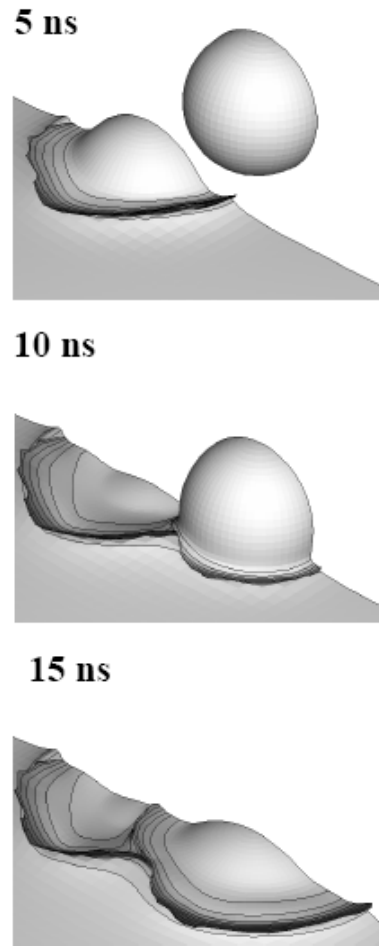
Cold Spray

Cold Spray: A Solid State Deposition Process

- A high-velocity low-temperature gas jet accelerates particles
- The impact velocity is high enough for “cold welding” the particles forming a coating
- Main advantages:
 - Very low oxidation
 - No grain growth or phase transformation

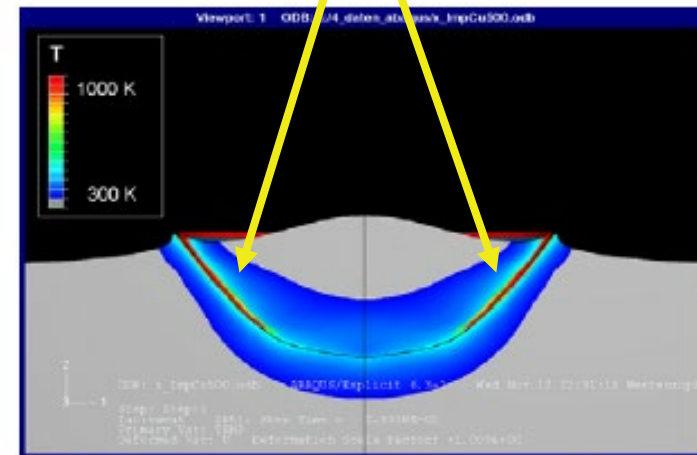


Impact Deformation and Welding



F. Gärtner, *et al.*

Adiabatic shear instability



Tobias Schmidt et al

Operation Parameter

Stagnation jet pressure, MPa (psi)	1–4 (145–600)
Stagnation jet temperature, °C (°F)	0–1000 (32–1832)
Gas flow rate, m ³ /min (ft ³ /min)	1–2 (35–70)
Powder feed rate, kg/h (lb/h)	2–8 (4–18)
Spray distance, mm (in.)	10–50 (0.4–2)
Power consumption, kW (for heating gas)	5–25
Particle size, μm	1–50

After ASM Handbook 5A p. 55

Cold Spray Deposition

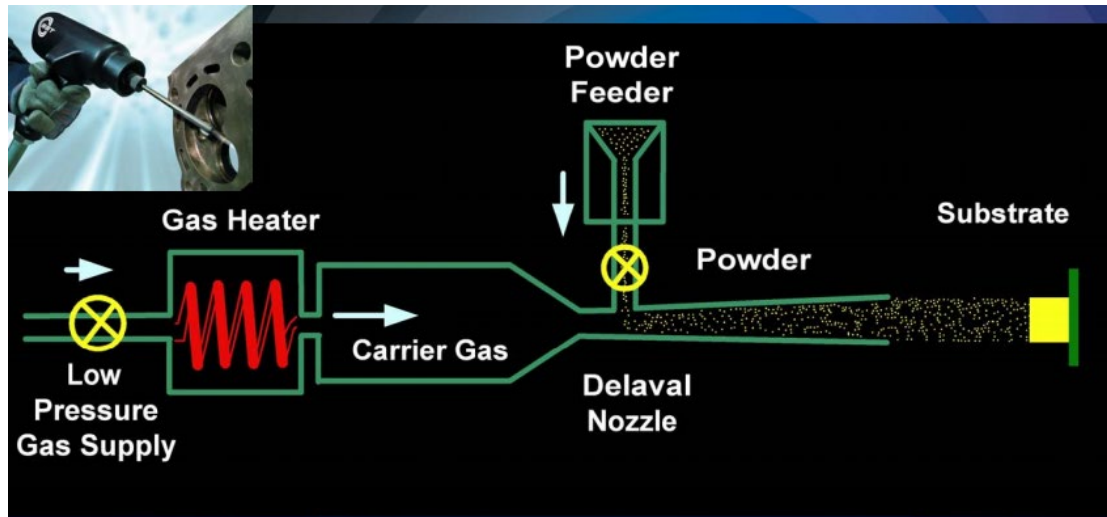


*Courtesy of NRC Canada

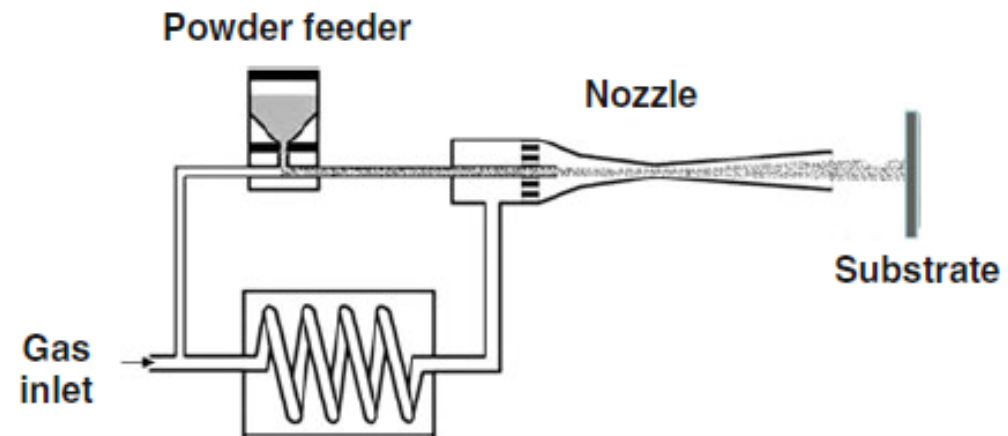
Cold Spray

- Particle characteristics
 - temperature $\sim 0-100^{\circ}\text{C}$
 - speed $\sim 400-1000\text{ m/s}$
- Materials - metals and cermets
 - spray rate $\sim 3\text{ to }5\text{ kg/hour}$
- Coating characteristics
 - density $\sim 1-10\%$ porosity
 - No oxidation, no phase change

Low and High Pressure Cold Spray Systems

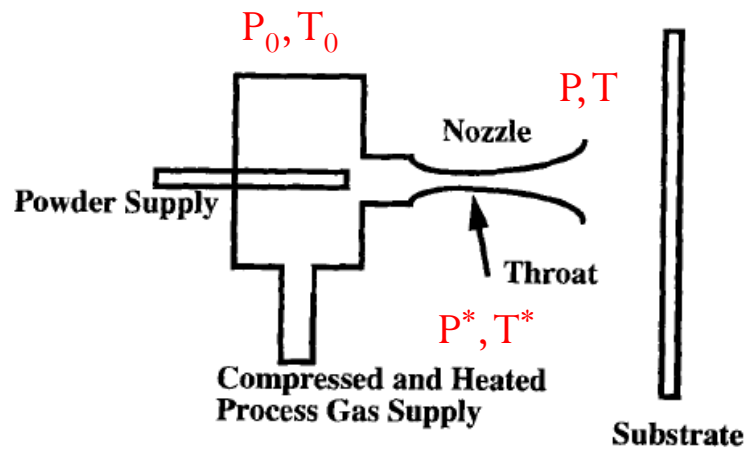


High Pressure Cold Spray



One-dimensional Isentropic Flow

- Well described in “Gas Dynamic Principles of Cold Spray, R.C. Dykhuizen and M.F. Smith, JTST 7(1998)205-212



0 = stagnation
 $*$ = Throat

- \dot{m} = mass flow rate fixed
- γ = ratio of specific heats (1.66 or 1.4 for monoatomic or diatomic gases)
- M = Mach number
- R = Universal gas constant / gas molecular weight

One-dimensional Isentropic Flow

- At the throat $M = 1$ (choked flow)

$$\frac{T_o}{T^*} = 1 + \frac{\gamma - 1}{2} \quad V^* = \sqrt{\gamma R T^*} \quad \rho^* = \frac{\dot{m}}{V^* A^*}$$

$$P^* = \rho^* R T^* \quad \frac{P_o}{P^*} = \left(1 + \frac{\gamma - 1}{2}\right)^{\gamma/(\gamma - 1)}$$

- At the nozzle exit (assuming $P < \text{atm}$, overexpanded flow)

$$\frac{A}{A^*} = \left(\frac{1}{M}\right) \left[\left(\frac{2}{\gamma + 1}\right) \left(1 + \frac{\gamma - 1}{2} M^2\right) \right]^{(\gamma + 1)/2(\gamma - 1)} \quad \frac{P}{P^*} = \left(\frac{\gamma + 1}{2 + (\gamma - 1) M^2}\right)^{\frac{\gamma}{\gamma - 1}}$$

$$\frac{T_o}{T} = 1 + \frac{\gamma - 1}{2} M^2 \quad V = M \sqrt{\gamma R T} \quad \frac{\rho_o}{\rho} = \left(1 + \frac{\gamma - 1}{2} M^2\right)^{1/(\gamma - 1)}$$

Particle Acceleration

- Particle acceleration due to drag force:

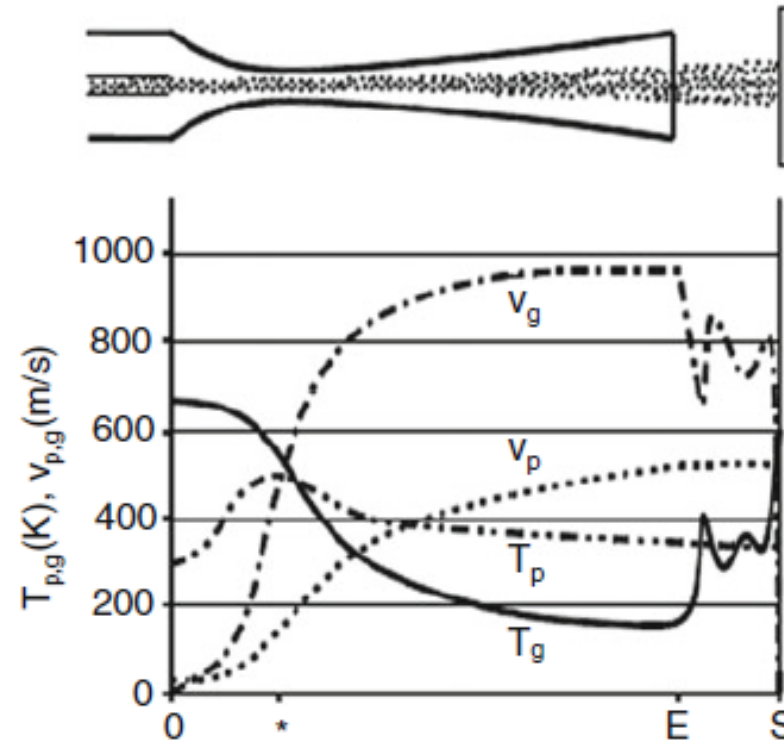
$$m \frac{dV_p}{dt} = m V_p \frac{dV_p}{dx} = \frac{C_D A_p \rho (V - V_p)^2}{2}$$

- For low values of the spray particle velocity (as compared to the gas velocity):

$$V_p = V \sqrt{\frac{C_D A_p \rho x}{m}}$$

Cold Spray Modeling

Fig. 6.13 Gas temperature, T_g , and velocity, v_g , evolutions along the nozzle axis for a N_2 flow ($T_0 = 573$ K, $p_0 = 2.5$ MPa, standard nozzle), and Cu particle ($15\ \mu\text{m}$) velocity, v_p and temperature, T_p , evolutions along the axis (* nozzle throat, E nozzle exit, S substrate). Reprinted with kind permission of ASM [31]



Cold Spray Modeling

Fig. 6.15 Dependence of the particle temperature and velocity at the nozzle exit with the inlet gas pressure for a standard nozzle, an initial temperature of 673 K and N₂ gas. Reprinted with kind permission of ASM [31]

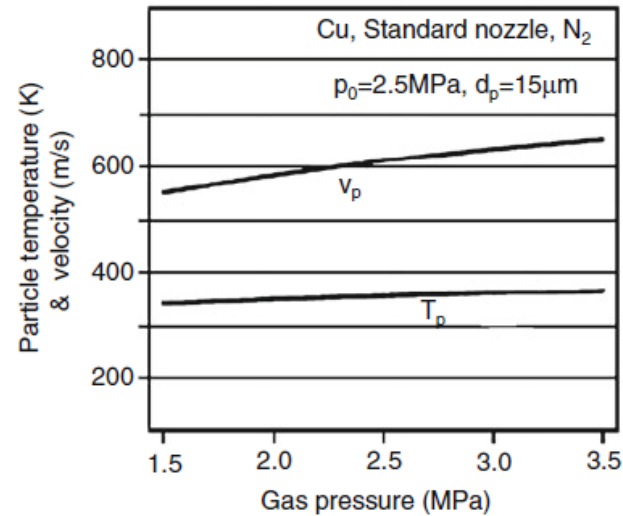
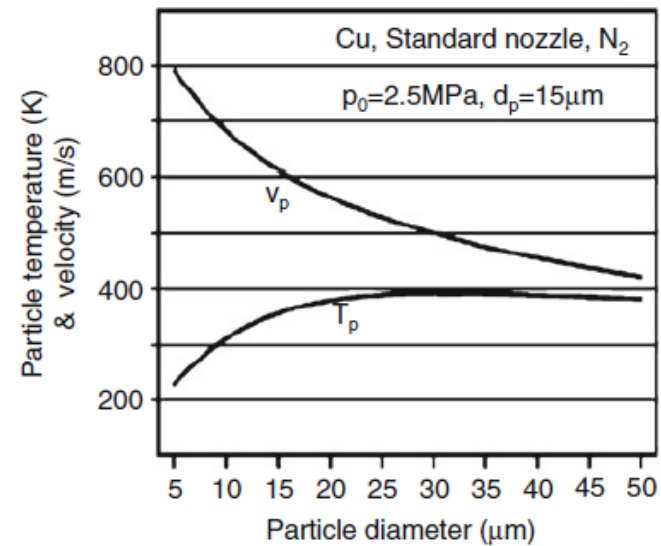


Fig. 6.16 Dependence of the Cu particle temperature and velocity on its size at the nozzle exit: standard nozzle, N₂ as process gas, 2.5 MPa, 673 K. Reprinted with kind permission of ASM [31]



Shear Instability

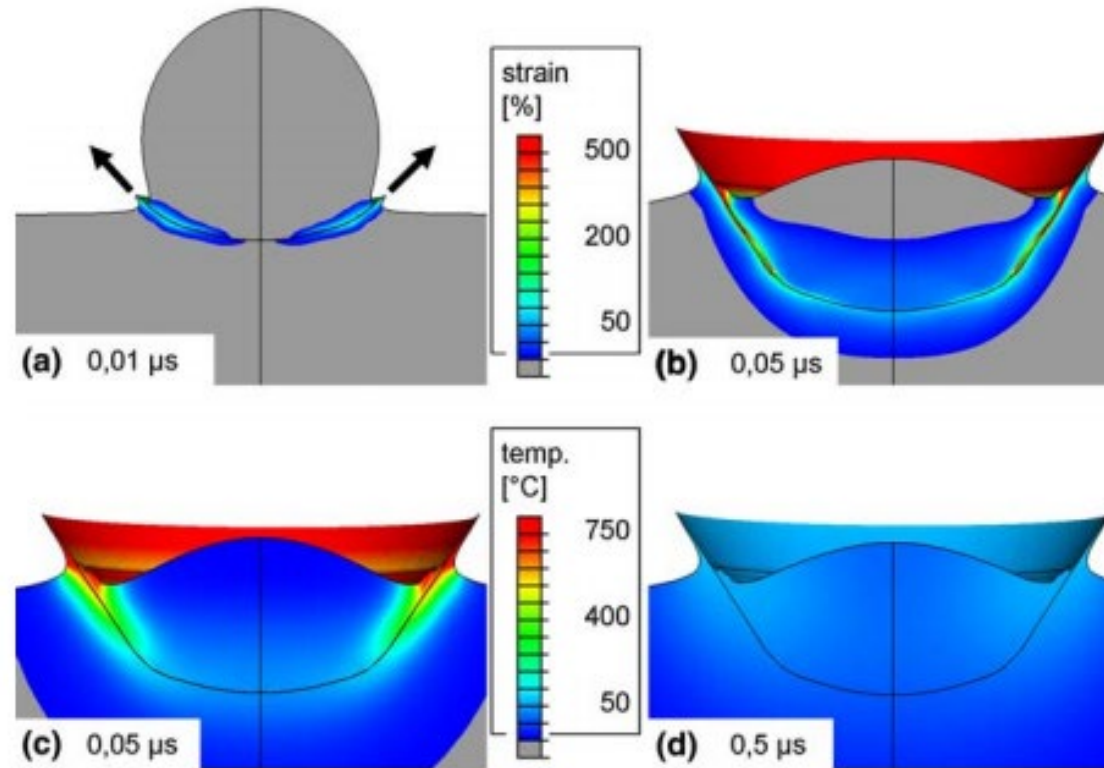


Fig. 11 Single sequences of an impact of a 25 μm Cu particle to a Cu substrate with 500 m/s at an initial temperature of 20 $^{\circ}\text{C}$. (a, b) Strain field and (c, d) temperature field. For the analysis a thermally coupled axisymmetric model was used

T. Schmidt et al., JTST, 18 (2009) 794–808

Fundamental investigation of impact behavior

Critical velocity (d=25 μm)

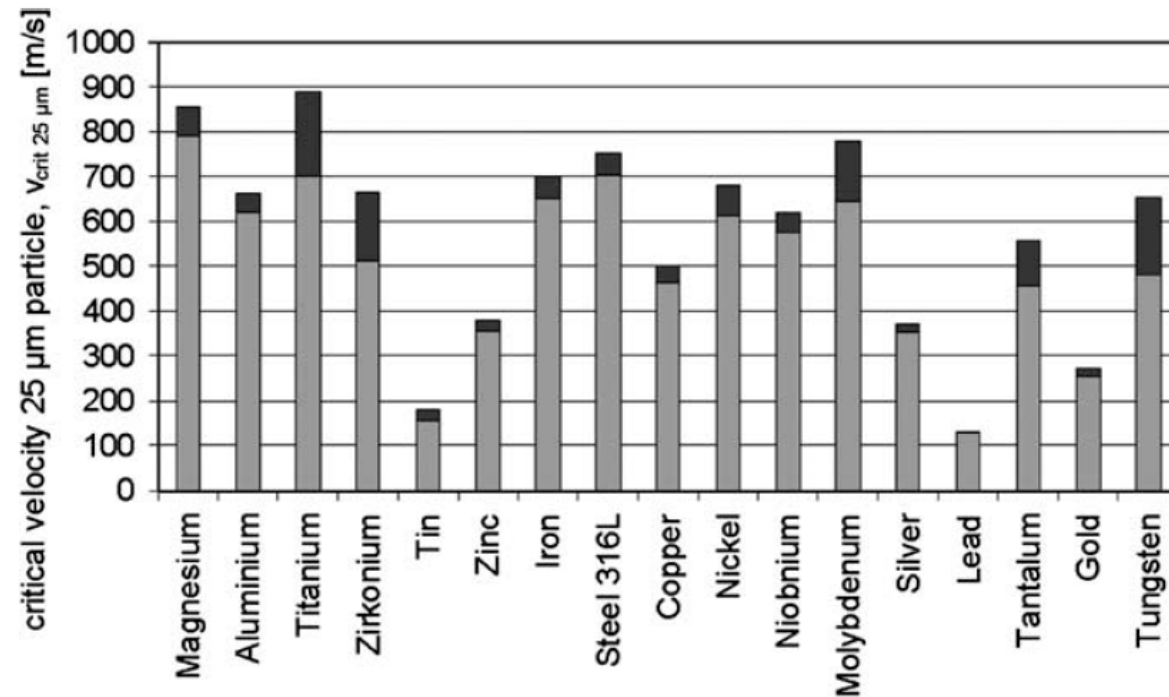
F_1, F_2 : empirical factors

σ_{TS} : tensile strength

T_i, T_R, T_m : initial, reference and melting temperatures

c_p : specific heat

$$v_{crit}^{th,mech} = \sqrt{\frac{F_1 \cdot 4 \cdot \sigma_{TS} \cdot \left(1 - \frac{T_i - T_R}{T_m - T_R}\right)}{\rho}} + F_2 \cdot c_p \cdot (T_m - T_i)$$



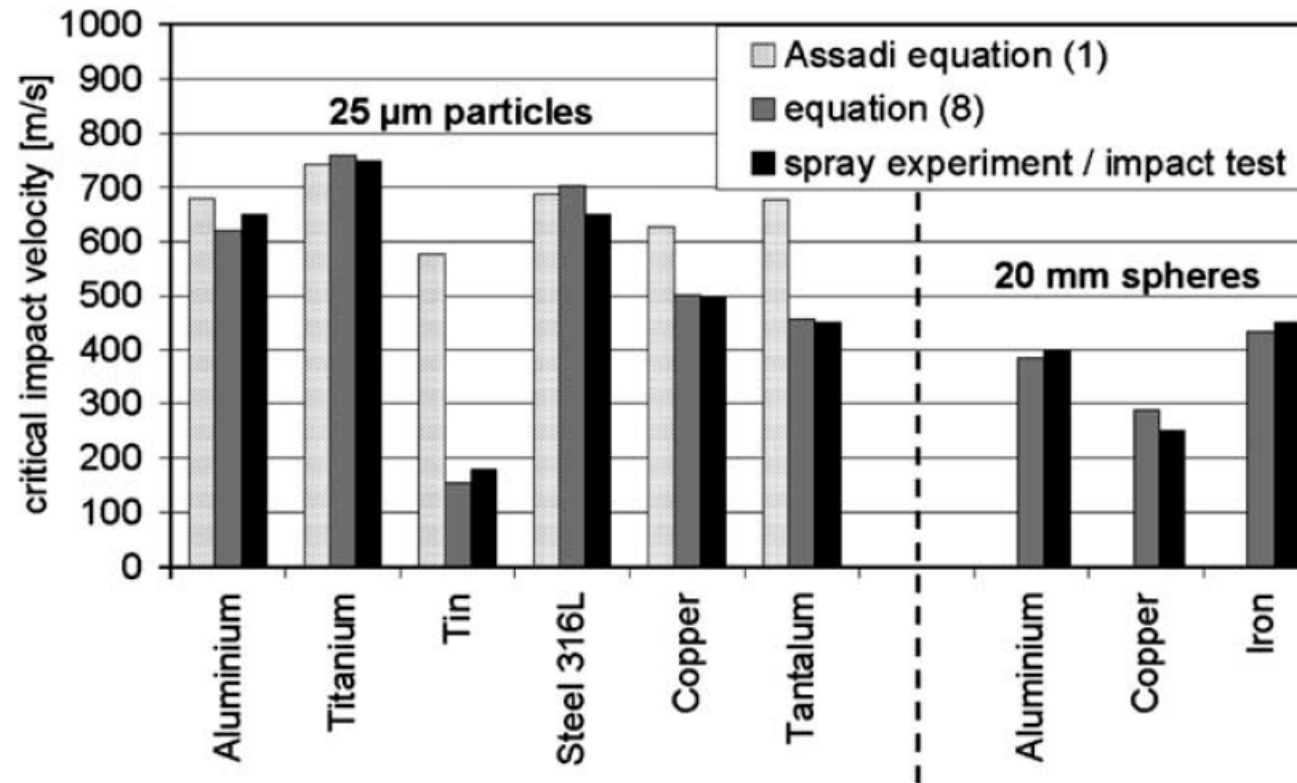
$$v_{cr} = 667 - 14\rho_{part} + 0.08T_m + 0.1\sigma_u - 0.4T_i$$

Assadi *et al.*, *Acta Materialia*, 51, 4379–4394 (2003)

T. Schmidt *et al.*, *Acta Materialia*, 54 729-742, (2006)

Fundamental investigation of impact behavior

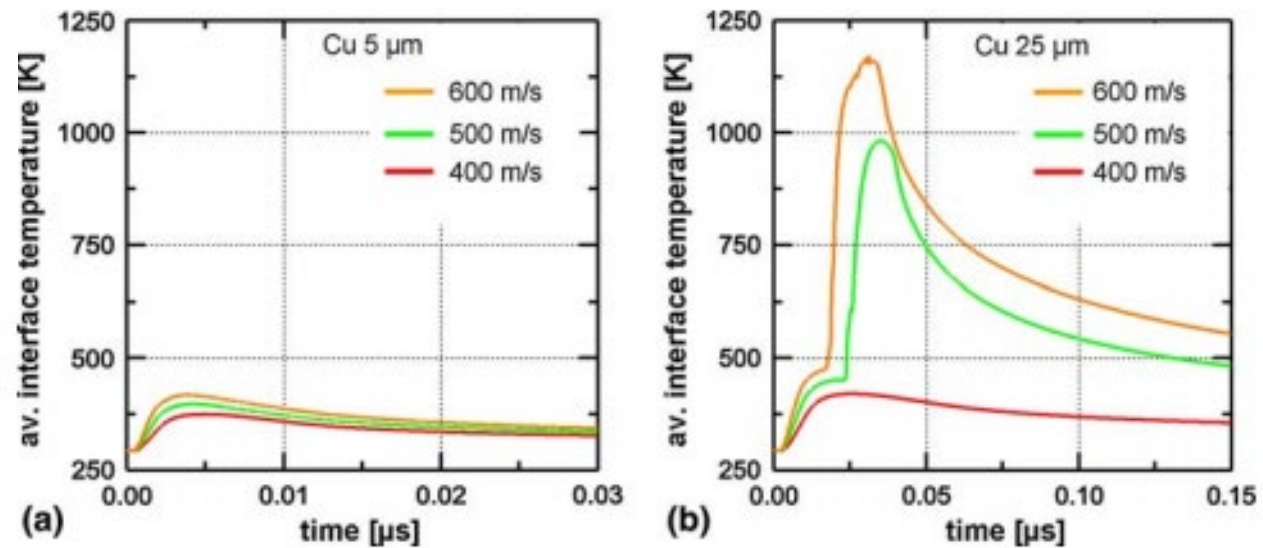
Critical velocity (experiment vs modeling)



T. Schmidt *et al.*, *Acta Materialia*, 54 729-742, (2006)

Effect of Particle Size

Fig. 6.27 Temporal evolution of the temperature at the monitored volume (sheared interface) of copper particles with different impact velocities and two sizes: (a) 5 μm and (b) 25 μm . Reprinted with kind permission from Springer Science Business Media [45], copyright © ASM International



T. Schmidt et al., JTST, 18 (2009) 794–808

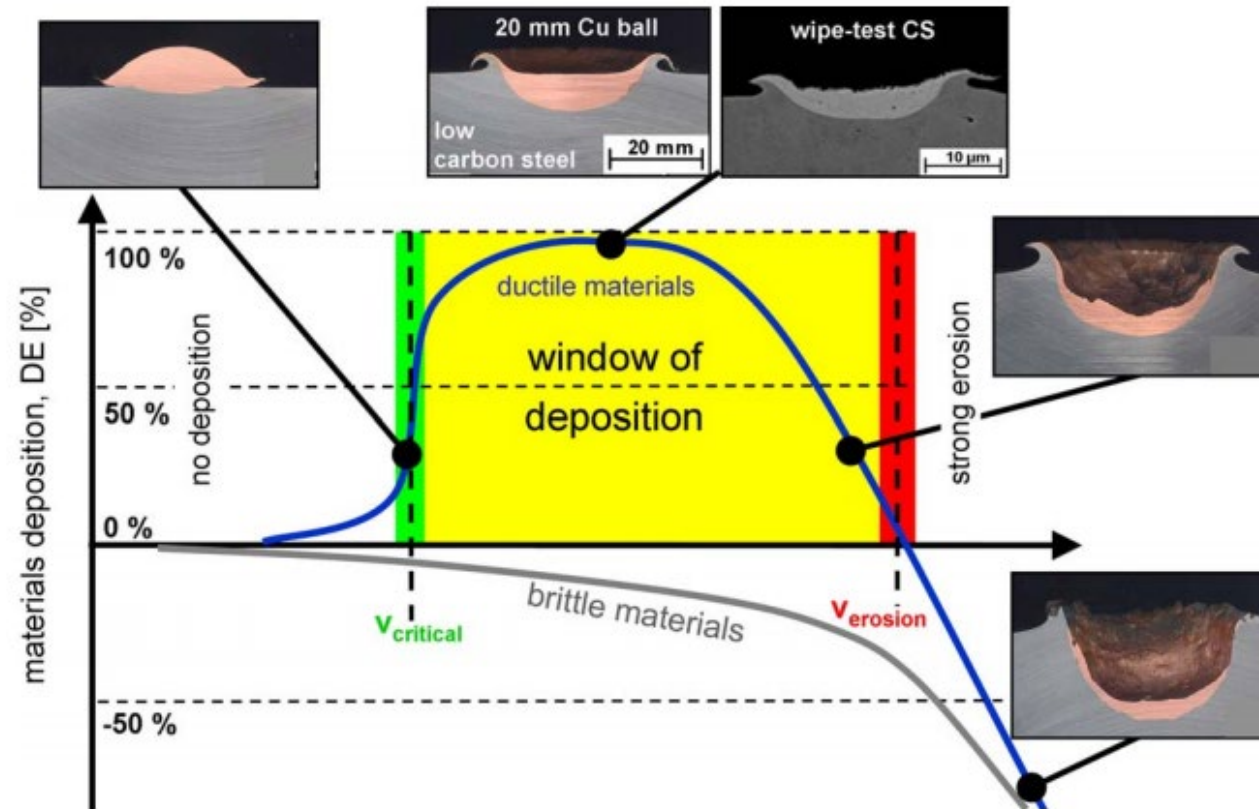
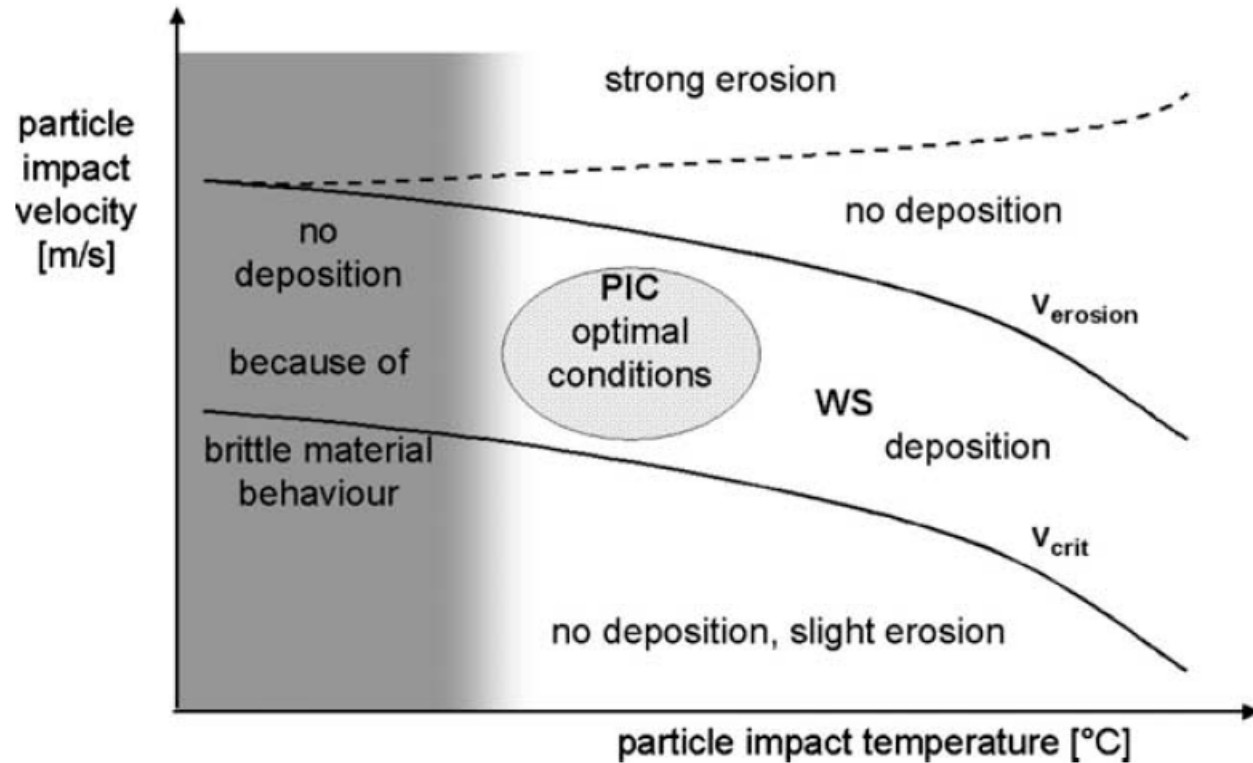


Fig. 8 Schematic correlation between particle velocity, deposition efficiency (DE) and impact effects for a constant impact temperature. Deposition is only observed for ductile materials in a certain velocity range for a given powder size and temperature, the so-called “window of deposition”

Fundamental investigation of impact behavior



WS = Window of sprayability
PIC = Particle impact condition

Ductile to Brittle Transition

T. Schmidt *et al.*, Acta Materialia, 54 729-742, (2006)

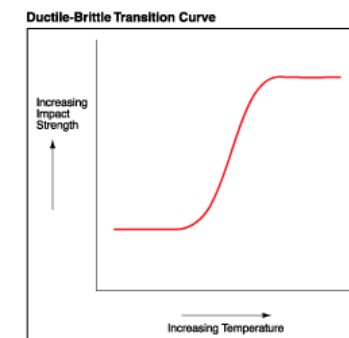
Exemple: Tin

$T_{trans} = 13^{\circ}C$

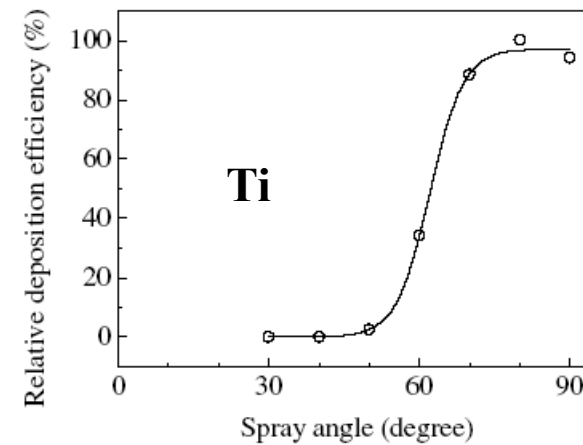
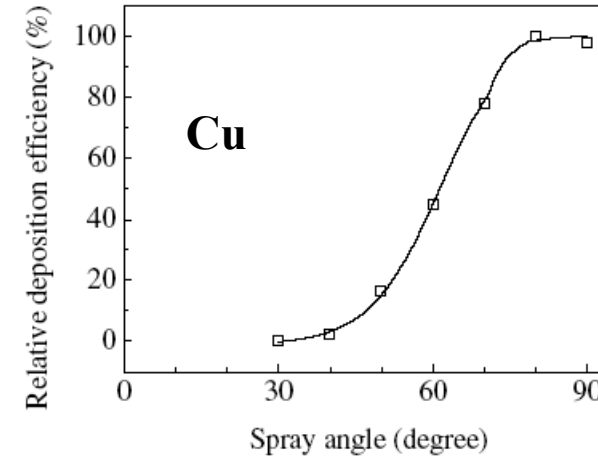
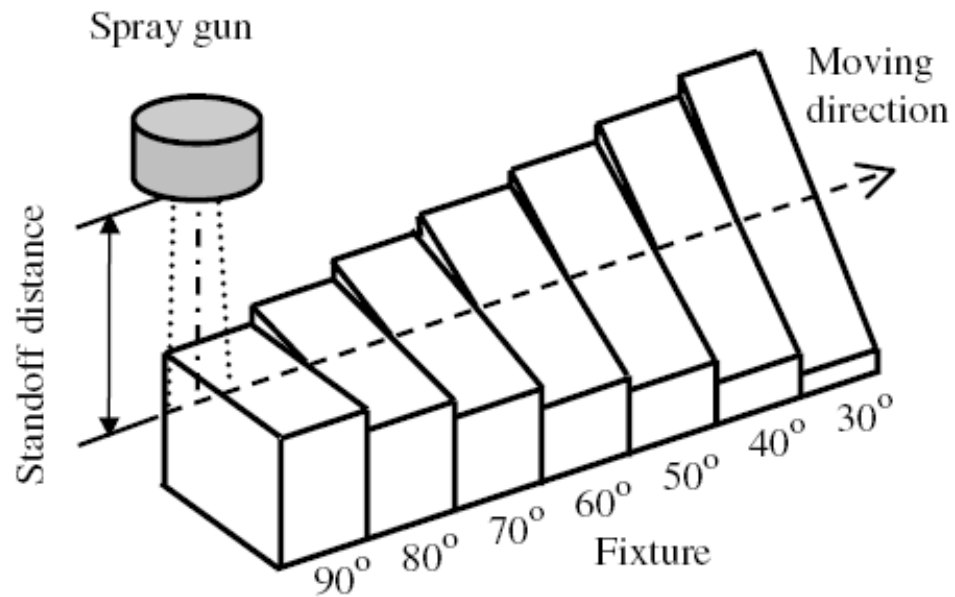
Temperature range
50-200 °C

At 50 °C
 $v \sim 150-340$ m/s

At 200 °C
 $v \sim 70-150$ m/s



Effect of angle of deposition



C. J. Li *et al.* ITSC 2003: International Thermal Spray Conference, pp.pp. 91-96, (2003)

Coating Structure: Aluminum

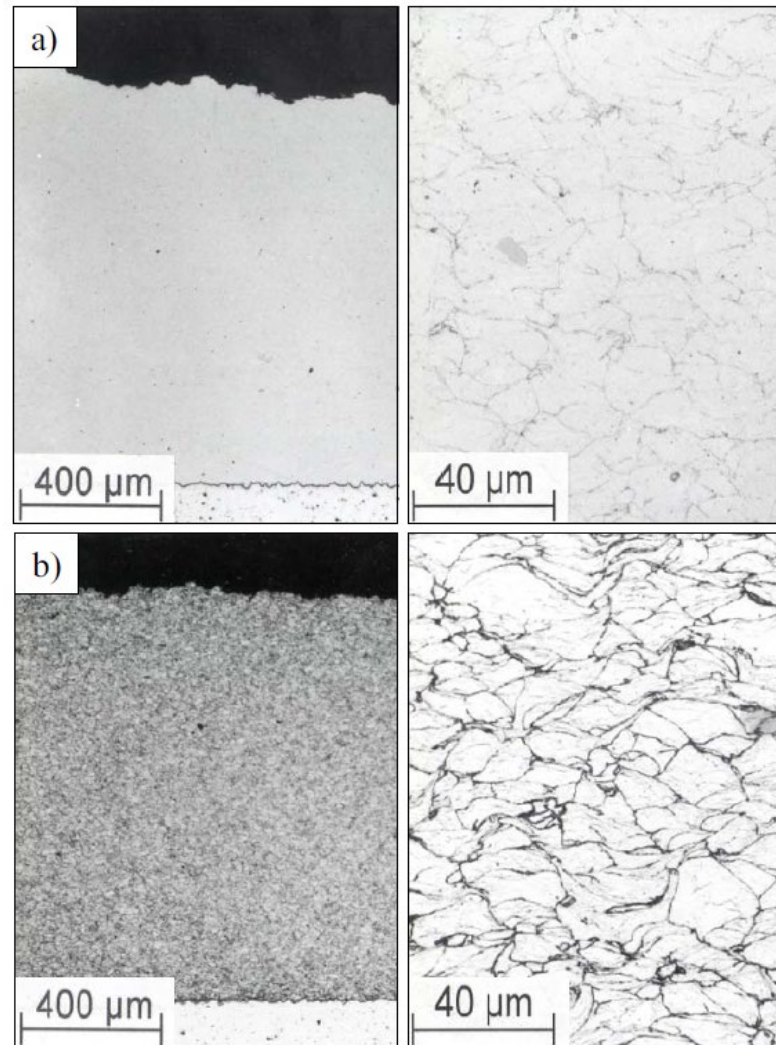


Figure 7: Microstructure of a Cu coating Cold Gas sprayed using N_2 as process gas onto an Al substrate, a) as-polished and b) etched.

Coating Structure: 316L Steel

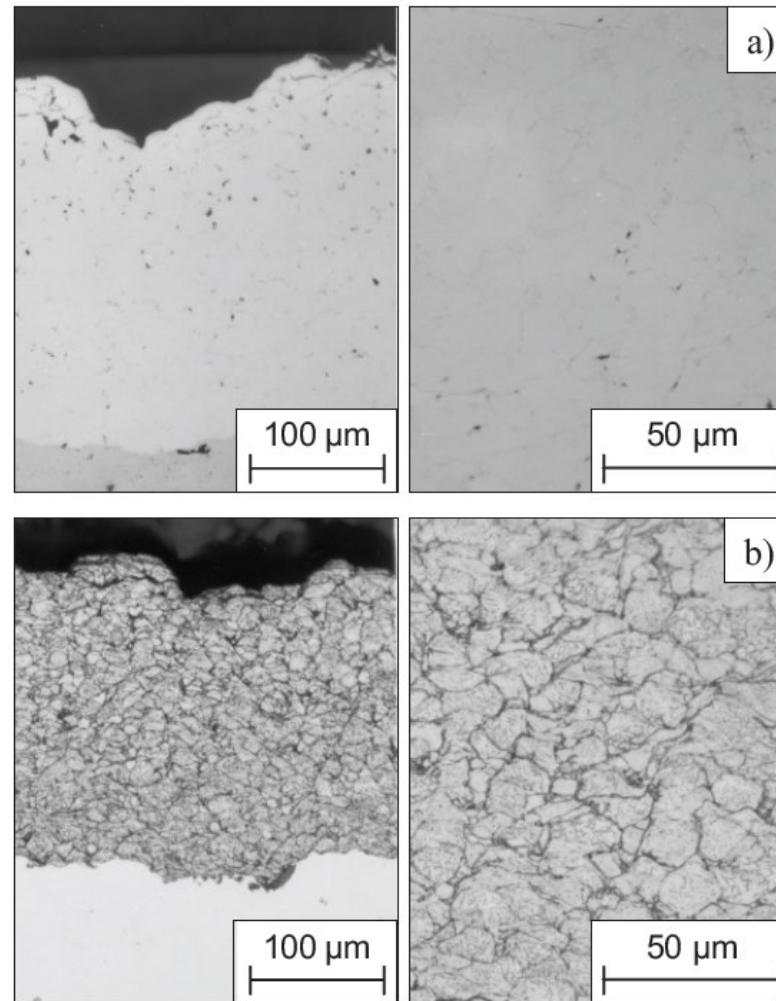
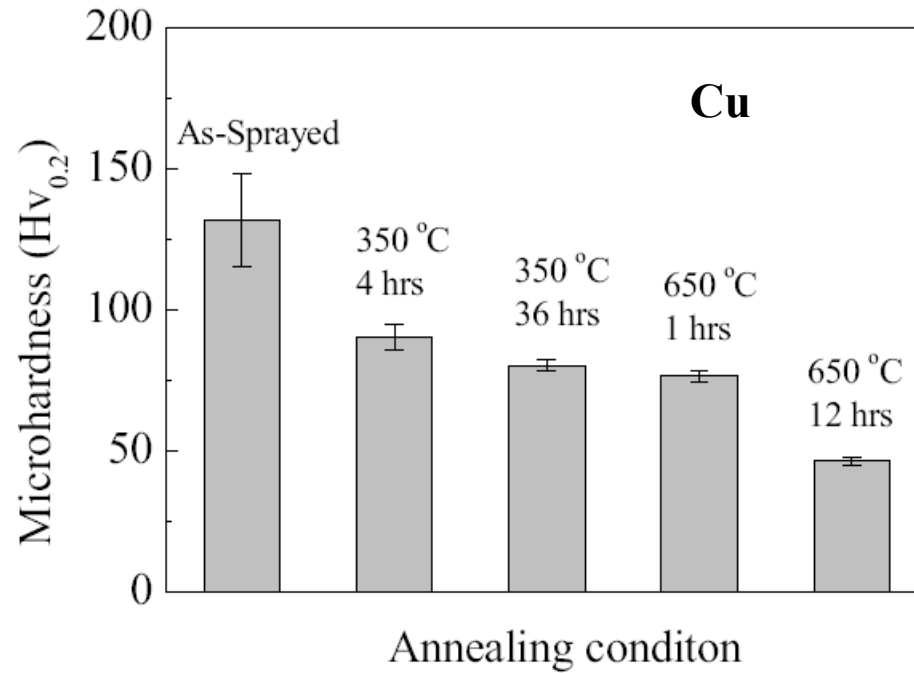


Figure 9: Microstructure of a 316L coating Cold Gas sprayed using N_2 as process gas onto an Al substrate: a) as-polished and b) etched.

Coating Properties

Hardness



Steel:

Microhardness

As sprayed : 193 HK

Annealed (1100C 24h): 105-115 HK

Mild steel sheet : 120 HK

Cu:

Microhardness

As sprayed : 153 HK

Annealed (650C 24h): 52 HK

CS Coatings have higher hardness than wrought materials probably due to cold work hardening during plastic deformation

Vacuum Cold Spray – Aerosol Spray

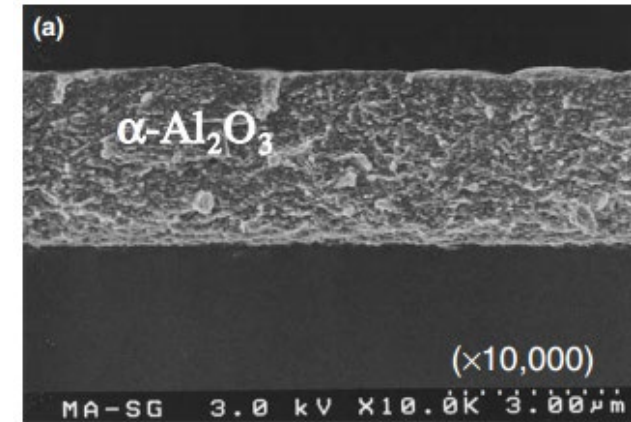
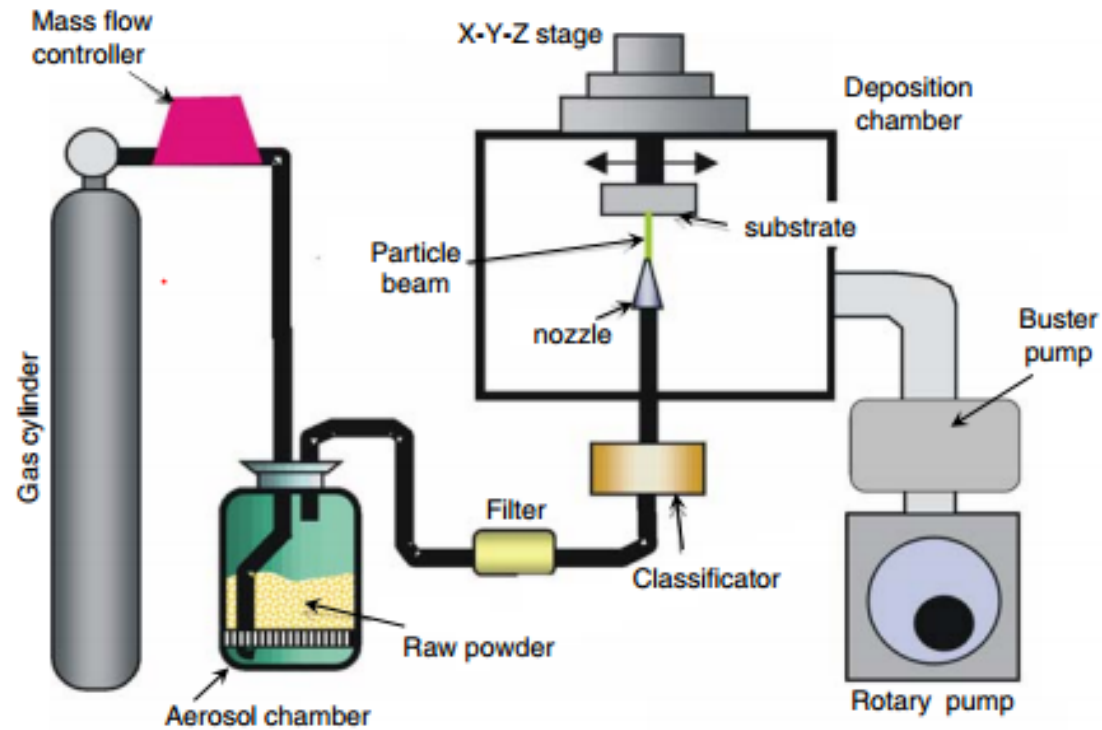


Table 2 Mechanical properties of as-deposited AD layers

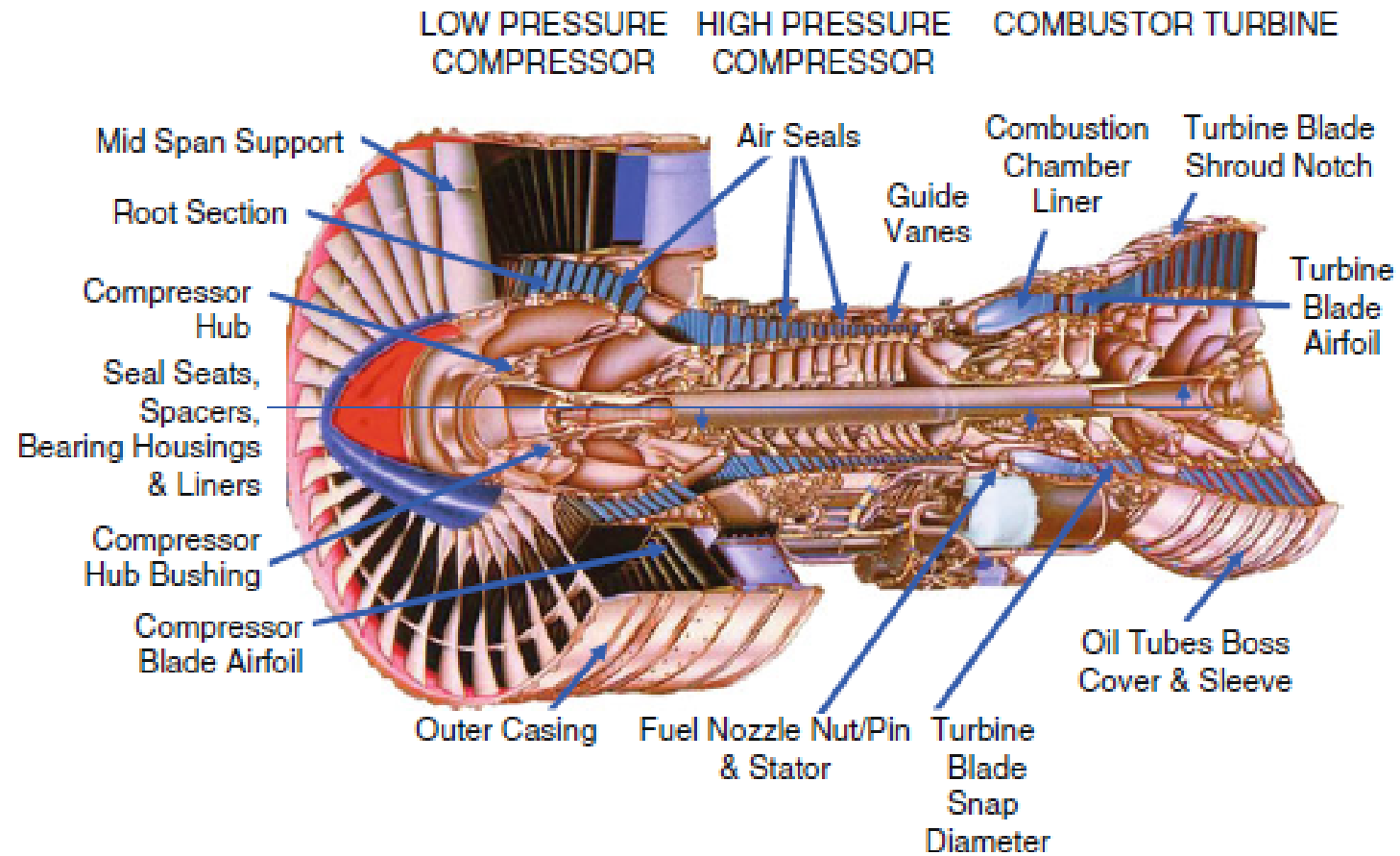
Material	Hardness (Hv)		Average crystallite size of the layer (nm)	Particle velocity at the collision (m/s)
	Layer (deposited at R.T.)	Bulk (a)		
<i>Oxide</i>				
A-Al ₂ O ₃	1200-2100	1900 ± 100	13-20	150-500
PZT	400-550	350 ± 50	10-30	100-300
(Ni,Zn)Fe ₂ O ₃	700-750	1040 ± 80	5-20	250-600
<i>Non-oxide</i>				
AlN	1100-1470	1180 ± 90	5-15	200-600
MgB ₂	700	...	5-20	300-550

(a) Bulk sample were prepared from the same starting powder as layers, by conventional sintering procedure (at temperature over 1200 °C)

J. Akedo, JTST, 17 (2008) 181-198

Applications

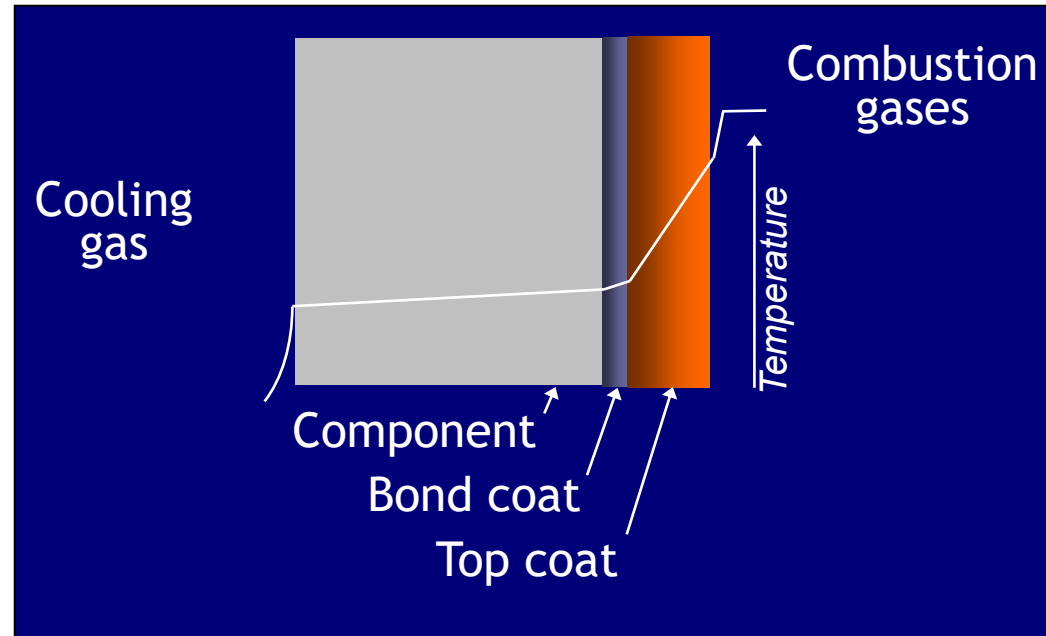
Aerospace Applications



*Walser B (2003), Spraytime 10(4) pp 1-7

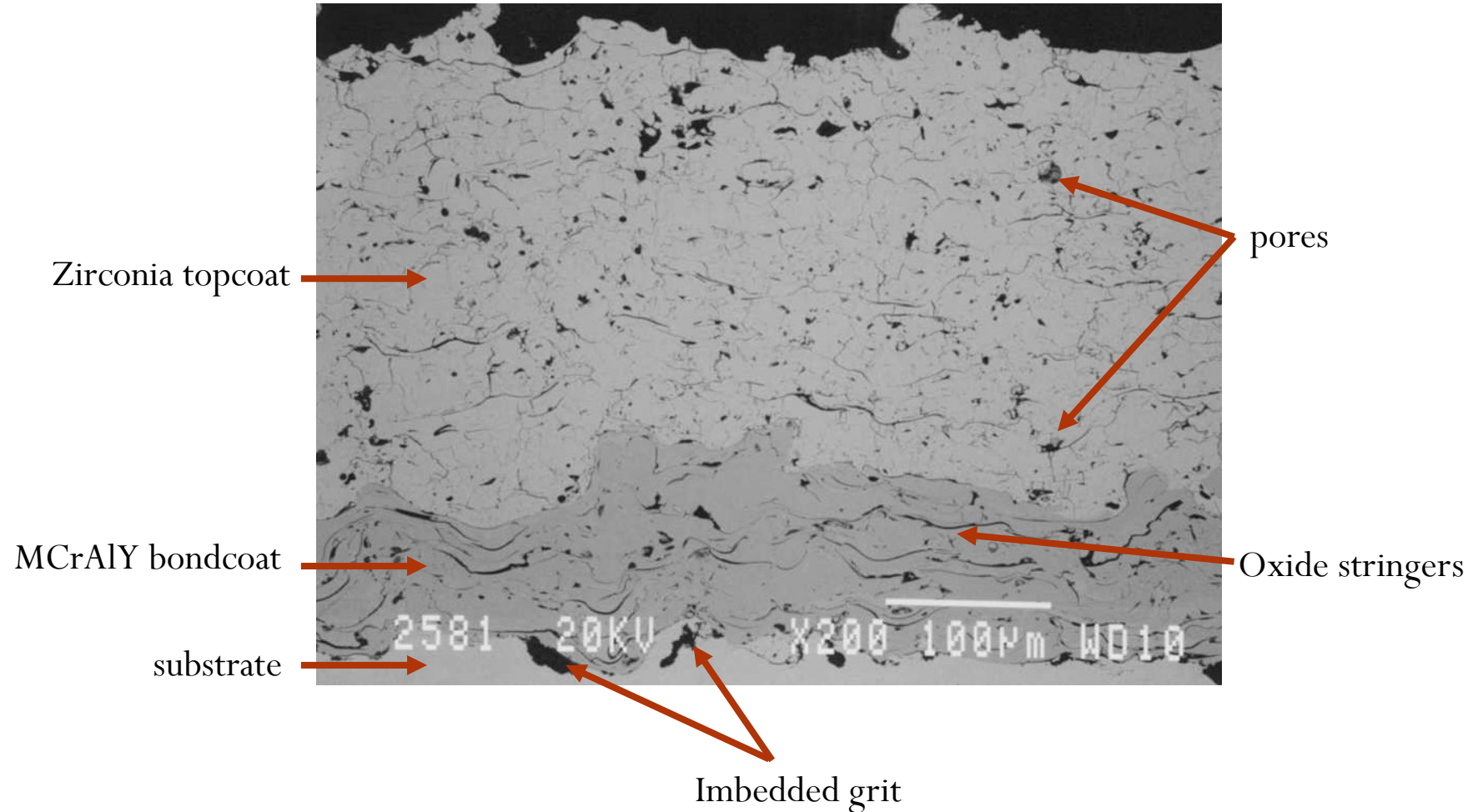
Thermal Barrier Coatings

- Bond coat
 - MCrAlY
- Top coat
 - Y-Stabilized ZrO₂

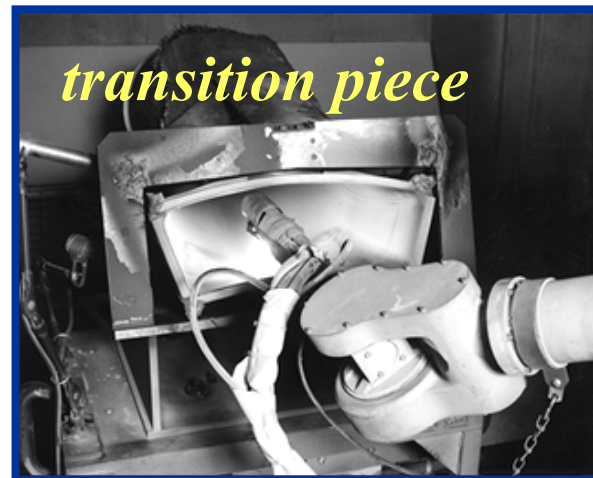
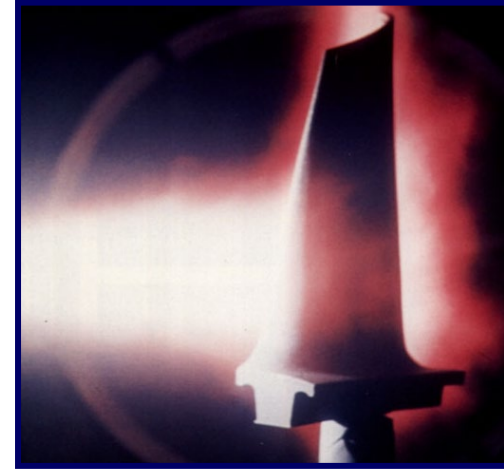
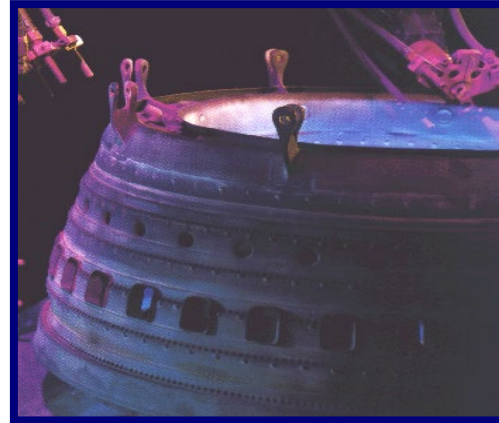


- Main function: Protect the underlying component from high temperature gases
- Operating temperature (TBC surface): Up to $\sim 1200^{\circ}\text{C}$ \Rightarrow temperature drop of up to $\sim 150^{\circ}\text{C}$

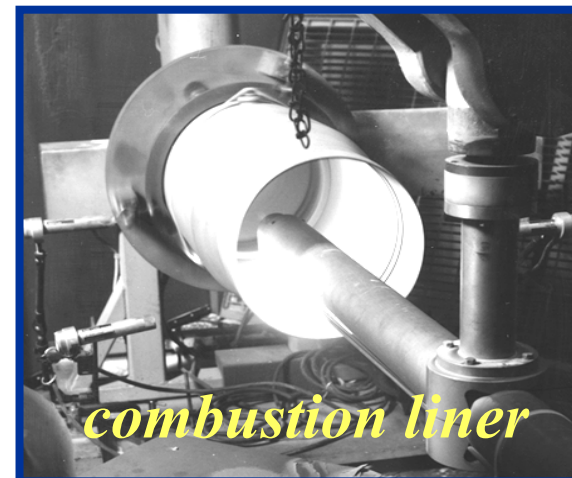
Thermal Barrier Coating System



Thermal Barrier Coatings



Courtesy of General Electric



Courtesy of Praxair Tafa

Plasma Spraying: Internal Surfaces

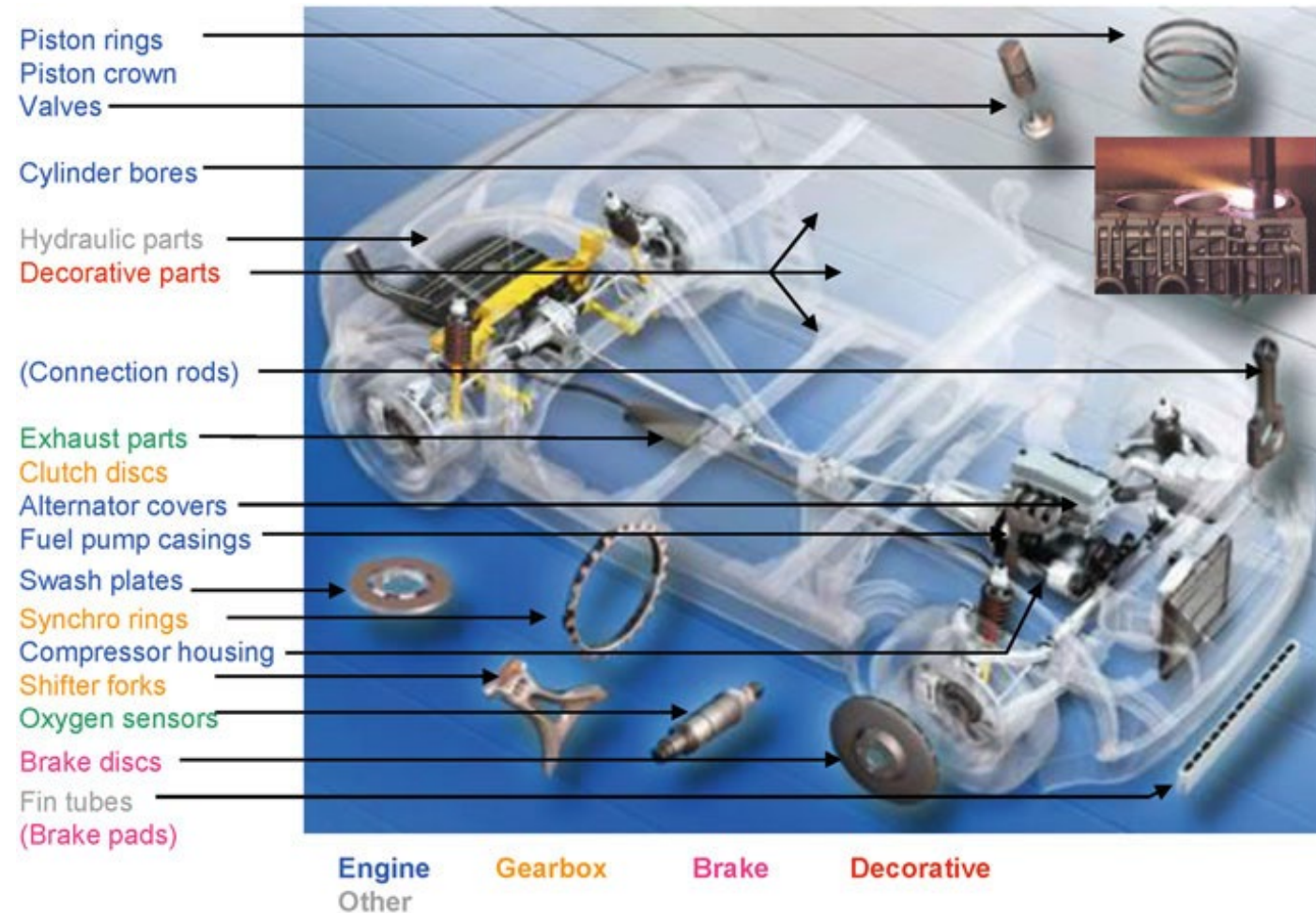


Applications:

- Combustion chamber, transition ducts in gas turbines
- Cylinders bores of ICE Al blocks

Video courtesy of NRC Canada

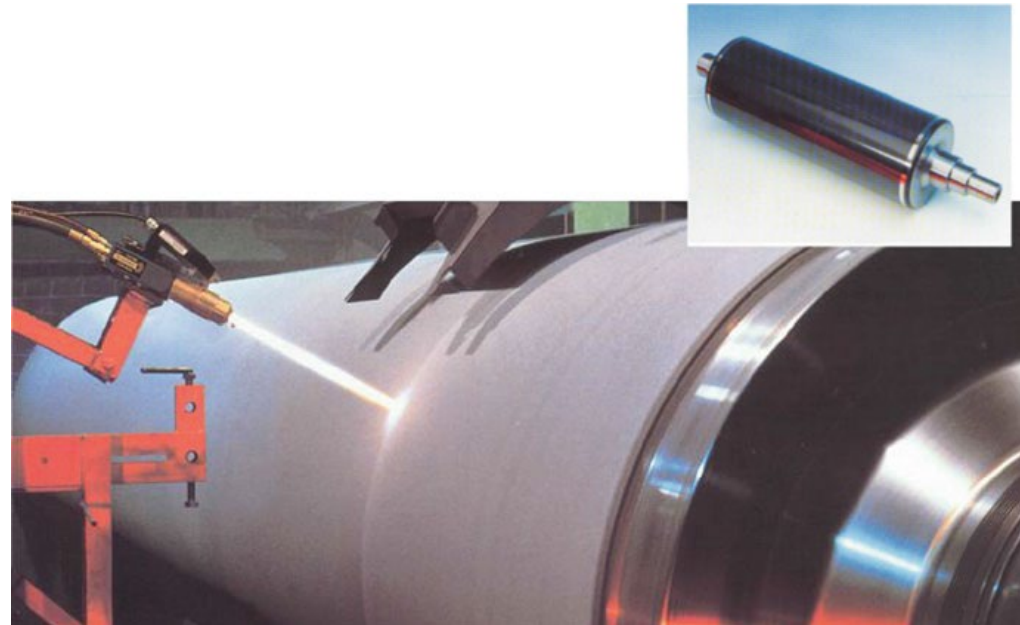
Automotive Applications



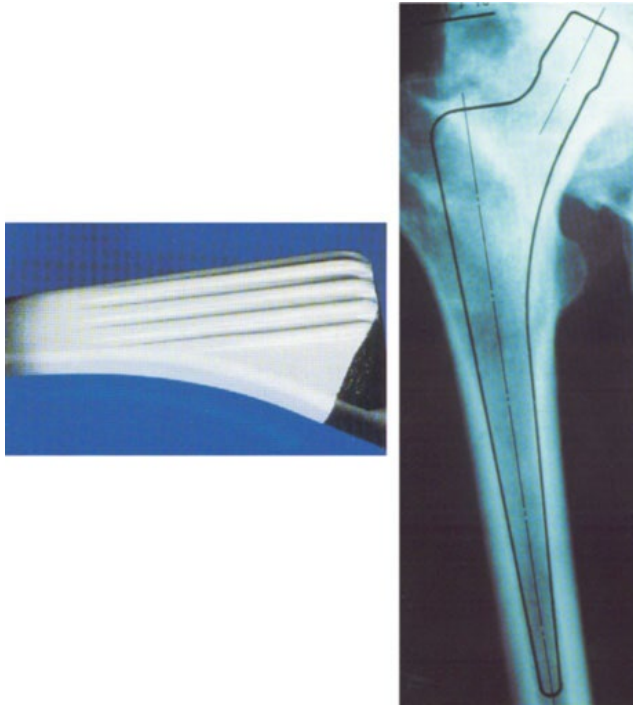
*Walser B (2003), Spraytime 10(4) pp 1-7

Pulp and Paper

- Coatings applied for wear and corrosion protection



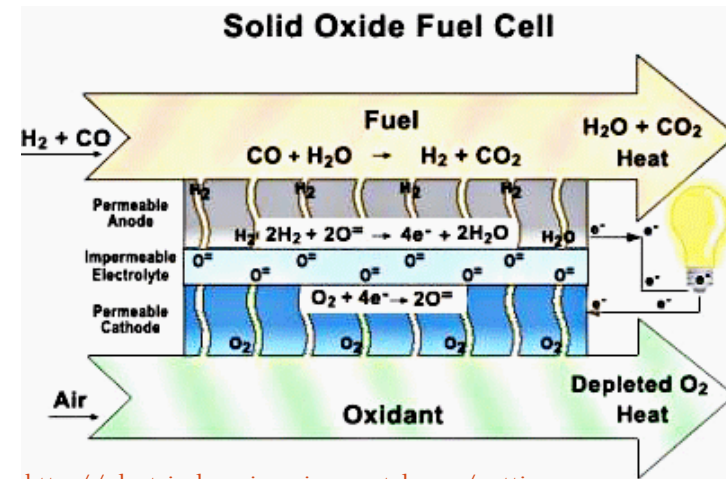
Biomedical Applications



- Thermal spray hydroxyapatite (HA) coatings for improved bone adhesion for hip and dental implants
- HA is the main inorganic bone constituent

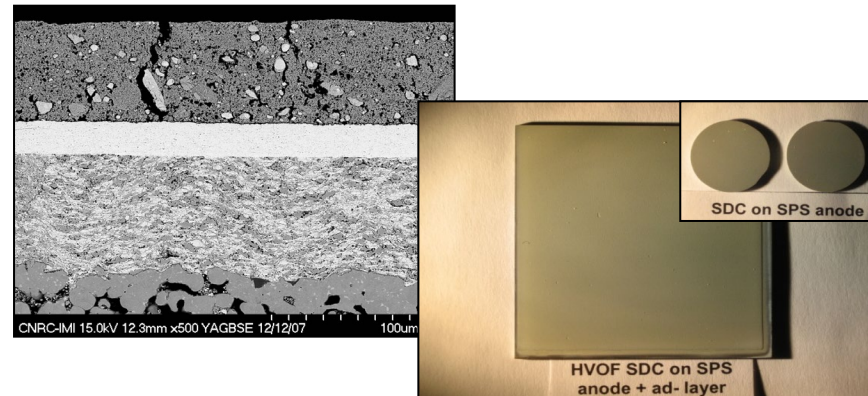
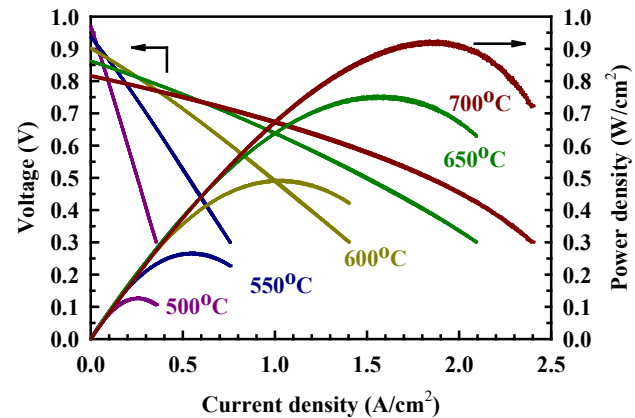
Solid Oxide Fuel Cell

- Highly efficient devices to convert chemical energy into electrical energy and heat with low environmental impact



<http://electrical-engineering-portal.com/getting-electricity-from-solid-oxide-fuel-cell>

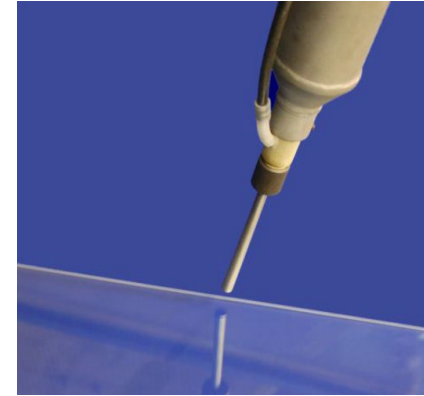
Reduction of component and overall manufacturing cost for next-generation Solid Oxide Fuel Cells (SOFC).



*Images courtesy of NRC Canada

Cold Spray Applications

- Coatings for wear, corrosion and oxidation protection
- Repair (magnesium components)
- Additive manufacturing
 - 2D printing (busbars on tin oxide coated glass)
 - 3D manufacturing



Current Trends in Cold Spray Technology:
Looking at the Future in Metal
finishing.com; 8 Jan 2010



Heat Exchangers: Brayton Energy Canada

Final Comments

- Thermal spray processes are used intensively in the industry and the market is rapidly growing
- Spray materials have unique properties that can be tailored according to the targeted application
- Innovative processes, such as suspension plasma spray and cold spray, are in active development and stimulate important research efforts for new high performance coatings and new applications